THE EFFECTS OF DECENTRALIZATION AND TRUST ON THE OPTIMIZATION OF INFORMATION GATHERING ACTIVITIES FOR COOPERATIVE AUTONOMOUS VEHICLES

by

Héctor J. Ortiz-Peña

June 15, 2015

A dissertation submitted to the

Faculty of the Graduate School of

the University at Buffalo, State University of New York

in partial fulfillment of the requirements for the

degree of

Doctor of Philosophy

Department of Industrial and Systems Engineering

UMI Number: 3714656

UMI

Dissertation Publishing

UMI 3714656

ProQuest

To Jesselyn and Héctor Adrián... for being my pillars of strength
and motivation throughout this journey.

Acknowledgment

First, I want to thank my parents, Héctor and Gema, and my sisters, Gemarie, Michelle and Melissa, for their love, support throughout my entire life, and for teaching me that perseverance and hard work are indispensable to successfully face any challenges in life.

I want to thank my thesis advisors, Dr. Mark Karwan and Dr. Moises Sudit, for their guidance and motivation during the entire doctoral program. I will always be grateful for their understanding and willingness to accommodate their busy schedules to my work, academic and personal commitments. It is was an honor working with them. I also want to thank Dr. Rakesh Nagi for his helpful suggestions and support on this process.

I want to acknowledge Dr. Michael Hirsch for motivated me to pursue this goal for which I am grateful. I cannot thank him enough for his contributions and advice, but more importantly, for being a friend and mentor, always challenging me to be a better researcher and professional. I look forward to continue working with him on new research challenges and ideas.

I also want to acknowledge CUBRC, Inc. in Buffalo, New York, for their financial support and for trusting me to expand my job responsibilities while I was completing my degree. Also, I want to thank my colleagues at CUBRC, Inc. and the graduate school of the Department of Industrial and Systems Engineering at the University at Buffalo for always having words of encouragement for me to complete the doctoral degree.

Finally, I want to thank my wife, Jesselyn Torres, and my son, Héctor Adrián. This dissertation simply would not have been possible were it not for their unconditional support and endless love. I will be forever on their debt.

Contents

List of Tables

List of Figures

Abstract

One of the main technical challenges facing intelligence analysts today is the efficient utilization of limited resources (both in quantity and capabilities) to maximize the accuracy and timeliness of collected data to address information gaps. The challenges on this problem increase when the communication between the information gathering assets is limited, preventing constant coordination of collection activities and information sharing among the assets. This work addresses the problem of routing cooperative autonomous vehicles (e.g., unmanned vehicles) operating in a dynamic environment to maximize overall information gain. Vehicles (collection assets) are collecting information on multiple objectives, subject to communication network constraints. In addition, this research studies the degradation of solution quality (i.e., information gain) as a centralized system synchronizing information gathering activities for a set of cooperative autonomous vehicles moves to a decentralized framework.

A mathematical programming model to determine routes in (de)centralized frameworks was developed. This model is based on a representation of potential information gain in discretized maps, the effectiveness of the assets collecting information and an obsolescence rate on the areas visited by the assets. The model assumes that information is only exchanged when assets are part of the same network, allowing a multi-perspective optimization of the information gathering activities in which each asset develops its own decisions based only on its perspective of the environment (i.e., potential information gain). This framework is used to evaluate the degradation of solution quality as a centralized system moves to a decentralized framework. This research extends the concept of "price of anarchy" (a measure on the inefficiency of a system when individuals (i.e., agents) maximize decisions without coordination) by considering different levels of decentralization.

Different communication network topologies are considered. Collection assets are part of

the same communication network (i.e., a connected component) if: (1) a fully connected network exists between the assets in the connected component, or (2) a path (consisting of one or more communication links) between every asset in the connected component exists. Multiple connected components may exist among the available collection assets supporting a mission. Trust (with a suitable decay factor as a function of time) on the potential location of assets that are not part of a connected component is considered as part of an extension to the optimization model. A solution approach based on multiple aggregation strategies to obtain satisficing solutions that are computational efficient was developed.

Chapter 1

Introduction

One of the main technical challenges facing intelligence analysts today is the efficient utilization of limited resources (both in quantity and capabilities) to maximize the accuracy and timeliness of collected data to address information gaps. The challenges on this problem increase when the communication between the information gathering assets is limited, preventing constant coordination of collection activities and information sharing among the assets. This work addresses the problem of routing cooperative autonomous vehicles (e.g., unmanned vehicles) operating in a dynamic environment to maximize overall information gain. Vehicles (collection assets) are collecting information on multiple objectives, subject to communication network constraints. In addition, this research studies the degradation of solution quality (i.e., information gain) when a centralized system synchronizing information gathering activities for a set of cooperative autonomous vehicles moves to a decentralized framework. The concept of "price of anarchy", a measure referring to the inefficiency of a system when decisions are made without coordination, is extended by considering different levels of decentralization.

The objective of this chapter is to present an overview and a roadmap of the research documented in this dissertation: from the definition of potential information gain maps to the computation and comparison of the "price of decentralization" for different network configurations. Mathematical tools are developed to facilitate the measurement and analysis of the loss of effectiveness (i.e., level of performance accomplishing a goal [2]) of information gathering systems operating with some degree of decentralization when compared to its centralized version. The main interest

is to represent the effects of the lack of overall coordination of resources, for example UAVs, on a system-level measure of performance (e.g., number of detected targets, accuracy of information, information gain, etc.). This chapter is used then as a means to clarify terms and concepts, to characterize the research problem, and to highlight potential areas of additional research.

Collection assets are represented in this research as entities characterized by three main components: (1) the platform (also referred to as the vehicle), (2) an on-board sensor suite, and (3) the communication network. The Area of Operation (AO) where assets are collecting information is discretized and represented by a set of grid cells. A numerical value, the potential information gain, is associated to each cell. An Information Gain Map (IGM) represents a characterization of the subareas in the AO based on its potential of having features addressing identified information deficits and objectives in the mission. When considering the IGMs, a higher value among cells represent a higher opportunity to obtain information of interest between them; thus, a rating system to define IGMs is developed. The concept of *entropy*, a measure of the amount of information required on the average (i.e., a measure of the uncertainty) to describe a random variable, is exploited in the rating system.

A Mixed-Integer Linear Program (MILP) was developed to determine the optimal routes (i.e., the sequence of moves) of the information collection assets in the AO to maximize the overall potential information to be gained. The model is based on the representation of potential information gain in discretized maps (i.e., IGMs), the effectiveness of the assets collecting information and an obsolescence rate on the areas visited by the assets. The model assumes assets operate on a decentralized framework. In a centralized framework, the information is propagated from node to node in the network until it reaches a "central" node responsible of determining and disseminating expected decisions (e.g., path definition, tasks assignments) to all lower nodes. This requires high computational burden at the central node and a robust and reliable communication network that allow virtually perfect information flow among all the agents in the system and the central node. Decentralized frameworks rely on local processing of information, including information from nearby agents, and local decision-making. This framework reduces the computational and communication requirements of a centralized framework, allowing scalability of the system to large group sizes [3]. Moreover, in the assumed decentralized framework, information is only exchanged when assets are part of the same communication network, allowing a multi-perspective optimization of the informa-

tion gathering activities in which each asset develops its own decisions based only on its perspective of the environment.

Different communication network topologies are considered. First, a fully connected network between the collection assets in the same communication network (i.e., a connected component) was assumed. For this communication network topology a direct communication link between each pair of assets is required. Multiple connected components may exist among the available collection assets supporting a mission. A different communication network topology is possible in which assets use other assets as intermediary (or "bridge") nodes to exchange information. In this case, assets are not required to have a direct communication link (within its communication range) to all other assets in the network: information is exchanged between assets as long as there is a communication path between them. Mathematical model was updated in order to relax the constraints of the direct communication link topology and allow assets to identify communication paths to exchange information. Other extensions, including the evaluation of the potential location of assets that are not part of a connected component, were derived and described in Chapter 6.

A solution approach based on multiple aggregation strategies to obtain satisficing solutions that are computational efficient was developed. Instead of trying to solve the complete route for each asset at once, a strategy is defined in which only a subset of time-steps are evaluated at a time. This subset of time-steps is referred to as a *rolling horizon* and it constitutes a subproblem to be solved using the mathematical model described above. Within this rolling horizon, only a number of time-steps from the solution obtained while solving this subproblem will be considered in the final solution. This subset of time-steps is considered as the *fixed window*. Once this *cascade* (i.e., a subproblem defined, solved and appropriate solution fixed) is completed, a new rolling horizon is defined from the last fixed time-step in the solution. A new cascade is then solved. When the rolling horizon includes the last time-step in the planning horizon, the solution from that subproblem completes the final solution.

Using the time aggregation approach described above provides the opportunity to also reduce the number of grid cells considered in each cascade, reducing even more the complexity of solving the MILP. Given the number of time-steps in each rolling horizon and the (known) kinematic constraints of each vehicle, only the cells that could be reached in each cascade are considered. In addition to time aggregation, we consider a spatial aggregation whereby gain information for cells that cannot

be reached in the current rolling horizon are "combined" with the rolling horizon boundary cells. This space aggregation approach is used to update the value of selected cells considered on each rolling horizon, complementing the developed solution approach.

The developed mathematical programming model and solution approach are used as a framework to evaluate the degradation of solution quality as a centralized system moves to a decentralized framework. This research extends the concept of "price of anarchy", a measure referring to the inefficiency of a system when individuals (i.e., agents) maximize decisions without coordination [4, 5, 6, 7, 8]. The Price of Decentralization (PoD) is defined as a measure on the degradation of solution quality as a centralized system moves to different levels of decentralization. Price of Anarchy (PoA) is then only the extreme case of the PoD concept, wherein all collection assets defined their best route to maximize the potential information gain, without coordination. Network connectivity is represented by a set of binary variables in the mathematical model so a connectivity matrix can be defined capturing what assets are in the same communication network and enabled to exchange information. Levels of decentralization will be determined by redefining the structure of this connectivity matrix and computing the PoD metric against the information gain from the best-known solution for a centralized framework.

This dissertation is organized as follow: In Chapter 2 a review of relevant research is presented. The concepts of centralized and decentralized architectures are described in detail. Research efforts and results on the areas of planning and control systems are also discussed. In Chapter 3, a rating system is discussed to characterize the potential information gain in an area of operation. In Chapter 4, a mathematical programming model for multi-perspective optimization is developed. Chapter 5 discusses multiple heuristic approaches to allow evaluation of the mathematical programming model while considering larger problem sizes and operational timelines. Extensions to the mathematical model, including theoretical mathematical proofs and numerical examples of the derived constraints to allow assets to identify communication paths to exchange information are presented in Chapter 6. A characterization of the price of decentralization is then presented in Chapter 7 by evaluating different network topologies and asset collection parameters operating in different conditions (as captured by different types of IGM). Finally, conclusions and future research topics are presented in Chapter 8.

Chapter 2

Literature Review

2.1   Introduction

This chapter is a literature review on the general area of planning and control systems on centralized and decentralized frameworks, with particular emphasis on the control of cooperative autonomous vehicles (e.g., Unmanned Aerial Vehicles (UAVs)). The main thrust of the chapter is to highlight relevant previous work in this area. The chapter is organized as follows: In Section 2.2, the concepts of centralized, decentralized and hierarchical architectures are defined in the context of this work. Research efforts and results on the area of planning and control of UAV systems are then discussed, highlighting its application to centralized or decentralized frameworks. In Section 2.3, a review of the literature on cost of anarchy, or loss of effectivity, when moving from a centralized to a decentralized system is provided, including a description of a game-theoretic perspective on resource allocation problems, the price of anarchy and the price of fairness.

2.2   Planning and Control Systems of Autonomous UAVs

Autonomous systems are playing an increasingly important role in both civilian and military applications. Systems of UAVs, for example, are allowing military personnel to focus on more important issues like interpreting gathered information, as opposed to determining how to acquire it [9]. The planning and control component on these autonomous systems is responsible for determining the

trajectory the vehicles will follow. For the purpose of this discussion, a trajectory is defined as an assignment of the UAVs to set of tasks with a location associated to them, a set of waypoints or simply an area in a discretized environment (i.e., a cell in a grid representing the area of operation of the UAVs). The terms *trajectory*, *route* and *path* are used interchangeably throughout this dissertation and refer to the described assignment. A general description of the different architectures in which planning and control systems are implemented, with the purpose of clarifying the terminology used throughout the paper, is presented in Section 2.2.1. A literature review on centralized and decentralized algorithms and results for planning and control of UAV systems is discussed in Section 2.2.2.

2.2.1   Centralized, Decentralized and Hybrid Frameworks

Frameworks for planning and control of autonomous systems, similar to an information fusion system, can be classified into three types of topologies [10, 11]: (1) centralized, (2) decentralized, and (3) hierarchical (hybrid).
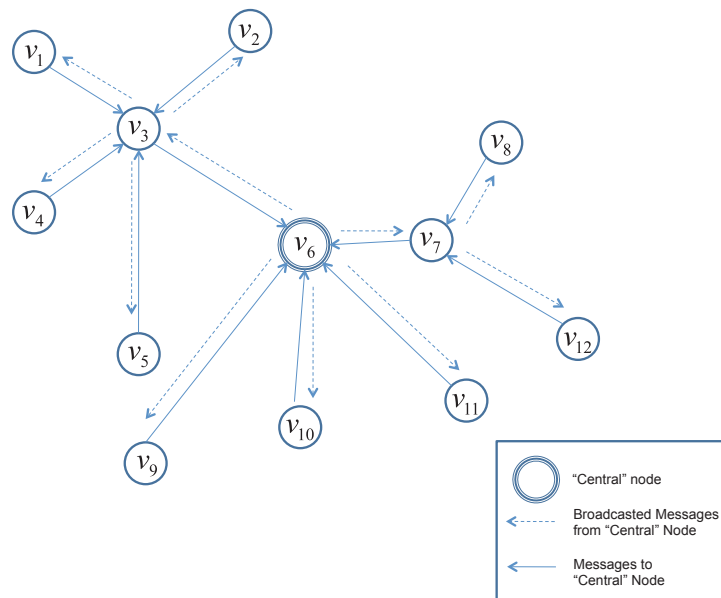
Figure 2.1: Example of a Centralized Framework
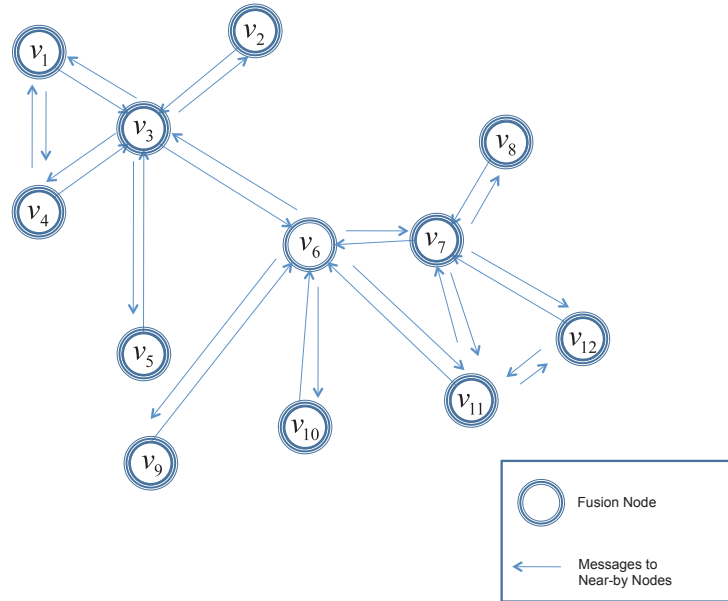
Figure 2.2: Example of a Decentralized Framework
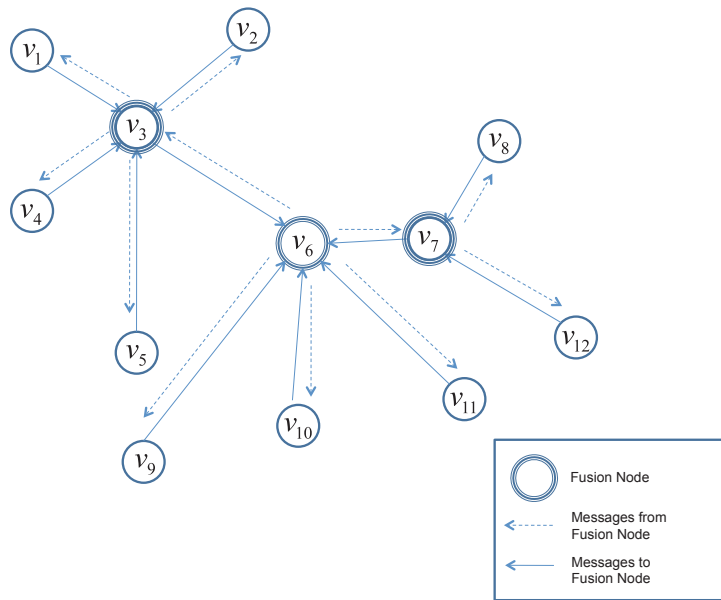
Figure 2.3: Example of a Hierarchical Framework

In a centralized architecture, the information is propagated from node to node in the network until it reaches a "central" node responsible of determining and disseminating expected decisions (e.g., path definition, tasks assignments) to all lower nodes (Figure 2.1). This requires high computational burden at the central node and a robust and reliable communication network that allows virtually perfect information flow (i.e., all relevant information to make decisions is available, uncorrupted and with no delay) among all the agents in the system and the central node.

Decentralized frameworks (Figure 2.2) rely on local (i.e., by each agent) processing of information, including information from nearby agents, and local decision-making. This framework reduces the computational and communication requirements of a centralized framework, allowing scalability of the system to large group sizes [3]. Jameson [12] compared a few distributed architectures based on a set of general requirements for distributed information fusion. In his work, nodes on the network consisted of fusion centers (e.g., command and control center) and/or sensors. For the purpose of this discussion, it is at these fusion nodes where planning and control decisions are made. The first architecture analyzed was the single composite picture implemented by the US Navy in the Cooperative Engagement Capability (CEC) system [13]. This architecture consists of high speed communication links connecting peer nodes. Each node consists of high quality sensors. All nodes in this architecture fuse data using the same algorithm so, given the low latency provided by the network, all nodes maintain virtually the same "fused" picture. A "fused" picture refers to the representation of entities (e.g., targets, assets) in the environment by combining data from multiple sensors. As would be expected, the requirements, particularly on communication bandwidth, to maintain such an accurate and high-speed network are substantial. The grapevine architecture is also a decentralized, peer to peer architecture in which each node is capable of fusing the data collected by local sensors, as well as the data received from peer nodes. At each node, a Grapevine manager is responsible for the interchange of data with peer nodes to mitigate the communication bandwidth requirements on CEC. This manager evaluates the information needs and capabilities of peer nodes and, as data is received, it is propagated to the appropriate node. This is referred to as an intelligent push of data. The Grapevine manager on each node is also responsible to communicate the local information needs to peer nodes. Since the peer nodes will identify information to satisfy those needs, Jameson refers to it as an intelligent pull of data. A similar approach, but from a goal-driven (rather than a data driven) perspective is presented by Perugini et al. [14]. Finally, Jameson describes the Distributed Hierarchical Information Fusion architecture. The nodes on this

network correspond to military units in a command and control hierarchy. Each node is responsible for propagating the collected information to its parent node and child nodes (Figure 2.3). In addition, each node has its local fused picture and a computed fused picture of the nodes it is propagating information to. This proxy fused picture is necessary to avoid fusing repeated information. Since data is propagated only to adjacent nodes, flow of information is faster than in a centralized architecture.

As will be discussed in Section 2.2.2 most planning and control algorithms assumed a centralized framework. When the challenges of a decentralized frameworks are addressed, an architecture such as the one implemented by CEC is usually assumed: each UAV collects information from on-board sensors and, over a low latency network, exchanges information with *neighbor* UAVs (i.e., peer nodes). Information is processed and a trajectory is (re) defined.

2.2.2   Algorithms for Planning and Control Systems

Research in the area of planning and control systems has resulted in the development of algorithms assuming, mostly, a centralized framework [15, 16]: information is collected in a single, "central" node and optimal or near-optimal plans (or re-plans) are defined and communicated to the agents (e.g., UAV) in the system. Just a small fraction of the research on this area has been concerned with the more realistic coordination of resources in a decentralized environment.

Jin, Minai and Polycarpou [17] considered two classes of UAVs, target recognition UAVs and attack UAVs, for the search-and-destroy problem over an area. All UAVs were assumed to have sensors needed for search. A distributed assignment, mediated through centralized mission status information, was developed. At each potential target location (environment was discretized as a set of cells), UAVs can Search, Confirm, Attack, perform Battle Damage Assessment (BDA), or Ignore. A centralized information base kept essential information updated for the coordination of the UAVs. Information include, for each target location, the Target Occupancy Probability (TOP), certainty, task status, and assignment status. In addition, the information base includes state information of each UAV. A set of rules, based on the information contained in the information base, determined the assignment of tasks to UAVs. Each UAV accesses and updates the information base at each step. Two measures of performance were considered to evaluate the proposed algorithm: the time needed to neutralize all a priori known (stationary) targets, and the total number of steps needed

to bring all cells to the Ignore status.

Shetty, Sudit, and Nagi [18] considered the routing of multiple unmanned (combat) vehicles to service multiple potential targets in space. They formulated this as a Mixed-Integer Linear Program (MILP), and decomposed the problem into: (1) the vehicle to target assignment problem, and (2) determining the tour for each vehicle to service their assigned targets. Each problem was solved using a tabu-search heuristic.

A modeling framework for the dynamic rerouting of a set of heterogeneous vehicles was presented by Murray and Karwan in [19]. Vehicles were constrained by fuel- and payload- capacity. The defined MILP maximizes overall mission effectiveness and minimizes changes to the original vehicles' task assignments. Tasks were characterized by priority values, service duration, limits on the minimum and maximum number of resources that may perform them, precedence relationships among tasks, and multiple time windows in which resources may be assigned to the tasks. In addition, tasks were classified as required or optional. Vehicles were characterized by a value indicating the resource's relative capability of performing a task.

A planning algorithm to maximize the visibility of a set of UAVs monitoring multiple moving ground targets in an urban area is discussed by Kim and Crassidis [20]. The shape and location of each urban obstacle (e.g., buildings) were assumed to be known. The algorithm consisted of three main parts: (i) an optimal grouping of (known) targets, and assignment of UAVs to each defined group, (ii) definition of an optimal circular path for each UAV, and (iii) an optimal transition path (i.e., from one circular path to another) for each UAV . Full information was assumed to be shared among all UAVs, in a centralized control framework, for the first two steps of the algorithm.

Several authors [21, 22, 23] have taken an information-theoretic approach to the resource allocation problem. From this perspective, the purpose of the resource management algorithm is to reduce the uncertainty about the environment. McIntyre and Hintz [21] demonstrated the effectiveness of this approach for sensor management on the problem of searching and tracking targets. For this problem, the area of operation was represented as a grid divided into $m \times n$ cells. Information about targets was represented as a discrete probability density function (pdf) on the $m \times n$ area. The pdf represents the sensors' estimate of the location of the targets. Two types of uncertainty where considered on this problem: (i) the location of undetected targets, and (ii) an estimate of the target state vector. The manager decides which sensor to use and whether to continue

tracking a target (already represented as a track) or to search for new ones. When a cell is observed by a sensor, two conditional entropies are computed, $H(X|Y = D)$ and $H(X|Y = ND)$, where D and ND represent detection and no detection, respectively. The amount of information gained was defined as the change in entropy prior to and proceeding a sensor measurement. The information gained by observing a cell on the grid depends on the probability of getting a detection or not. The information gained by updating a (detected) target state vector considers a norm of the respective track's error covariance matrix. The sensor management control algorithm consists of comparing the potential information gain from each sensor and target combination. Once a target is detected, the amount of information gain is computed and a decision on whether to update the track or to search is made. If search was decided, the cell with the highest probability of detecting a target determined where a sensor is aimed. Also using an information-theoretic approach, Kreucher et al. [23] presented their results on a decentralized sensor management algorithm. The sensor actions were determined by maximizing the expected Rényi Divergence, subject to sensors' kinematic and physical constraints. The Rényi Divergence, also known as the α divergence, is a measure of the difference between two probability distributions (i.e., information gain). In the distributed implementation, each node transmits its information to neighbor nodes within a "radius of communication".

Mullen, Avasarala and Hall [24] explored the application of market-based concepts to sensor management in a single-platform. Market-oriented programming refers to the design of a process in which distributed agents determine prices and exchange goods, facilitating a resource allocation mechanism. This approach usually involves an auction mechanism where resource allocation is determined from the bids submitted by agents seeking and selling resources. The authors considered a network of sensors with processing and communication capabilities in a system with multiple, cooperating decision makers. A specialized architecture, the Market Architecture for Sensor Management (MASM), was developed for sensor management. The main components of MASM are the mission manager and sensor manager. The mission manager component evaluates mission-level decisions (e.g., task priorities) and the assignment of tasks to consumer agents. At this component, consumer agents's budgets to accomplish these tasks is also determined. The sensor manager component is responsible for the allocation of sensors to various tasks, schedules and necessary sensor resources (e.g., bandwidth and battery power). Bids for resources include a description of the task (in terms of products) and the minimum acceptable task quality. Bids also include the price consumers are willing to pay for the service. A service chart database captures the products that consumers may

obtain from the measurement made by the sensor. This database include detailed domain information such as sensor's field location and available bandwidth. A *bid formulator* translates the bids using the service chart and submits them to a combinatorial auctioneer module. An auction is conducted to set prices and allocate sensors so that revenue is maximized. The authors use a genetic algorithm to solve this problem. The authors left as future work the extension of their algorithm to distributed sensor systems by incorporating distributed auction design.

Hirsch et al. [9] mathematically formulated the problem of dynamically tracking targets of interest by a set of autonomous UAVs in a centralized cooperative control framework. A decentralized control approach for UAVs with the goal of tracking moving ground targets was developed by Hirsch, Ortiz-Peña and Eck [1]. Targets and UAVs were moving through an urban domain, simulated as a set of buildings. The shape and location of each building was assumed to be known by each UAV. Areas in the urban domain in which an accurate representation of the ground targets was more important were represented by an importance function. This function was modeled as the sum of Gaussian pdfs (each pdf represented an important area). The vehicles operate in a decentralized manner, in which each UAV was responsible to plan its route to maintain an accurate representation of detected targets. A nonlinear optimization problem was defined and solved at each time-step of the duration of the simulation. The Continuous Greedy Randomized Adaptive Search Procedure (GRASP) [25] was utilized to approximately solve this optimization problem. The vehicles were modeled as non-holonomic point masses on a two-dimensional plane with a minimum turning radius (i.e., a Dubins vehicle), and a minimum and maximum speed. Communication among UAVs was restricted to a maximum communication range, beyond which UAVs cannot share information. A minimum distance among UAVs and between buildings was also considered as a collision avoidance mechanism. UAVs were assumed to be flying at a constant altitude, below the height of the buildings. Additional constraints considered in the formulation include line of sight to targets due to the presence of buildings and minimum/maximum detection range. Every UAV operated following its own dynamic feedback loop in which, at each time-step:

1. the UAV moved according to its plan.

2. the UAV sensed the environment with on-board sensors and received measurements from neighbor UAVs on the targets they have been tracking.

3. sensor measurements were fused (i.e., tracks' states representing targets in the environment

were created, updated or deleted).

4. if a new route was needed (based on some criteria on the fused picture, or the time since the
   last route was defined)

   (a) targets' states and neighbor UAVs' routes were predicted over the planning horizon

   (b) a new route was defined by solving the nonlinear optimization problem described above

This dynamic feedback loop is depicted in Figure 2.4.
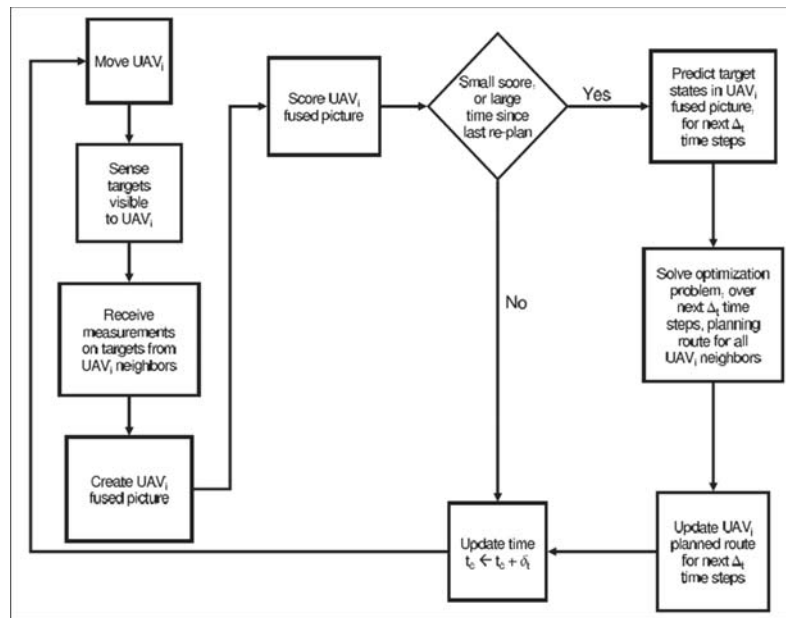
Figure 2.4: Dynamic Feedback Loop Used by Hirsch et al. [1]

In [26], Hirsch, Ortiz-Peña and Sudit studied the effects of this decentralized control ap-
proach for the cooperative tracking of ground targets in an urban environment, as a function of
the number of UAVs. It was shown, experimentally, that the decentralized approach exploits the
availability of multiple UAVs by defining routes that resulted in an accurate representation of the
targets.

In [27], Hirsch and Ortiz-Peña extended their work in [1] by considering the decentralized
control of a set of autonomous UAV consisting of two sets of UAV (determined *a priori*):

1. a set of "Low-level" UAVs responsible of sensing the environment with the goal of accurately
   tracking targets of interest in the urban domain, and

2. a set of "High-level" UAVs responsible of providing the communication back-bone for the autonomous UAVs tracking the targets of interest.

Low-level UAVs were modeled as in [1], with the additional constraint that they could only communicate with high-level UAVs. High level UAVs, also in a decentralized cooperative control framework, maximized the potential communication of the low-level UAVs by planning routes that will keep them within communication range to both, low-level UAVs, and other high-level UAVs. A nonlinear optimization problem was defined and solved (using the GRASP heuristic) at each time-step of the duration of the simulation. This optimization problem maximizes the number of potential direct connections of the UAVs over the planning horizon. High-level UAVs were assumed to be flying at a higher altitude than the low-level UAVs and the buildings. The created communications back-bone by the high-level UAVs is the mechanism by which UAVs shared, with other UAVs, the information on the targets they were tracking.

Another decentralized algorithm for the routing of cooperative UAVs is presented by Shima, Rasmussen and Chandler [3]. UAVs were modeled as a Dubin's vehicle. They considered a set of UAVs performing tasks on a set of targets. The task assignment was performed using an iterative capacitated transshipment problem and auction algorithms. In each iteration, every vehicle computes the cost of performing the available tasks, based on its own information. This information consists of an estimate of its own state (i.e., position and velocity), the teammates' states and its state, as viewed by the teammates. This estimation is based on an information filter and accounts for communication delays. The total accumulated cost for all of the vehicles to perform all of the tasks on all of the targets was used as the cost function. Since each UAV knows the cost function of the members of the group, and an estimate of the teammates' states is being maintained by each UAV, it enables each UAV to estimate the cost of assigning new tasks to all UAVs, allowing a sub optimal decentralized coordination among them.

The multiple vehicle coordination problem in which vehicles pursue private as well as global objectives is considered by Raffard, Tomlin and Boyd [28] from a decentralized perspective. For each vehicle, $i \in \{1, ..., N\}$, x_i and u_i represent the state and control input of vehicle i, respectively. Private objectives were specified by linear equalities on $x_i : A_i x_i = b_i$ and may represent vehicle's fuel consumption minimization or trajectory optimization for a previously specified path, for example. Common objectives, in particular the case of flight formation, were also a set of linear equalities of

the form $y_i - yj = \Delta y_{ij\text{desired}}$. The key quantity of the proposed algorithm is the deviation from common objectives: $d_{ij} = C(x_i - x_j) - \Delta y_{ij}, j \in R(i), i = 1, \ldots, N$, where $R(i)$ represents the set of vehicles which communicate with vehicle i. The proposed decentralized algorithm is derived from the dual decomposition method: each UAV, iteratively, submits its deviation from common objectives to neighbor UAVs, $(d_{ij}, \forall \text{J} \in Ri$, from UAV i's perspective), UAVs recompute their routes, and update their deviation to common objectives; new deviations are submitted again to neighbor UAVs and the process is repeated until the deviations to common objectives converge.

A decentralized policy, the Multi-Vehicle Receding Horizon Median/TSP policy (mRH), is proposed in [29] by Frazzoli and Bullo for the motion coordination of a group of autonomous vehicles. The mRH is defined so the expected waiting time to service stochastically-generated targets is minimized. Letting Q represent the environment as a convex, compact set with unit volume, and m vehicles at positions $P = (p_1, ..., p_m) \in Q$, $V(P, Q)$ is defined as the Voronoi partition of the environment Q and the set P. $P_m^*(Q)$ is referred to the m-median of the set Q. Each vehicle is assumed to have sufficient information to determine: (1) its Voronoi cell, and (2) the locations of outstanding events in its Voronoi cell . The Single-Vehicle Receding Horizon Median/TSP policy (sRH) is proposed to define the path for a single vehicle servicing targets in the set D: when there are no targets to service, the vehicle should move towards $P_1^*(P, Q)$ if $p_1 \neq P_1^*(P, Q)$, otherwise, stop; while D is not empty, a path that maximizes the number of targets reached within τ time units is defined. Under the mRH, each vehicle computes its Voronoi cell $V_i(P, Q)$ and executes the sRH($V_i(P, Q)$), removing all targets already serviced by other vehicles. This process is repeated as new targets might be added to and removed from D.

2.3   Measuring the Cost of Decentralization

Implementation of planning and control algorithms for UAV systems is in most situations, as discussed in 2.2.1, in a decentralized architecture. Given that reality, how can a system designer quantify the potential loss of a system's efficiency when the planning and control system is implemented in a decentralized framework, when it is compared to a centralized implementation? Having a model of the system, we are interested in measuring the effects of the lack of an overall, "central" controller to the optimal value that would be obtained when such a centralized coordination is available. One

measure of this is to quantify the value of the communication links that, if available, would allow the overall system to obtain the same optimal value as a centralized framework. In Section 2.3.1 the concept of *shadow prices* and its interpretation in economic theory as the value of a particular good is presented. In Section 2.3.2 the game theoretic "price of anarchy" is presented. In addition, the price of "fairness" is discussed. Under slightly different assumptions, both are proposed measures to quantify (and bound) the efficiency loss of a system due to the lack of overall coordination of players.

2.3.1   Duality and its Economic Interpretation

Whenever a (primal) resource allocation problem is solved, the (dual) resource valuation problem is solved simultaneously. Following the description in [30], consider $z^* = cx^*$ as the optimal objective function value of a primal Linear Programming (LP) problem, then the dual variable corresponding to the ith constraint (say w_i^*), is the rate of change of the optimal objective value with a unit increase in i^{th} in the right-hand side value, b_i $\left(\text{i.e., } \frac{\partial z^*}{\partial b_i} = w_i^*\right)$.

From LP and economic theory, if the ith constraint represents a demand for production of at least b_i units of the ith product and cx represents the total cost of the production, then w_i^* is the *incremental cost* of producing one more unit of the ith product. The values of the vector w^* are referred to as "shadow prices" and provide an indication of the value of a particular good. These estimates have been used in a variety of applications, including cost-benefit analyses and investment decisions, or as a weighting method for comparing the relative severity of different environmental impacts.

Soest, List and Jeppesen [31] used the concept of "shadow prices" to measure the impact of environmental policies and its relationship to international competitiveness. They assumed that environmental regulation imposes a constraint on a firm's use of polluting inputs (such as energy) either because it artificially reduces firm-level profitability or because it directly imposes a cap on the amount of polluting inputs. One implication is that environmental policies create a gap between the firm's willingness to pay for an additional unit of a polluting input and the input's purchase price. In this case, the value (i.e., the input's shadow price) of the firm's willingness to pay is equivalent to the benefits of using one additional unit that cannot be captured due to the environmental policy constraints. In [32, 33], "shadow prices" were used to provide an indication of the value of water

and the impact on productivity performances.

Examples of the use of "shadow prices" is not limited to applications in the economic sector. Fare, Grosskopf and Weber [34] defined a framework for measuring the shadow prices of nonmarket, undesirable byproducts of some agricultural production process. Xue, Li and Nahrstedt [35] proposed a price-based resource allocation framework for wireless ad hoc networks to achieve optimal resource utilization and fairness by considering the value of data links among competing end-to-end flows. Shadow prices were associated to a wireline link in previous research to reflect the relation between the traffic load of the link and its bandwidth capacity. These results motivated the proposed pricing framework by relating individual links in a wireline network to the notion of maximal cliques in wireless ad hoc networks. A clique refers to a complete subgraph; a maximal clique is a clique that is not contained in any other cliques. A utility function was associated with the end-to-end flow to reflect its resource requirement.

2.3.2   Game Theory and the Price of Anarchy

Game theory is emerging as a popular tool for distributed control of multi-agents systems [5]. It has been applied to a variety of scenarios including, for example, counter-terrorism operations and disaster relief recovery coordination [36]. Theoretical computer scientists used the decentralized systems described by economic game theory to model the Internet [37].

The cost for the lack of coordination was investigated in [38] to quantify the performance lost in the Internet where users act selfishly without an overarching authority regulating network operations. Modeling this network routing problem as a non-cooperative game, the ratio of the worst-case *Nash equilibrium* and the global optimum was proposed as such a measure. A Nash equilibrium is a combination of actions for each agent in the system from which no agent has an incentive to unilaterally change their actions [39]. Mathematically, for a given set N of n-players in a non-cooperative game, where each player $i \in N$ is represented by a strategy vector $x_i \in X_i \subset \mathbb{R}^{m_i}$ (m_i is a positive integer) and a utility function $u_i : X \to \mathbb{R}$, where $X \equiv \prod_{i=1}^{N} X_i$ and $u = (u_1, u_2, u_3, \ldots, u_N)^T$, a Nash equilibrium, $x^* \in X$, could be expressed as

$$u_i \left(x_i^*, x_{-i}^* \right) \geq u_i \left(x_i, x_{-i}^* \right), \quad \forall x_i \in X_i$$

where $x_{-i} = x_{N \setminus \{i\}} = (x_j : j \in N, j \neq i)$

It is known (for example, the Prisoner's Dilemma) that there may be no Nash equilibrium which optimizes overall performance. The Prisoner's Dilemma is a classic example in game theory to describe this situation. It is usually phrased in terms of two crime suspects, Prisoner A and Prisoner B, arrested and interviewed separately. Figure 2.5 shows a typical payoff matrix to describe the Prisoner's Dilemma:

- If Prisoner A confesses and Prisoner B denies, Prisoner A will be convicted for 1 year, while Prisoner B will be convicted for 4 years, and vice versa.

- If both confess, they will both serve a three-years sentence.

- If both deny, they will both serve a two-years sentence.

The best scenario for both prisoners (i.e., Nash equilibrium) is for each of them to deny involvement, earning them the shortest sentence of two-years in prison. But not knowing what the other prisoner intends to do might deter them from denying the crime.

		Prisoner B			
		Confess		Deny	
Prisoner A	Confess	3	3	1	4
	Deny	4	1	2	2

Figure 2.5: Prisoner's Dilemma - By cooperation (both denying) a better result could be obtained than by deciding individually.

Conditions under which the best Nash equilibria can achieve the overall optimum have been studied extensively, mainly with the intent to quantify the effectiveness of approximation algorithms and "on-line" algorithms [37]. The term Price of Anarchy (PoA) was used in [4] to refer to the inefficiency of a system when individuals (i.e., agents) maximize decisions without coordination. Researchers have continued using this term to refer to the efficiency-loss ratio described above.

A general framework for investigating the feasibility of non-cooperative resource allocation and designing desirable utility functions, utilizing a game-theoretic perspective and the concept of *distributed welfare game*, was presented by Marden and Wierman [16]. A *distributed welfare game*

was defined as a non-cooperative resource allocation game with each player's utility function having a specific structure. A *resource allocation game* consists of a set of players $N := \{1, ..., n\}$ and a (finite) set of resources R that are to be shared by the players. Each player $i \in N$ is assigned an action set $A_i \subseteq 2^R$ and a utility function of the form $U_i : A \to \mathbb{R}$. Consider an action profile $a = (a_1, a_2, \ldots, a_n) \in A$. Let a_{-i} denote the profile of player actions *other than* player i. In distributed welfare games, each player's utility function is defined as some portion of the welfare, $W(a)$, and satisfies the following properties:

(i) $U_i(a) \geq 0$

(ii) $\sum_{i \in N} U_i(a) \leq W(a)$

Moreover, separable welfare functions are restricted to the form $W(a) = \sum_{r \in R} W^r(a)$. Consider a distribution rule $f_i(r, a)$ for any player $i \in N$, resource $r \in R$ and action profile $a \in A$, satisfying the following properties:

(i) $f_i(r, a) \geq 0$

(ii) $r \notin a_i \Rightarrow f_i(r, a) = 0$

(iii) $\sum_{i \in N} f_i(r, a) \leq 1$

Then the utility function of each player is restricted to the form $U_i(a_i, a_{-i}) = \sum_{r \in a_i} f_i(r, a) W^r(a)$. Using this definition, the authors explored three different categories of utility functions:

Equally Shared Utilities $U_i(a_i, a_{-i}) = \sum_{r \in a_i} \left(\frac{1}{\sum_j I\{r \in a_j\}} W^r(a) \right)$

Marginal Contribution Utility $U_i(a_i, a_{-i}) = W^r(a_i, a_{-i}) - W^r(a_i^0, a_{-i})$ where a_i^0 is the null (i.e., default) action for player i.

Shapley Value Utility $U_i(a_i, a_{-i}) = \sum_{r \in a_i} Sh_i^r(a^r)$

in which, $Sh_i^r(a^r)$ is referred to as the Shapley value and it is defined as

$$Sh_i^r\left(\tilde{N}\right) = \sum_{S \subseteq \tilde{N} : i \in S} \frac{\left(|\tilde{N}| - 2\right)! \, (|S| - 1)!}{|\tilde{N}|!} \left(W^r(S) - W^r(S \setminus \{i\})\right)$$

The PoA for any distributed welfare game in which players are assigned any of these utility functions is equal to $\frac{1}{2}$.

The Shapley value utility function was also used by Marden and Roughgarden in [5] for the vehicle to target assignment problem. This work was an application of their main research in the area of routing traffic on the Internet, in which users act selfishly without an overarching authority regulating network operations. Roughgarden and Tardos [6] considered a model of selfish routing in which the latency on an edge of the network is a function of the edge congestion, and network users are assumed to selfishly route traffic on minimum latency paths. Using this model, the price of anarchy for linear edge latency functions was determined. Roughgarden [7] extended this work by determining the PoA for a common set of edge latency functions (e.g., quadratic, cubic functions).

Finally, the price of fairness is defined by Bertsimas, Farias and Trichakis [8] as a measure of the relative system efficiency loss under a ''fair'' allocation compared to the one that maximizes the sum of player utilities.

$$POF(U;S) = \frac{SYSTEM(U) - FAIR(U;S)}{SYSTEM(U)}$$

where U is the utility set and S the fairness scheme. Be definition, $SYSTEM(U)$ is the sum of the utilities of the players. The price of fairness is then a value between 0 and 1. Two fairness schemes were discussed in this work: proportional fairness and max-min fairness, which maximizes the minimum utility that all players derive. Although its definition is slightly different and more restrictive than the PoA above, it is of interest in the study of decentralized systems, particularly for cooperative control of UAV systems in which a balance utilization of available resources is of interest. PoA assumes a formulation of the problem as a *non-cooperative game* and, moreover, selfish behavior of players. In the design of decentralized cooperative control algorithms, both approaches should be considered. As will be discussed in Chapter 7, a categorization of UAVs' missions may highlight the applicability of these type of utility functions and criteria on the design of the decentralized systems in order to minimize the efficiency loss when compared to the centralized framework.

Chapter 3

An Entropy-based Relative Rating System for Potential Information Gain

3.1 Introduction

In this chapter, *Potential Information Gain Maps*, or simply Information Gain Maps (IGMs), are defined. An IGM is a characterization of subareas in the Area of Operation (AO) based on its potential to have information about relevant features that may address information deficits for a mission. Relevant features for an information deficit as well as the deficits identified for a mission are assumed to be known. The area of operation is represented as a discrete set of grid cells. A numerical value, its potential information gain, is associated with each cell. When considering an IGM, a higher value represents a higher opportunity to obtain relevant information from a cell in the AO to address one or more deficits. A rating and ranking system is defined to generate IGMs. As will be discussed in Chapter 4, IGMs are a main input to the mathematical programming model for the cooperative control of multiple autonomous vehicles collecting information for a mission.

3.2   Information, Entropy and Other Terms Defined

Information is a very difficult and broad concept to be defined in a single definition [40]. Information theory, for example, is based on probability theory and statistics. For this paradigm, information in a random variable is referred to as *entropy*. Entropy is a measure of the amount of information required on the average (i.e., a measure of the uncertainty) to describe the random variable. Others define *information* as "facts provided or learned about something or someone" [41]. While defining IGMs, both concepts will be applied. A set of facts, or features, are assumed to be related *a priori* to each information deficit. Moreover, the probability of each feature occurring on each subarea of the AO is assumed to be known. This information may be provided by Subject Matter Experts (SMEs) or gathered from a probabilistic framework modeling these features and the conditions in the area of interest.

Mathematically, the entropy $H(X)$ of a discrete random variable X is defined by

$$H(X) = H(p) = -\sum_{x \in X} p(x) \log_2(p(x)) \tag{3.1}$$

For example, the graph of $H(p)$ for the Bernoulli random variable X defined in Equation (3.2) is shown in Figure 3.1.

$$X = \begin{cases} 1 & \text{with probability } p \\ 0 & \text{with probability 1 - } p \end{cases} \tag{3.2}$$

The concept of *entropy* and Equation (3.1) are used in the rating system defined in Section 3.4. Let X_{jk} be a Bernoulli random variable as defined in Equation (3.2) where p_{jk} refers to the probability of feature j be found in cell k. Figure 3.1 provides insights into the benefits of using $H(p)$ as the basis for the rating system. For a particular feature j on cell k:

(1) as $p_{jk} \to 0$, knowledge about feature j on cell k is actually increasing (i.e., it is unlikely that cell k contains information about feature j) so the opportunity to gain information decreases ,

(2) similarly, as $p_{jk} \to 1$, knowledge about feature j on cell k is also increasing (i.e, it is likely that cell k contains information about feature j) so the opportunity to gain information decreases.

Moreover, from [40], $H(p) \geq 0$ and is concave in p, characteristics that will prove beneficial while
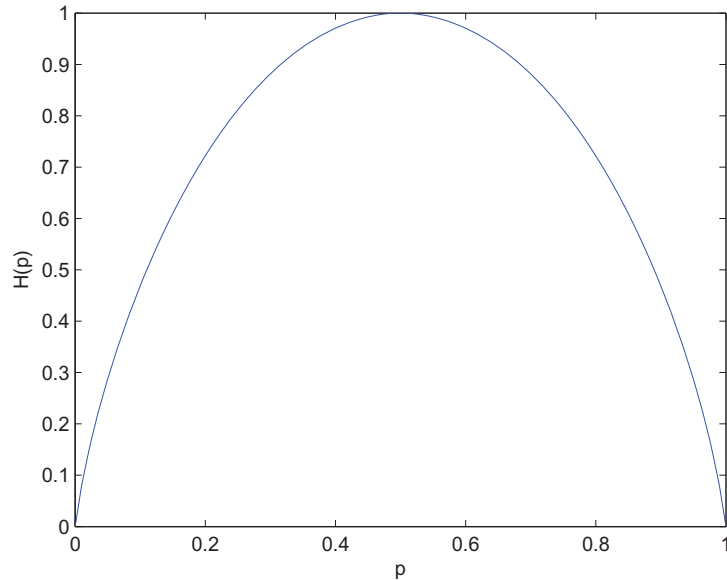
Figure 3.1: Entropy function $H(p)$ for the Bernoulli random variable X

defining the statistics and scoring function for the rating system. In Section 3.3 different rating methods are described. Key to these methods are the scoring mechanism selected to establish the comparison among the items being rated.

3.3   Rating and Ranking Systems

A rating assigns a numerical score to each item in a set. A rating list, when sorted, creates a ranking list [42]. Rating and ranking are everywhere in our daily lives, from presidential elections [42], to sports leagues [43], to information retrieval systems [44]. The ranking system on each of these applications requires a deep understanding of the relevant factors that should be considered to design an effective rating criteria.

In 1997, Massey [45] created a method for ranking college football teams. The fundamental philosophy of this method is summarized by the idea that the difference in the ratings of two teams i and j, ideally, predicts the margin of victory in a game between these two teams. This is represented with the following equation,

$$r_i - r_j = y_k,$$
(3.3)

where y_k is the margin of victory for game k, and r_i and r_j are the rating of teams i and j, respectively. Massey defined a least squares system relating these variables as

$$\mathbf{Mr} = \mathbf{p} \tag{3.4}$$

where $\mathbf{M}$ is the $n \times n$ Massey matrix, $\mathbf{r}$ is the $n \times n$ vector of unknown ratings, and $\mathbf{p}$ is a $n \times 1$ vector of cumulative point differentials. n is the number of teams in the college football league. $\mathbf{M}$ is formed by using the fact that diagonal elements $\mathbf{M}_{ii}$ are the total number of games played by team i and the off-diagonal element $\mathbf{M}_{ij}$, for $i \neq j$, is the negation of the number of games played by team i against team j. Massey's method has been applied in the Bowl Champion Series (BCS) to select the National Collegiate Athletic Association (NCAA) football bowl matchups.

In 2002, Colley [46] wrote about a new method for ranking sports teams. To obtain the Colley rating vector $\mathbf{r}$, the system $\mathbf{Cr} = \mathbf{b}$ is solved, where $\mathbf{C}$ is a $n \times n$ real, symmetric, positive definite matrix. $\mathbf{C}$ is called the Colley matrix and it is defined by

$$C_{ij} = \begin{cases} 2 + t_i, & i = j, \\ -n_{ij} & i \neq i \end{cases}$$

where

t_i is the total number of games played by team i,

n_{ij} is the number of times teams i and j faced each other,

$\mathbf{b}_{n \times 1}$ is the right-hand side vector and $b_i = 1 + \frac{1}{2}(w_i - l_i)$,

w_i is the total number of wins accumulated by team i,

l_i is the total number of losses accumulated by team i, and

n is the number of teams.

Some properties of the Colley method include:

- Ratings are generated using only win-loss information and not point score data. The ratings are considered bias-free as they are unaffected by score differentials.

- The Colley ratings follow a conservation property in which the average of all ratings is $\frac{1}{2}$.

The Massey and the Colley methods are related by the Equation 3.5:

$$\mathbf{C} = \mathbf{2I} + \mathbf{M} \tag{3.5}$$

The reader is referred to [42] for the details of the derivation of this equation.

Keener [47] proposed a rating method relating the rating for a given team to the absolute strength of the team. The strength of a team should be based on its interactions with opponents, together with the strength of these opponents. The rating for each team should be uniformly proportional to the strength of the team. Mathematically, if s_i and r_i are the strength and rating values for team i respectively, then there should be a proportionality constant λ such that $s_i = \lambda r_i$, and λ must have the same value for each team. Keener's method was updated and evaluated as the rating framework to define the relative potential information gain for each information deficit in an IGM.

The concept of entropy has been applied in information retrieval while selecting the words to be used to characterize a document [48]. Given this characterization, relevant documents are identified for a given search query.

3.4   Computing Potential Information Gain Maps

Consider a deficit (or any combination of them) on a mission, consisting of multiple features describing the relevant information to address it. The probability of each feature occurring on each subarea (a cell) of the AO is assumed to be known. The AO is discretized by a number of `rows` $\times$ `columns`. The total number of cells $K =$ `rows` $\times$ `columns`. Each cell in the resulting grid will be indexed as k or k', where $k, k' \in K$ as shown in Figure 3.2. The relative priority of each cell k in the AO to address the information deficits of the mission will be determined. Assuming an information gathering asset can collect information on any cell in the AO, the most uncertain cell about an information deficit provides the highest potential to gather relevant information about that deficit. The defined rating system should then rank this cell highest (and hence have the highest rating) on the list of cells to evaluate while obtaining information about that deficit. Moreover, while aggregating multiple deficits into the computation of the IGM, the rating system should preserve the relative priority of each deficit in the mission.

(rows-1)*cols + 1	(rows-1)*cols + 2	. . .	rows*cols
. . .	. . .	. . .	. . .
(2*cols) + 1	(2*cols) + 2	. . .	3*cols
cols + 1	cols + 2	. . .	2*cols
1	2	. . .	cols

Figure 3.2: Definition of Cell Index k for the Discretization of AO

A tournament in which cells will be ranked based on an assessment of their potential to contain the information requested will be establish to represent an IGM. The concept of *strength* in Keener's method and the rating algorithm defined around it, will be updated and applied to the defined rating system. This rating system will be compared to the Colley' rating method described in Section 3.3 applied to this domain.

Let the value of the statistic when cell k is compared to cell k' be $a_{k,k'}$. Using Keener's proposed definition for this statistic, $a_{k,k'}$ is defined as

$$a_{k,k'} = \frac{S_{k,k'} + 1}{S_{k,k'} + S_{k',k} + 2} \tag{3.6}$$

The key of the rating system is then the definition of $S_{k,k'}$, the score of cell k when compared to cell k'. The defined scoring function is based on the entropy function shown in Figure 3.1. Let this function be represented by $H(p_{jk})$ and defined by Equation (3.1), where p_{jk} refers to the probability that feature j will be found in cell k. Then,

$$S_{k,k'} = (K - 1) \cdot \max \left\{ \sum_{j=1}^{J} w_j \left(H(p_{jk}) - H(p_{jk'}) \right), 0 \right\} \tag{3.7}$$

where w_j is a predefined priority on feature j. Priorities w_j can be defined based on the mission

objectives. J is the total number of features under consideration.

$$w_j \geq 0, \quad \forall j \in J \tag{3.8}$$

$$\sum_{j \in J} w_j = 1 \tag{3.9}$$

As described above, K is the number of cells in the discretized representation of the AO. $S_{k,k'}$ is a measure on the differential in uncertainty between cells k and k'. The defined scoring function in Equation (3.7) meets all constraints required by Keener's method in [47]. These constraints are:

1. **Nonnegativity**. The statistic $a_{k,k'}$ is a nonnegative number so that $\mathbf{A} \geq \mathbf{0}$ is a nonnegative matrix. From Equation (3.6) - Equation (3.9) it is easy to see that this constraint is met.

2. **Irreducibility**. This constraint requires that the items being compared are "connected" by a series of past comparisons involving other items. In the case of a sports tournament for example, not all teams will have the opportunity to play each other. However, this constraint requires a series of games between other teams so a comparison between i and j is possible. For the definition of IGMs, all cells are compared against each other so this constraint is met.

3. **Primitivity**. More restrictive than irreducibility, this constraint requires that all cells are connected by the same number of comparisons. This is equivalent to $\mathbf{A}^p > \mathbf{0}$ for some power p. Similar to the above discussion on irreducibility, there are $K - 1$ comparisons for each cell in the application of this method so this constraint is also met.

Using the $a_{k,k'}$ defined using Equation (3.6) - Equation (3.9), consider the matrix

$$\mathbf{A} = [a_{k,k'}]_{K \times K}, \text{where } K \text{ is the number of cells in the AO.}$$

Assuming r_k is the (so far, unknown) rating of cell k, and using Keener's terminology for strength and rating, the relative strength of cell k compared to cell k' is defined as

$$s_{k,k'} = a_{k,k'} \, r_k$$

The absolute strength of cell k can be defined as

$$s_k = \sum_{k'=1}^{K} s_{k,k'} = \sum_{k'=1}^{K} a_{k,k'} \, r_k$$

Letting $\mathbf{s}$ and $\mathbf{r}$ be the strength and rating vectors, respectively.

$$\mathbf{s} = \begin{pmatrix} \sum_{k=1}^{K} a_{1,k} \, r_k \\ \sum_{k=1}^{K} a_{2,k} \, r_k \\ \vdots \\ \sum_{k=1}^{K} a_{K,k} \, r_k \end{pmatrix} = \begin{pmatrix} a_{1,1} & a_{1,2} & \cdots & a_{1,K} \\ a_{2,1} & a_{2,2} & \cdots & a_{2,K} \\ \vdots & \vdots & \ddots & \vdots \\ a_{K,1} & a_{K,2} & \cdots & a_{K,K} \end{pmatrix} \begin{pmatrix} r_1 \\ r_2 \\ \vdots \\ r_k \end{pmatrix} = \mathbf{Ar}$$

Following the assumption that the rating for each team should be uniformly proportional to the strength of the team,

$$\mathbf{Ar} = \lambda \mathbf{r} \tag{3.10}$$

In [42], Equation (3.10) is referred to as *"the keystone of Keener's method"*. From Equation (3.10), the rating vector $\mathbf{r}$ is then the eigenvector associated with the maximum eigenvalue of $\mathbf{A}$. The rating vector $\mathbf{r}$ is normalized as

$$\tilde{\mathbf{r}} = \mathbf{r} / \sum_{k}^{K} r_k \tag{3.11}$$

$$\bar{\mathbf{r}} = \tilde{\mathbf{r}} / \max_{k \in K} \{\tilde{r}_k\} \tag{3.12}$$

Equation (3.6) - Equation (3.12) constitute the rating method used to compute IGMs. This will be referred to as the *Modified Keener's Method* in this dissertation.

3.5 Results

A mission consisting of 2 information deficits is used to illustrate the computation of IGMs. The mission is over an area represented by a discrete 10×10 grid set. Each information deficit is represented by a set of features: for information deficit 1, two features are being monitored; for information deficit 2, three features are being monitored. For each information deficit, the features are equally weighted in Equation (3.6): $w_1 = w_2 = \frac{1}{2}$ for information deficit 1, $w_1 = w_2 = w_3 = \frac{1}{3}$

for information deficit 2. Table 3.1 and Table 3.2 capture the probabilities of feature 1 and feature 2 from information deficit 1 occurring on each cell of the mission area, respectively. Similarly, Table 3.3, Table 3.4 and Table 3.5 capture the probabilities of feature 1, feature 2 and feature 3 from information deficit 2 occurring on each cell of the mission area, respectively. A heat map of the probabilities for each feature is shown in Figure 3.3 - Figure 3.7.

Table 3.1: Probability of Feature 1 of Information Deficit 1 Occurring in the AO

	1	2	3	4	5	6	7	8	9	10
10	0.0000	0.0000	0.0000	0.0000	0.0000	0.0000	0.0000	0.0000	0.0000	0.0000
9	0.0000	0.0000	0.0000	0.0000	0.0000	0.0000	0.0001	0.0000	0.0000	0.0000
8	0.0000	0.0000	0.0001	0.0002	0.0003	0.0005	0.0005	0.0004	0.0002	0.0001
7	0.0000	0.0001	0.0005	0.0013	0.0025	0.0036	0.0037	0.0027	0.0014	0.0005
6	0.0001	0.0006	0.0024	0.0066	0.0132	0.0188	0.0192	0.0140	0.0074	0.0028
5	0.0004	0.0023	0.0089	0.0247	0.0491	0.0700	0.0715	0.0523	0.0274	0.0103
4	0.0011	0.0061	0.0238	0.0660	0.1312	0.1869	0.1908	0.1395	0.0731	0.0275
3	0.0022	0.0117	0.0455	0.1262	0.2509	0.3574	0.3649	0.2669	0.1399	0.0525
2	0.0030	0.0161	0.0623	0.1729	0.3438	0.4898	0.5000	0.3657	0.1917	0.0720
1	0.0029	0.0158	0.0612	0.1698	0.3376	0.4810	0.4910	0.3591	0.1882	0.0707
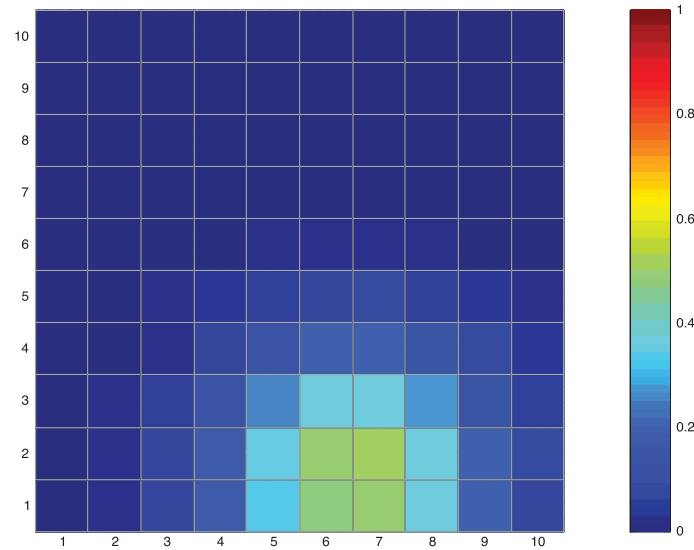
Figure 3.3: Heat Map of Probabilities for Information Deficit 1 - Feature 1 in AO

For this example, three IGMs will be computed:

1. An IGM representing the potential information gain only considering the features of informa-

Table 3.2: Probability of Feature 2 of Information Deficit 1 Occurring in the AO

	1	2	3	4	5	6	7	8	9	10
10	0.0006	0.0041	0.0210	0.0765	0.1996	0.3732	0.5000	0.4800	0.3301	0.1627
9	0.0005	0.0039	0.0198	0.0720	0.1879	0.3513	0.4706	0.4517	0.3107	0.1531
8	0.0004	0.0026	0.0133	0.0486	0.1267	0.2369	0.3174	0.3046	0.2095	0.1033
7	0.0002	0.0013	0.0064	0.0235	0.0612	0.1145	0.1534	0.1472	0.1013	0.0499
6	0.0001	0.0004	0.0022	0.0081	0.0212	0.0396	0.0531	0.0510	0.0351	0.0173
5	0.0000	0.0001	0.0006	0.0020	0.0053	0.0098	0.0132	0.0126	0.0087	0.0043
4	0.0000	0.0000	0.0001	0.0004	0.0009	0.0017	0.0023	0.0022	0.0015	0.0008
3	0.0000	0.0000	0.0000	0.0000	0.0001	0.0002	0.0003	0.0003	0.0002	0.0001
2	0.0000	0.0000	0.0000	0.0000	0.0000	0.0000	0.0000	0.0000	0.0000	0.0000
1	0.0000	0.0000	0.0000	0.0000	0.0000	0.0000	0.0000	0.0000	0.0000	0.0000
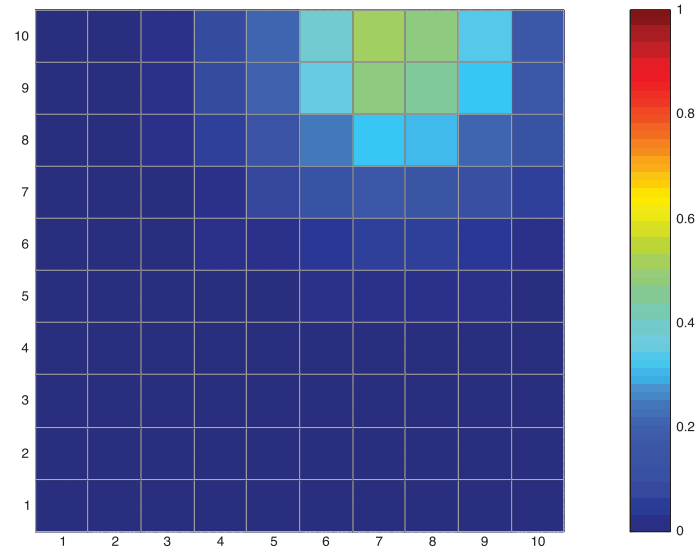
Figure 3.4: Heat Map of Probabilities Information Deficit 1 - Feature 2 in AO

tion deficit 1.

2. An IGM representing the potential information gain only considering the features of informa-
   tion deficit 2.

3. An IGM representing the potential information gain aggregating both information deficit 1
   and information deficit 2.

IGMs are represented as heat maps as a visualization aid of the resulting rating.

The priority of the different information deficits to the mission may vary. The case of

Table 3.3: Probability of Feature 1 of Information Deficit 2 Occurring in the AO

10	0.0001	0.0007	0.0026	0.0069	0.0130	0.0177	0.0173	0.0120	0.0060	0.0022
9	0.0005	0.0027	0.0098	0.0261	0.0495	0.0673	0.0656	0.0458	0.0229	0.0082
8	0.0014	0.0072	0.0268	0.0710	0.1347	0.1831	0.1784	0.1246	0.0623	0.0223
7	0.0027	0.0141	0.0523	0.1384	0.2627	0.3572	0.3481	0.2430	0.1216	0.0436
6	0.0038	0.0198	0.0731	0.1935	0.3672	0.4993	0.4865	0.3396	0.1699	0.0609
5	0.0038	0.0198	0.0732	0.1938	0.3677	0.5000	0.4872	0.3401	0.1701	0.0610
4	0.0028	0.0142	0.0525	0.1390	0.2639	0.3588	0.3496	0.2441	0.1221	0.0438
3	0.0014	0.0073	0.0270	0.0715	0.1357	0.1845	0.1797	0.1255	0.0628	0.0225
2	0.0005	0.0027	0.0099	0.0263	0.0500	0.0680	0.0662	0.0462	0.0231	0.0083
1	0.0001	0.0007	0.0026	0.0070	0.0132	0.0179	0.0175	0.0122	0.0061	0.0022
	1	**2**	**3**	**4**	**5**	**6**	**7**	**8**	**9**	**10**
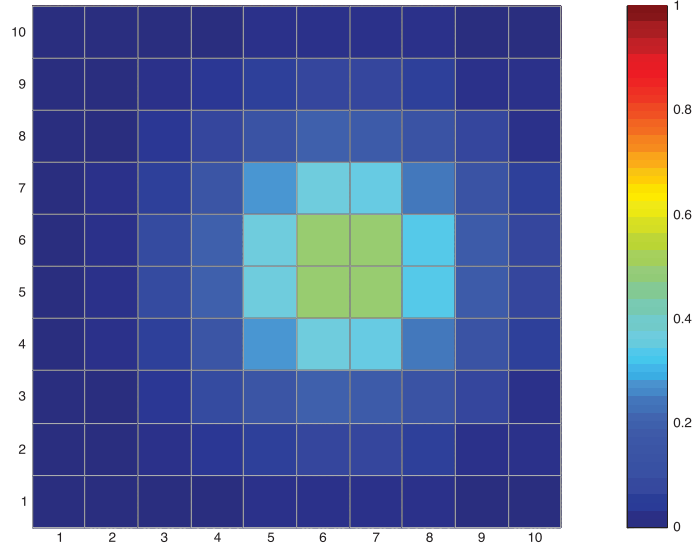
Figure 3.5: Heat Map of Probabilities Information Deficit 2 - Feature 1 in AO

equally weighted deficits as well as cases where the deficits are weighted differently is presented below. To represent this case, let w_j in Equation (3.6) be updated to w_{j_i} where j_i refers to feature j characterizing information deficit i. $w_{j_i} = w_j * \bar{w}_i$ where w_j remains the priority of feature j and $\bar{w}_i$ is a weighting parameter on information deficit i when it is aggregated with other information deficits in an IGM. Note that weighting parameter $\bar{w}_i$ may represent the relative importance of gathering information about deficit i for the mission. Let I be the set of information deficits being aggregated into the IGM

$$\bar{w}_i \geq 0, \quad \forall i \in I \tag{3.13}$$

Table 3.4: Probability of Feature 2 of Information Deficit 2 Occurring in the AO

	1	2	3	4	5	6	7	8	9	10
10	0.0000	0.0000	0.0000	0.0000	0.0000	0.0000	0.0000	0.0000	0.0000	0.0000
9	0.0000	0.0000	0.0000	0.0000	0.0000	0.0001	0.0002	0.0003	0.0003	0.0003
8	0.0000	0.0000	0.0000	0.0001	0.0003	0.0009	0.0017	0.0025	0.0026	0.0020
7	0.0000	0.0000	0.0001	0.0004	0.0017	0.0047	0.0096	0.0140	0.0146	0.0109
6	0.0000	0.0000	0.0003	0.0017	0.0066	0.0186	0.0379	0.0552	0.0576	0.0430
5	0.0000	0.0001	0.0009	0.0047	0.0186	0.0528	0.1072	0.1561	0.1629	0.1218
4	0.0000	0.0002	0.0017	0.0095	0.0377	0.1070	0.2175	0.3167	0.3304	0.2470
3	0.0000	0.0003	0.0025	0.0139	0.0548	0.1555	0.3161	0.4602	0.4802	0.3590
2	0.0000	0.0003	0.0026	0.0144	0.0571	0.1620	0.3291	0.4792	0.5000	0.3738
1	0.0000	0.0003	0.0019	0.0108	0.0426	0.1208	0.2456	0.3576	0.3731	0.2789
	1	**2**	**3**	**4**	**5**	**6**	**7**	**8**	**9**	**10**
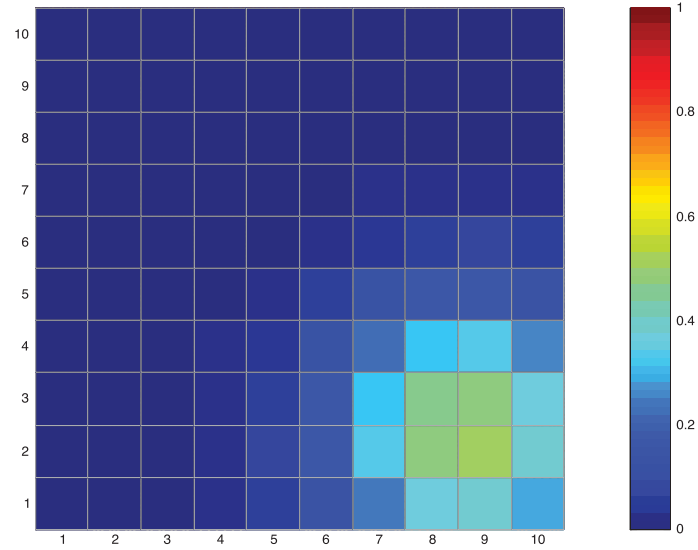
Figure 3.6: Heat Map of Probabilities Information Deficit 2 - Feature 2 in AO

$$\sum_{i \in I} \bar{w}_i = 1 \qquad (3.14)$$

The Modified Keener's method (i.e., Equation 3.6 - Equation 3.14) will be used to define the IGMs. The resulting IGMs will be compared to the rating obtained while using Colley's method described in Section 3.3. For the Colley's rating method, the following values were defined:

K = number of cells = 100

t_k = total number of cells compared to cell $k = K - 1$

$n_{k,kp}$ = number of times cells k and k' were compared to each other = number of features

Table 3.5: Probability of Feature 3 of Information Deficit 2 Occurring in the AO

10	0.0001	0.0007	0.0040	0.0168	0.0501	0.1071	0.1641	0.1801	0.1417	0.0798
9	0.0002	0.0014	0.0079	0.0329	0.0983	0.2101	0.3219	0.3533	0.2778	0.1566
8	0.0002	0.0019	0.0111	0.0463	0.1381	0.2953	0.4524	0.4965	0.3905	0.2200
7	0.0002	0.0019	0.0112	0.0466	0.1391	0.2974	0.4555	0.5000	0.3932	0.2216
6	0.0002	0.0014	0.0081	0.0336	0.1004	0.2146	0.3287	0.3608	0.2837	0.1599
5	0.0001	0.0007	0.0042	0.0174	0.0519	0.1109	0.1699	0.1865	0.1467	0.0827
4	0.0000	0.0003	0.0015	0.0064	0.0192	0.0411	0.0630	0.0691	0.0543	0.0306
3	0.0000	0.0001	0.0004	0.0017	0.0051	0.0109	0.0167	0.0183	0.0144	0.0081
2	0.0000	0.0000	0.0001	0.0003	0.0010	0.0021	0.0032	0.0035	0.0027	0.0015
1	0.0000	0.0000	0.0000	0.0000	0.0001	0.0003	0.0004	0.0005	0.0004	0.0002
	1	**2**	**3**	**4**	**5**	**6**	**7**	**8**	**9**	**10**
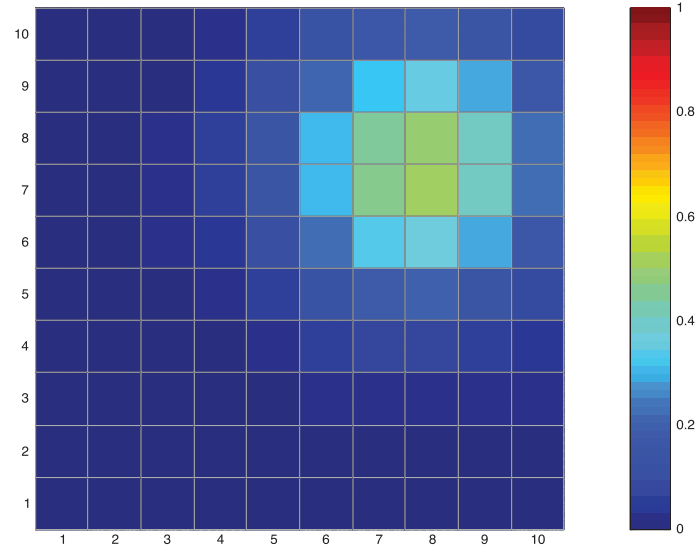
Figure 3.7: Heat Map of Probabilities Information Deficit 2 - Feature 3 in AO

$Sc_{k,k',j} = H(p_{jk}) - H(p_{jk'}) =$ scoring function based on the difference of entropy values on cell k and k', for feature j

$w_k =$ number of times $Sc(k, k', j) > 0$

$l_k =$ number of times $Sc(k, k', j) < 0$

Note that different scoring functions $Sc(k, k', j)$ for Colley's method could be defined to compare the cells in the AO. All IGMs were computed using `MATLAB R2011B` [49].

Table 3.6 shows the resulting potential information gain values for the IGM of information

deficit 1 applying the Modified Keener's and Colley's methods. Figure 3.8 shows the IGM representing the potential information gain for information deficit 1 using the Modified Keener's method. Similarly, Figure 3.9 shows the IGM representing the potential information gain for information deficit 1 using Colley's method.
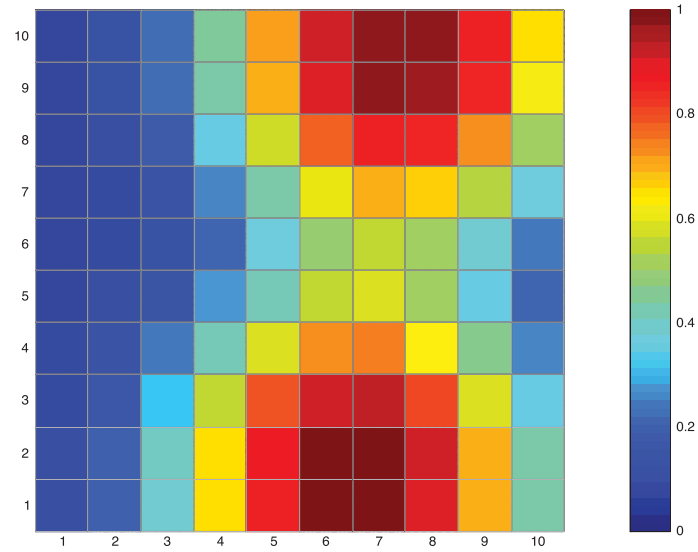
Figure 3.8: Information Gain Map for Information Deficit 1 Using Modified Keener's Method
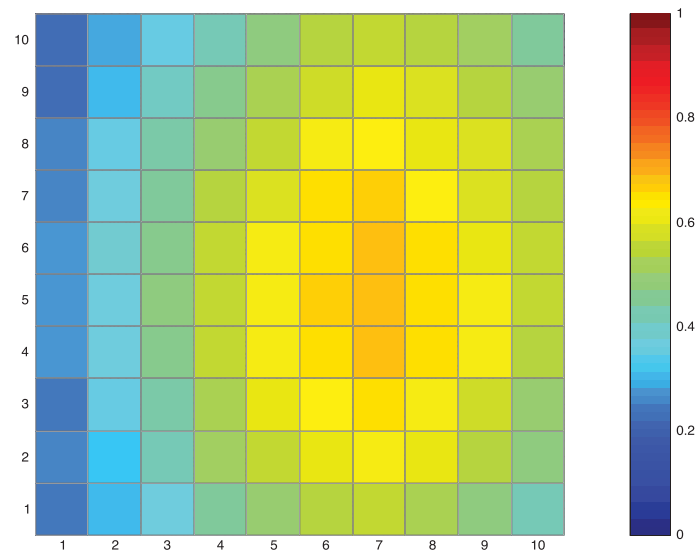
Figure 3.9: Information Gain Map for Information Deficit 1 Using Colley's Method

Table 3.6: Potential Information Gain for Information Deficit 1

	IGM Value			IGM Value	
Cell	Modified Keener's Method	Colley's Method	**Cell**	Modified Keener's Method	Colley's Method
1	0.0917	0.2376	51	0.0638	0.2673
2	0.1849	0.3020	52	0.0747	0.3812
3	0.3848	0.3713	53	0.1143	0.4604
4	0.6498	0.4406	54	0.2085	0.5495
5	0.8794	0.4950	55	0.3575	0.6188
6	0.9968	0.5396	56	0.4965	0.6535
7	0.9983	0.5594	57	0.5635	0.6782
8	0.9112	0.5297	58	0.5133	0.6535
9	0.6909	0.4802	59	0.3814	0.6089
10	0.4231	0.4109	60	0.2385	0.5495
11	0.0922	0.2525	61	0.0643	0.2574
12	0.1867	0.3218	62	0.0791	0.3614
13	0.3896	0.4059	63	0.1338	0.4505
14	0.6573	0.5000	64	0.2589	0.5347
15	0.8889	0.5495	65	0.4356	0.5941
16	0.9991	0.6040	66	0.6007	0.6436
17	1.0000	0.6238	67	0.6951	0.6683
18	0.9223	0.5990	68	0.6631	0.6337
19	0.7004	0.5446	69	0.5348	0.5891
20	0.4289	0.4703	70	0.3621	0.5396
21	0.0846	0.2376	71	0.0666	0.2475
22	0.1592	0.3515	72	0.0926	0.3416
23	0.3230	0.4307	73	0.1791	0.4356
24	0.5581	0.5248	74	0.3505	0.4950
25	0.7872	0.5990	75	0.5749	0.5545
26	0.9179	0.6337	76	0.7803	0.6139
27	0.9318	0.6535	77	0.8768	0.6337
28	0.8121	0.6238	78	0.8535	0.6040
29	0.5939	0.5743	79	0.7363	0.5842
30	0.3520	0.4901	80	0.5146	0.5198
31	0.0743	0.2673	81	0.0689	0.2178
32	0.1195	0.3663	82	0.1053	0.3069
33	0.2314	0.4604	83	0.2195	0.3960
34	0.4126	0.5495	84	0.4316	0.4653
35	0.5902	0.6188	85	0.6935	0.5297
36	0.7298	0.6584	86	0.9047	0.5792
37	0.7508	0.6881	87	0.9825	0.5990
38	0.6354	0.6535	88	0.9752	0.5842
39	0.4628	0.6188	89	0.8505	0.5446
40	0.2615	0.5446	90	0.6221	0.4901
41	0.0666	0.2624	91	0.0693	0.2178
42	0.0874	0.3614	92	0.1076	0.2822
43	0.1481	0.4752	93	0.2269	0.3515
44	0.2648	0.5594	94	0.4459	0.4158
45	0.4162	0.6188	95	0.7140	0.4802
46	0.5530	0.6683	96	0.9248	0.5347
47	0.5909	0.6881	97	0.9847	0.5594
48	0.5052	0.6485	98	0.9827	0.5396
49	0.3526	0.6188	99	0.8775	0.5000
50	0.2023	0.5495	100	0.6454	0.4505

Two clusters of high potential information gain are recognized from Figure 3.8: (1) around cells 87, 88, 97 and 98, and (2) around cells 6, 7, 16 and 17. These cells are the most uncertain cells from the features characterizing information deficit 1 (see Table 3.1 and Table 3.2). Note that for this case, the rating defined by Colley's method identifies an area of relatively high value cells (rating > 0.60) for this IGM, between the two areas of the most uncertain cells. However, although the area with relatively high potential gain value extends to the areas most uncertain of this information deficit, it does not rate cells 6, 7, 16, 17, 87, 88, 97 and 98 as high.

Table 3.7 shows the resulting potential information gain values for the IGM of information deficit 2 applying the Modified Keener's and Colley's methods. Figure 3.10 shows the IGM representing the potential information gain for information deficit 2 using Keener's method. Similarly, Figure 3.11 shows the IGM representing the potential information gain for information deficit 2 using Colley's method.
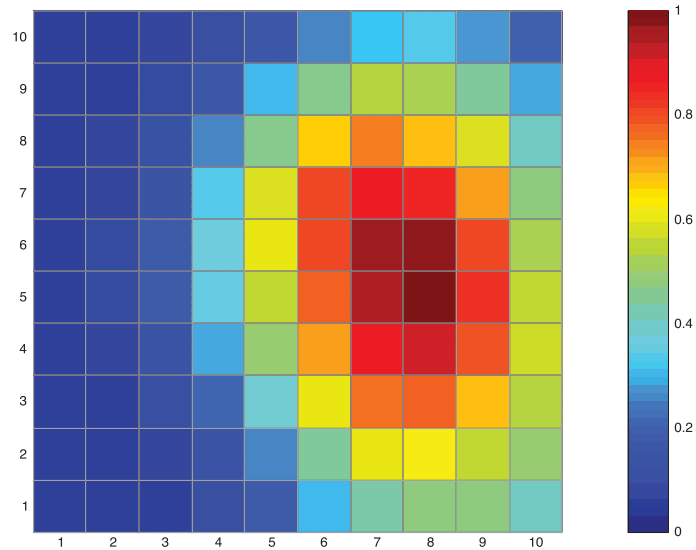
Figure 3.10: Information Gain Map for Information Deficit 2 Using Modified Keener's Method
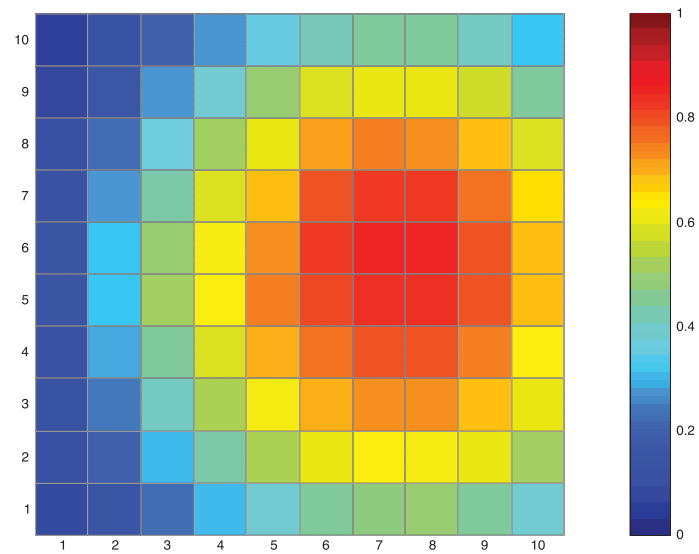
Figure 3.11: Information Gain Map for Information Deficit 2 Using Colley's Method

Table 3.7: Potential Information Gain for Information Deficit 2

Cell	IGM Value Modified Keener's Method	Colley's Method	Cell	IGM Value Modified Keener's Method	Colley's Method
1	0.0405	0.0745	51	0.0474	0.1407
2	0.0427	0.1407	52	0.0764	0.3129
3	0.0536	0.2169	53	0.1756	0.4884
4	0.0904	0.2964	54	0.3704	0.6142
5	0.1737	0.3791	55	0.6066	0.7334
6	0.2983	0.4520	56	0.8168	0.8262
7	0.4210	0.4818	57	0.9616	0.8526
8	0.4832	0.4884	58	0.9812	0.8493
9	0.4690	0.4520	59	0.8150	0.7964
10	0.4008	0.3758	60	0.5290	0.6805
11	0.0413	0.0977	61	0.0457	0.1308
12	0.0465	0.1970	62	0.0685	0.2666
13	0.0675	0.2997	63	0.1494	0.4354
14	0.1318	0.4321	64	0.3319	0.5877
15	0.2613	0.5182	65	0.5895	0.6838
16	0.4428	0.6043	66	0.8077	0.7897
17	0.5975	0.6308	67	0.8955	0.8195
18	0.6157	0.6242	68	0.8503	0.8195
19	0.5625	0.5977	69	0.7091	0.7599
20	0.4846	0.5050	70	0.4747	0.6474
21	0.0428	0.1109	71	0.0434	0.0911
22	0.0538	0.2334	72	0.0576	0.2169
23	0.0955	0.4023	73	0.1117	0.3692
24	0.2009	0.5315	74	0.2464	0.5083
25	0.3831	0.6242	75	0.4638	0.6043
26	0.6028	0.6937	76	0.6677	0.7070
27	0.7693	0.7268	77	0.7432	0.7401
28	0.7720	0.7368	78	0.6857	0.7334
29	0.6830	0.6904	79	0.5835	0.6871
30	0.5458	0.6010	80	0.3968	0.5811
31	0.0452	0.1341	81	0.0416	0.0613
32	0.0648	0.2798	82	0.0491	0.1573
33	0.1323	0.4454	83	0.0776	0.2666
34	0.2820	0.5844	84	0.1554	0.3825
35	0.4945	0.6970	85	0.2949	0.4917
36	0.7155	0.7599	86	0.4577	0.5844
37	0.8922	0.7997	87	0.5422	0.6109
38	0.9259	0.7997	88	0.5238	0.6043
39	0.7993	0.7467	89	0.4375	0.5646
40	0.5743	0.6374	90	0.2935	0.4520
41	0.0472	0.1474	91	0.0406	0.0414
42	0.0749	0.3195	92	0.0436	0.1109
43	0.1679	0.5017	93	0.0570	0.1838
44	0.3461	0.6341	94	0.0934	0.2666
45	0.5628	0.7434	95	0.1627	0.3460
46	0.7722	0.8063	96	0.2525	0.4089
47	0.9490	0.8460	97	0.3223	0.4387
48	1.0000	0.8394	98	0.3289	0.4387
49	0.8456	0.7864	99	0.2694	0.3924
50	0.5628	0.6805	100	0.1880	0.3195

The IGM generated using the modified Keener's method for information deficit 2 rated cells 47 and 57 as the highest. This cluster, including the adjacent cells, correspond to the most uncertain cells of features 1 and 3 on information deficit 2. A rating greater than 0.60 was assigned to cells where feature 2 was most uncertain, a relatively high potential information gain but not as high as the cells were information collection could address multiple features. Similar for information deficit 1, a single cluster of high potential gain around the uncertain areas of the features of information deficit 2 is recognized by Colley's method.

For the third case, information deficits were combined into a single IGM to obtain an overall representation of the potential information gain for the mission. First, both deficits were equally weighted (i.e., $\bar{w}_1 = \bar{w}_2 = 0.5$). Table 3.8 shows the resulting potential information gain values for this IGM applying Modified Keener's and Colley's methods. For this case, areas of high potential information gain from the IGM for information deficit 1 (Figure 3.8) are expected to also be highlighted when the combined IGM is computed. Similarly, the areas of high potential information gain from the IGM for information deficit 2 (Figure 3.10) are also expected to be highlighted in the IGM in which all deficits are considered simultaneously. From Figure 3.12, the IGM generated by the rating system leveraging Keener's method clearly identifies the two areas ((1) around cell 77 and (2) around cell 27) where gain for individual deficits were identified. A third area between these two high potential information gain is also recognized from Figure 3.12. Ratings from Colley's method concentrated the potential information gain from all features evaluated around this area (Figure 3.13). However, even this rating is not as high as any of the ratings obtained in the three main areas identified from the Modified Keener's Method. The ability to rank highest all the cells with relatively high potential information gain from all the features considered is an important characteristic of IGMs since, as the basis for the routing of collection assets maximizing information gain, preserving the potential gain for all deficits that could be addressed by the same sensor capabilities (e.g., imagery, signals, etc.) is key. This will be described in detail in Chapter 4.
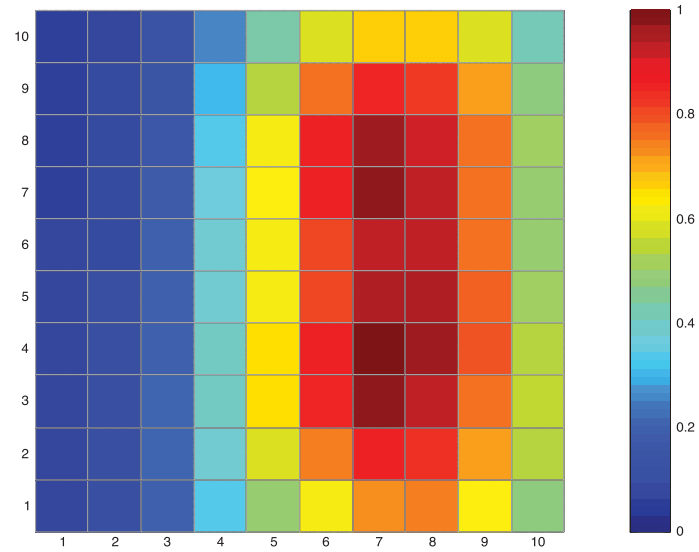
Figure 3.12: Information Gain Map for Information Deficits 1,2 Using Modified Keener's Method
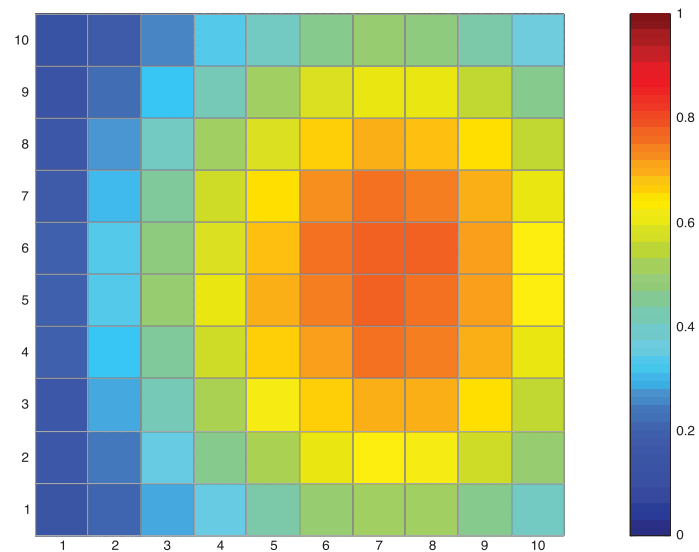
Figure 3.13: Information Gain Map for Information Deficits 1,2 Using Colley's Method

Table 3.8: Potential Information Gain for Combination of Equally Weighted Information Deficits

| Cell | IGM Value | | Cell | IGM Value | |
	Modified Keener's Method	Colley's Method		Modified Keener's Method	Colley's Method
1	0.0649	0.1384	51	0.0572	0.1902
2	0.1110	0.2042	52	0.0836	0.3396
3	0.2204	0.2779	53	0.1761	0.4771
4	0.3918	0.3536	54	0.3608	0.5886
5	0.5622	0.4253	55	0.5875	0.6882
6	0.6844	0.4871	56	0.7797	0.7580
7	0.7736	0.5129	57	0.8973	0.7839
8	0.7779	0.5050	58	0.8857	0.7719
9	0.6516	0.4631	59	0.7167	0.7221
10	0.4709	0.3894	60	0.4596	0.6285
11	0.0657	0.1584	61	0.0562	0.1803
12	0.1146	0.2460	62	0.0792	0.3038
13	0.2340	0.3416	63	0.1642	0.4412
14	0.4318	0.4592	64	0.3549	0.5667
15	0.6416	0.5309	65	0.6204	0.6484
16	0.8008	0.6046	66	0.8528	0.7321
17	0.9022	0.6285	67	0.9569	0.7600
18	0.8761	0.6145	68	0.9100	0.7460
19	0.7175	0.5767	69	0.7385	0.6922
20	0.5258	0.4910	70	0.4814	0.6046
21	0.0633	0.1604	71	0.0557	0.1524
22	0.1061	0.2799	72	0.0768	0.2659
23	0.2230	0.4133	73	0.1562	0.3954
24	0.4348	0.5289	74	0.3421	0.5030
25	0.6860	0.6145	75	0.6254	0.5847
26	0.8920	0.6703	76	0.8846	0.6703
27	1.0000	0.6982	77	0.9858	0.6982
28	0.9380	0.6922	78	0.9341	0.6823
29	0.7449	0.6444	79	0.7720	0.6464
30	0.5295	0.5568	80	0.5148	0.5568
31	0.0602	0.1863	81	0.0556	0.1225
32	0.0951	0.3137	82	0.0766	0.2161
33	0.2025	0.4512	83	0.1511	0.3177
34	0.4097	0.5707	84	0.3195	0.4153
35	0.6610	0.6663	85	0.5716	0.5070
36	0.8694	0.7201	86	0.8054	0.5827
37	0.9862	0.7560	87	0.8958	0.6066
38	0.9448	0.7420	88	0.8716	0.5966
39	0.7549	0.6962	89	0.7457	0.5568
40	0.5088	0.6006	90	0.5089	0.4671
41	0.0583	0.1922	91	0.0552	0.1106
42	0.0882	0.3357	92	0.0743	0.1783
43	0.1877	0.4910	93	0.1407	0.2500
44	0.3775	0.6046	94	0.2822	0.3257
45	0.6014	0.6942	95	0.4808	0.3994
46	0.7903	0.7520	96	0.6552	0.4592
47	0.9141	0.7839	97	0.7325	0.4871
48	0.9048	0.7639	98	0.7311	0.4791
49	0.7308	0.7201	99	0.6367	0.4353
50	0.4752	0.6285	100	0.4482	0.3715

Figure 3.14 shows an IGM where information deficit 1 and 2 were combined with the following weighting: $\bar{w}_1 = \frac{3}{4}$ and $\bar{w}_2 = \frac{1}{4}$. Table 3.9 shows the resulting potential information gain values for this IGM applying the Modified Keener's method. Figure 3.15 also shows an IGM of information deficit 1 and 2 combined, but with a different weighting: $\bar{w}_1 = \frac{1}{4}$ and $\bar{w}_2 = \frac{3}{4}$. Table 3.10 shows the resulting potential information gain values for this IGM applying the Modified Keener's method. For the case in which $\bar{w}_1 > \bar{w}_2$, the resulting IGM is very similar to the IGM generated when only the features of information deficit 1 were considered (Figure 3.8) and two high potential gain areas are identified. Rating of cells increased due to contributions of the features of information deficit 2. Following the same pattern, for the case in which $\bar{w}_1 < \bar{w}_2$, the resulting IGM is very similar to the IGM generated when only the features of information deficit 2 were considered. The high potential information gain area identified in Figure 3.10 is extended north and south due to the uncertainty of the features of information deficit 1 on cells 27, 28, 89 and 90.
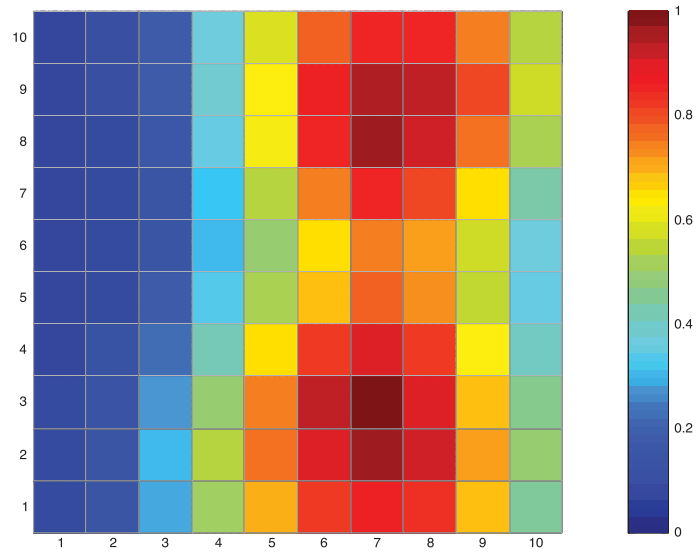
Figure 3.14: Information Gain Map for Information Deficit 1 and 2, with $w_1 = \frac{3}{4}$ and $w_2 = \frac{1}{4}$, using Modified Keener's Method

Table 3.9: Potential Information Gain for the Weighted Combination of Information Deficit 1, $\bar{w}_1 = \frac{3}{4}$ and Information Deficit 2, $\bar{w}_2 = \frac{1}{4}$

Cell	IGM Value Modified Keener's Method	Cell	IGM Value Modified Keener's Method
1	0.0755	51	0.0591
2	0.1428	52	0.0789
3	0.2925	53	0.1486
4	0.5091	54	0.2942
5	0.7037	55	0.4859
6	0.8178	56	0.6532
7	0.8763	57	0.7480
8	0.8451	58	0.7189
9	0.6747	59	0.5654
10	0.4517	60	0.3583
11	0.0762	61	0.0587
12	0.1458	62	0.0782
13	0.3032	63	0.1500
14	0.5380	64	0.3125
15	0.7598	65	0.5427
16	0.8977	66	0.7515
17	0.9614	67	0.8550
18	0.9132	68	0.8144
19	0.7174	69	0.6552
20	0.4861	70	0.4281
21	0.0715	71	0.0594
22	0.1287	72	0.0827
23	0.2697	73	0.1659
24	0.4985	74	0.3486
25	0.7471	75	0.6141
26	0.9291	76	0.8594
27	1.0000	77	0.9687
28	0.9054	78	0.9277
29	0.6876	79	0.7696
30	0.4567	80	0.5182
31	0.0653	81	0.0604
32	0.1050	82	0.0882
33	0.2161	83	0.1814
34	0.4169	84	0.3738
35	0.6479	85	0.6374
36	0.8273	86	0.8696
37	0.9034	87	0.9573
38	0.8257	88	0.9393
39	0.6299	89	0.8080
40	0.4011	90	0.5666
41	0.0609	91	0.0603
42	0.0870	92	0.0878
43	0.1706	93	0.1786
44	0.3313	94	0.3579
45	0.5269	95	0.5908
46	0.6889	96	0.7806
47	0.7737	97	0.8526
48	0.7295	98	0.8507
49	0.5623	99	0.7494
50	0.3532	100	0.5399

Table 3.10: Potential Information Gain for the Weighted Combination of Information Deficit 1, $\bar{w}_1 = \frac{1}{4}$ and information deficit 2, $\bar{w}_2 = \frac{3}{4}$

Cell	IGM Value Modified Keener's Method	Cell	IGM Value Modified Keener's Method
1	0.0534	51	0.0536
2	0.0773	52	0.0837
3	0.1397	53	0.1880
4	0.2500	54	0.3910
5	0.3833	55	0.6331
6	0.5109	56	0.8394
7	0.6236	57	0.9730
8	0.6593	58	0.9782
9	0.5847	59	0.8061
10	0.4556	60	0.5232
11	0.0542	61	0.0521
12	0.0812	62	0.0766
13	0.1541	63	0.1664
14	0.2943	64	0.3656
15	0.4737	65	0.6407
16	0.6490	66	0.8747
17	0.7812	67	0.9729
18	0.7766	68	0.9243
19	0.6667	69	0.7591
20	0.5252	70	0.5008
21	0.0539	71	0.0507
22	0.0809	72	0.0688
23	0.1642	73	0.1392
24	0.3346	74	0.3098
25	0.5633	75	0.5772
26	0.7821	76	0.8216
27	0.9218	77	0.9111
28	0.8925	78	0.8532
29	0.7444	79	0.7101
30	0.5596	80	0.4755
31	0.0537	81	0.0497
32	0.0821	82	0.0637
33	0.1757	83	0.1162
34	0.3661	84	0.2458
35	0.6099	85	0.4571
36	0.8320	86	0.6679
37	0.9823	87	0.7572
38	0.9795	88	0.7321
39	0.8153	89	0.6206
40	0.5704	90	0.4160
41	0.0540	91	0.0489
42	0.0849	92	0.0596
43	0.1893	93	0.0996
44	0.3860	94	0.1923
45	0.6168	95	0.3361
46	0.8218	96	0.4783
47	0.9764	97	0.5557
48	1.0000	98	0.5567
49	0.8320	99	0.4751
50	0.5520	100	0.3284
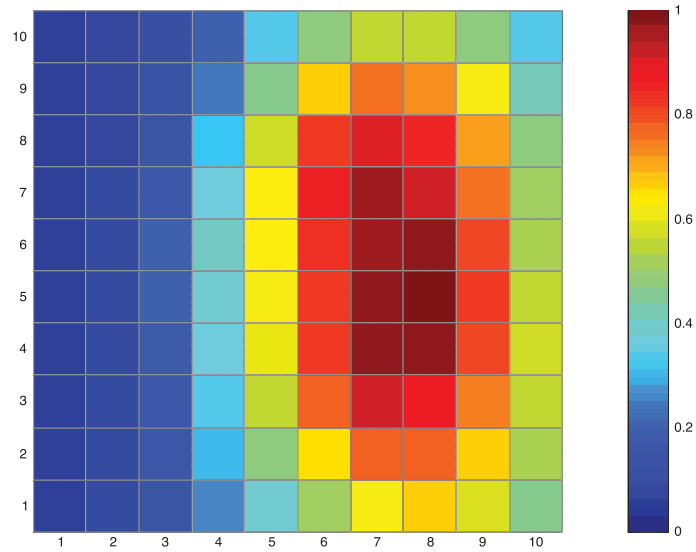
Figure 3.15: Information Gain Map for Information Deficit 1 and 2, with $\bar{w}_1 = \frac{1}{4}$ and $\bar{w}_2 = \frac{3}{4}$, using Modified Keener's Method

As information is collected and exploited (analyzed), the probability of the features on information deficits might change. When an information deficit for a mission is addressed, the probability for each associated feature, p_{jk}, is expected to be either 0 or 1. For this case, the relative priority among the cells in the AO is expected to be uniform, capturing the lack of information to establish any preference to collect information on a particular cell. The resulting IGM is shown in Figure 3.16.

Based on the results above, the ability of the Modified Keener's Method to establish a relative prioritization on the discretized areas of an AO based on the potential information gain to address information deficits will be exploited in Chapter 4. IGMs capturing this prioritization for different information collection requests in support of multiple mission objectives are the basis for the developed framework for the routing of cooperative assets maximizing overall information gain.
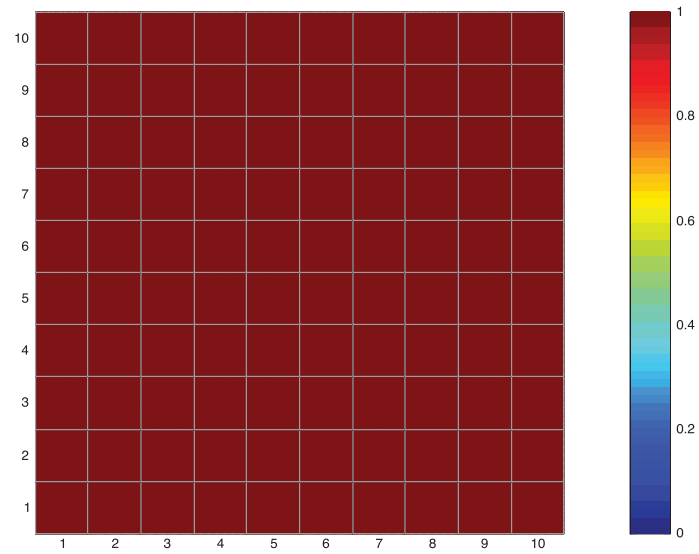
Figure 3.16: Information Gain Map using the Modified Keener's Method for an Information Deficit with $p_{jk} \approx 0$ or $p_{jk} \approx 1, \forall j, \forall k$

Chapter 4

A Mathematical Programming Framework for Decentralized Planning and Control Systems

4.1   Introduction

In this chapter, a Mixed-Integer Linear Program (MILP) to determine the routes of vehicles tasked to collect information on multiple objectives on a particular Area of Operation (AO) is presented. The main strategy is based on the discretization of the geographical space and time to represent the AO and the mission timeline, respectively. The mathematical model exploits the representation of potential information gain maps discussed in Chapter 3, the effectiveness of the assets collecting information and an obsolescence rate on the areas visited by the assets. The obsolescence rate captures the expected freshness on the information for a mission, increasing the information gain values when collection on a cell has not occurred over time. Each discretized subarea in the AO is referred to as a "cell". A mission is represented by a set of Information Gain Maps (IGMs), each capturing the potential information gain for a collection capability (e.g., imagery) required to accomplish mission objectives (see Figure 4.1), and a number of time-steps defining the planning horizon.
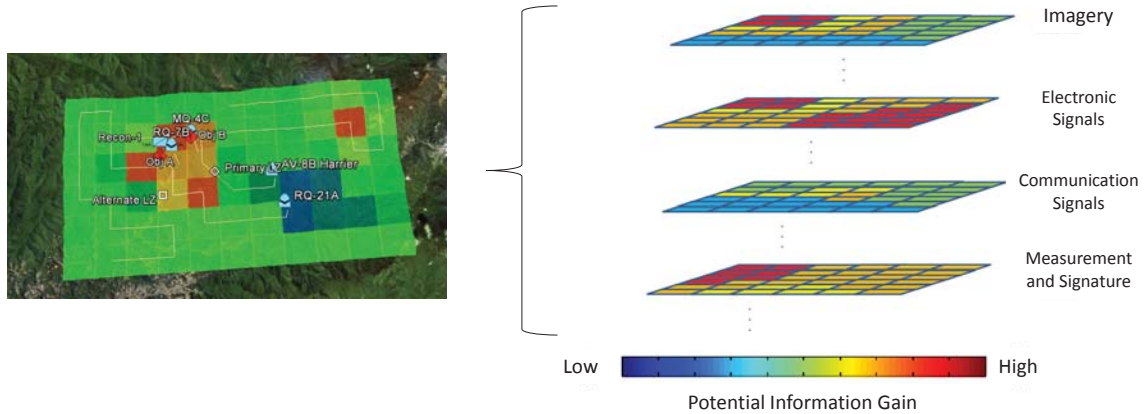
Figure 4.1: Representation of Collection Requirements for a Mission as Potential Information Gain Maps

A collection asset is represented in the mathematical model as an entity characterized by 3 main components:

1. the platform (also referred to as the vehicle)

2. an on-board sensor suite

3. the communication network

A platform can represent, for example, a manned aircraft, an unmanned ground vehicle or a ship. Movement of platforms is constrained and it is represented in the mathematical model by the cells the platform could reach from a given location over a given time horizon.

Collection assets are assumed to be equipped with a fixed set of on-board sensors. This sensor suite is not modifiable during the actual mission timeline. Each sensor is characterized by its effectiveness collecting a particular type of information (e.g., imagery) on each cell. Sensor effectiveness is assumed to be a function of time and the location of the sensor.

The communication network is represented in the MILP by a set of binary variables. Each binary variable represents a directed communication link between a pair of collection assets. Line-of-sight is assumed to be required to establish a communication link. A communication link is assumed to be required so two assets are considered ''connected'' and can exchange information.

This constraint is later relaxed as an extension to the model. The range to establish a communication link is limited.

Each collection asset is responsible for determining its own route plan over the planning horizon, considering its perspective of the environment and mission objectives. This implies that the collection asset has the necessary computational resources and authority to make those decisions autonomously. Note that this assumption does limit the applicability of the developed model and solution approaches to platforms with on-board computers with sufficient processing power. However, if decisions about the platform's routes over the planning horizon occur at a remote location, the latency to communicate that information to the platform is assumed to be insignificant.

Section 4.2 and Section 4.3 present the parameters and main decision variables defined in the mathematical model, respectively. Section 4.4 describes in detail the objective function and constraints in the MILP. Finally, in Section 4.5, a pictorial representation of the solutions obtained from the mathematical model for a simulated scenario is described. Solutions to this simulation were obtained by solving the MILP using `CPLEX` Interactive Optimizer 12.2 [50].

4.2   Mathematical Model Parameters

The following parameters are defined:

$$I \equiv \text{set of information collection assets}$$

$$T \equiv \text{set of discrete time-steps in planning horizon}$$

$$K \equiv \text{set of grid cells in the area of operation}$$

$$R \equiv \text{set of collection requirements (e.g., collection capabilities required for the mission)}$$

$$x_{ik0} \equiv \begin{cases} 1 & \text{if information collection asset } i \text{ is at cell } k \text{ at the time of planning} \\ 0 & \text{otherwise} \end{cases}$$

$$x_{ik,\text{-}1} \equiv \begin{cases} 1 & \text{if information collection asset } i \text{ was at cell } k \text{ a time-step prior to the time of planning} \\ 0 & \text{otherwise} \end{cases}$$

$$\psi_{ik''k'k} \equiv \begin{cases} 1 & \text{if information collection asset } i \text{ at cell } k'' \text{ at time } t-2 \text{ and at cell } k' \text{ at time } t-1 \text{ can be assigned to cell } k \text{ at time } t \\ 0 & \text{otherwise} \end{cases}$$

$$w_{rt} \quad \equiv \quad \text{weight (priority) of collection requirement } r \text{ at time-step } t$$

$$f_{rk0} \quad \equiv \quad \text{initial potential information gain from cell } k \text{ for collection requirement } r$$

$$\eta_{kk'} \quad \equiv \quad \text{distance between cell } k \text{ and cell } k', \ \eta_{kk'} \geq 0 \ \forall k, k' \in K$$

$$\overline{\text{CR}}_i \quad \equiv \quad \text{communication range of information collection asset } i, \ \overline{\text{CR}}_i \geq 0, \ \forall i \in I$$

$$e_{jrkt} \quad \equiv \quad \text{effectiveness of information collection asset } j \text{ on cell } k \text{ for collection requirement } r \text{ at time-step } t$$

$$D_{rkt} \quad \equiv \quad \text{maximum increase of potential information gain at time } t \text{ due to obsolescence of collected information for requirement } r \text{ on cell } k$$

$$M \quad \equiv \quad \text{large-enough constant used in Constraints (4.13), (4.14) and (4.23)}$$

4.3   Mathematical Model Main Decision Variables

The following decision variables are considered in the mathematical program:

$$x_{ikt} \quad = \quad \begin{cases} 1 & \text{if information collection asset } i \text{ is assigned to cell } k \text{ at time-step } t \\ 0 & \text{otherwise} \end{cases}$$

$$f_{rkt} \quad \equiv \quad \text{potential information gain from cell } k \text{ for collection requirement } r \text{ at time-step } t$$

$$d_{rkt} \quad \equiv \quad \text{increase in information value (due to obsolescence) of cell k for collection requirement } r \text{ at time-step } t$$

$$g_{rkt} \quad \equiv \quad \text{reduction of information value due to the sensor effectiveness of the team of information collection assets for collection requirement } r \text{ from cell } k \text{ at time-step } t$$

$$\Delta_{ijt} \quad \equiv \quad \text{distance from information collection asset } i \text{ to information collection asset } j \text{ at time-step } t$$

$$c_{ijt} \quad = \quad \begin{cases} 1 & \text{if information collection asset } j \text{ and information collection asset } i \text{ are within communication range at time-step } t \\ 0 & \text{otherwise} \end{cases}$$

4.4   Mathematical Model Objective Function and Constraints

4.4.1   Objective Function and Constraints

Consider the following objective for the mathematical formulation

$$\max \sum_{r \in R} \sum_{t \in T} w_{rt} \sum_{k \in K} g_{rkt} \tag{4.1}$$

The objective function in equation (4.1) maximizes the overall potential information to be gained by the set of information collection assets, for all collection requirements over the planning horizon.

4.4.2   Collection Assets Movement Constraints

Movement of collection assets is assumed to be constrained for realistic vehicle kinematics motion. The following constraints capture this behavior:

$$\sum_{k \in K} x_{ikt} = 1 \quad \forall i \in I, \forall t \in T \tag{4.2}$$

Constraint (4.2) ensures that each information collection asset i is assigned to a (single) cell at each time-step t.

$$\sum_{\substack{k \in K \\ k,k',k'' \in K \mid \psi_{ik''k'k}=1}} \sum_{k'} \sum_{k''} l_{ik''k'kt} = 1 \quad \forall i \in I, \forall t \in T \tag{4.3a}$$

$$l_{ik''k'kt} \leq \frac{x_{ikt} + x_{ik',t-1} + x_{ik'',t-2}}{3} \quad \forall i \in I, \forall k, k', k'' \in K \mid \psi_{ik''k'k} = 1, \forall t \in T \tag{4.3b}$$

Constraints (4.3) ensure that each information collection asset i is assigned to a cell k that can be reached at time-step t, given its assignment $x_{ik'',t-2}$ and $x_{ik',t-1}$ at times $t-2$ and $t-1$, respectively (see Section 4.2 for the definition of (parameter) $\psi_{ik''k'k}$).

4.4.3   Potential Information Gain Constraints

As described in Chapter 3, an IGM provides a characterization of the potential information gain available at a subarea of the AO at a particular time-step. At the time of planning, an initial set of IGMs, one for each collection requirement $r \in R$, is assumed to be an input parameter (see Section 4.2) to the mathematical model. Values on these maps need to be updated to account for the expected information collection from assets and information obsolescence rate on each cell.

Let f_{rkt} represent the potential information gain for collection requirement r from cell k at time-step t. It consists of three components:

$$f_{rkt} \quad \leq \quad \underbrace{f_{rk,t-1}}_{\substack{\text{potential} \\ \text{information} \\ \text{gain at } t\text{-1}}} \quad + \quad \underbrace{d_{rkt}}_{\text{temporal}} \quad - \quad \underbrace{g_{rkt}}_{\text{geospatial}} \qquad \forall r \in R, \forall k \in K, \forall t \in T \qquad (4.4)$$

$$f_{rkt} \quad \leq \quad 1.0 \quad \forall r \in R, \forall k \in K, \forall t \in T \qquad (4.5)$$

This relationship is shown in Figure 4.2.
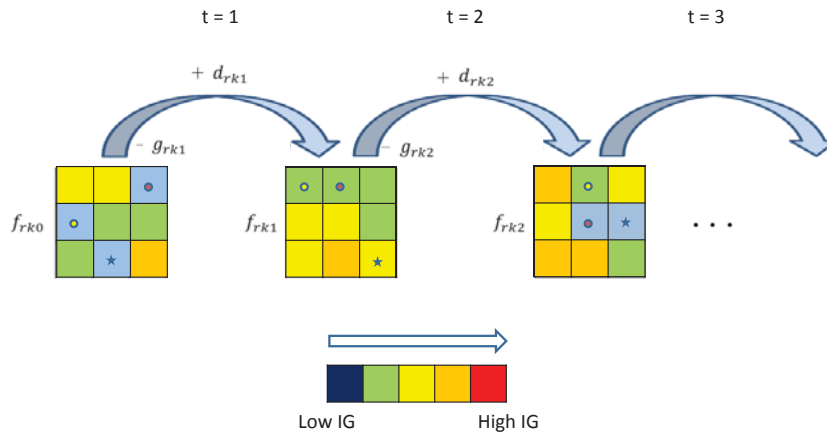
Figure 4.2: Concept of Potential Information Gain Update

In Figure 4.2, the AO is represented as a 3×3 grid. Three assets are moving in the area and cooperatively gathering information in support of the same collection request (thus, one IGM). The

initial IGM is captured by f_{rk0}. IGM values are represented by a heat map in which the color *blue* represents low information gain while the color *red* represents high information gain. For each time-step, a cell k may decrease its current potential information gain value due to the collection of assets (e.g., g_{rk1}) or increase it due to the decay in the value of previously collected information (e.g., d_{rk1}). Decay of information value is constrained by

$$d_{rkt} \leq D_{rkt} \quad \forall r \in R, \forall k \in K, \forall t \in T \tag{4.6}$$

where D_{rkt} is a constant indicating an upper bound on the decay contribution to the potential information gain.

In Constraint (4.4), d_{rkt} represents a decay on the value of the information on cell k. $g_{rk,t-1}$ represents the assumed gain of information on collection requirement r from cell k from time-step $t-1$ to t. g_{rkt} is represented as a set of constraints in the mathematical program as

$$g_{rkt} \quad = \quad \sum_{j \in I} g_{jrkt} \quad \forall r \in R, \forall k \in K, \forall t \in T \tag{4.7}$$

$$g_{jrkt} \quad \leq \quad e_{jrkt} \, x_{jkt} \, f_{jrkt} \quad \forall j \in I, \forall r \in R, \forall k \in K, \forall t \in T \tag{4.8}$$

Constraint (4.7) captures the overall information gain for collection requirement r from the set of collection assets I at time-step t on cell k. Constraint (4.8) captures the potential information gain from each collection asset j on cell k at time-step t, as a function of the effectiveness of the assets collecting information on r, the current potential information gain in cell k and the assignment of the collection asset to cell k. Note that decision variable f_{jrkt} was introduced in Constraint (4.8) to capture the perspective of each asset j on cell k from the IGM for collection requirement r at time-step t. This representation allows the mathematical model to capture the potential information gain when more than one asset collects information on the same cell and at the same time. Constraint (4.8) is nonlinear, and can be linearized as seen in Constraints (4.9) - (4.14).

$$g_{jrkt} \quad \leq \quad e_{jrkt} \, \zeta_{jrkt} \quad \forall j \in I, \forall r \in R, \forall k \in K, \forall t \in T \tag{4.9}$$

and

$$f_{0rkt} = f_{rkt} \quad \forall r \in R, \forall k \in K, \forall t \in T \tag{4.10}$$

$$f_{jrkt} = f_{j-1,rkt} - g_{jrkt} \quad \forall j \in I, \forall r \in R, \forall k \in K, \forall t \in T \tag{4.11}$$

$$\zeta_{jrkt} \leq f_{j-1,rkt} \quad \forall j \in J, \forall r \in R, \forall k \in K, \forall t \in T \tag{4.12}$$

$$\zeta_{jrkt} \geq f_{j-1,rkt} + (x_{jkt} - 1) M \quad \forall j \in I, \forall r \in R, \forall k \in K, \forall t \in T \tag{4.13}$$

$$\zeta_{jrkt} \leq x_{jkt} M \quad \forall j \in I, \forall r \in R, \forall k \in R, \forall t \in T \tag{4.14}$$

Also, note that g_{rk0} in Constraint (4.4) is

$$g_{rk0} = 0 \quad \forall r \in R, \forall k \in K \tag{4.15}$$

4.4.4   Communication Network Constraints

A communication link between collection assets i and j is possible if collection asset j is located within the communication range of collection asset i. As captured in Section 4.3, let c_{ijt} represent this communication link between assets i and j at time-step t.

$$c_{ijt} = \begin{cases} 1 & \text{if information collection asset } j \text{ and information collection asset } i \text{ are} \\ & \text{within communication range at time-step } t \\ 0 & \text{otherwise} \end{cases}$$

The following constraints are added to the mathematical model:

$$\Delta_{ijt} = \sum_{k} \sum_{k'} \eta_{kk'} \, x_{ikt} \, x_{jk't} \quad \forall i, j \in I, \, j \neq i, \forall t \in T \tag{4.16}$$

Constraint (4.16) is nonlinear and can be replaced by the following set of linear constraints, where the term $x_{ikt} \, x_{jk't}$ is replaced by the binary variable $a_{ikjk't}$.

$$a_{ikjk't} = \begin{cases} 1 & \text{if information collection asset } i \text{ is assigned to cell} \\ & k \text{ and information collection asset } j \text{ is assigned to} \\ & \text{cell } k' \text{ at time-step } t \\ 0 & \text{otherwise} \end{cases} \quad \forall i, j_{j \neq i} \in I, \forall t \in T \tag{4.17}$$

$$\Delta_{ijt} = \sum_k \sum_{k'} \eta_{kk'} \, a_{ikjk't} \quad \forall i,j \in I, \forall t \in T \tag{4.18}$$

$$a_{ikjk't} \leq x_{ikt} \quad \forall i,j \in I, \forall k,k' \in K, \forall t \in T \tag{4.19}$$

$$a_{ikjk't} \leq x_{jk't} \quad \forall i,j \in I, \forall k,k', \forall t \in T \tag{4.20}$$

$$a_{ikjk't} \geq x_{ikt} + x_{jk't} - 1 \quad \forall i,j \in I, \forall k,k' \in K, \forall t \in T \tag{4.21}$$

Decision variable c_{ijt} is defined by

$$c_{ijt} = \begin{cases} 1 & \text{if } \Delta_{ijt} \leq \overline{\text{CR}}_i \\ 0 & \text{otherwise} \end{cases} \quad \forall i,j \in I, \, j \neq i, \forall t \in T \tag{4.22}$$

Parameters $\eta_{kk'}$ and $\overline{\text{CR}}_i$ are defined in Section 4.2. For these communication objectives, consider the following constraint

$$\Delta_{ijt} \leq \overline{\text{CR}}_i + (1 - c_{ijt})M \quad \forall i,j, \forall t \in T \tag{4.23}$$

where M is a large-enough constant.

Given the equality in Constraint (4.18), Constraint (4.23) forces c_{ijt} to be 0 when, at time-step t, the assets i and j are assigned to cells with a distance between them greater than the communication radius $\overline{\text{CR}}_i$. Note that Constraint (4.23) by itself does not force c_{ijt} to be 1, even when the distance between assets i and j at time-step t is less than or equal to the communication radius CR_i. Decision variables c_{ijt} are forced to be 1 when possible (i.e., Constraint (4.23) is satisfied) and as needed by the communication network topology (see, for example Constraint (4.24) for a fully connected communication network.)

The information collection assets in set I are assumed to form a direct communication link topology. Under this communication network topology, a fully connected network is required among the assets: each asset is required to have a direct communication link to all other assets in the network. Figure 4.3 depicts a sample of this network topology for 3 Unmanned Aerial Vehicles (UAVs).

This can be represented mathematically by
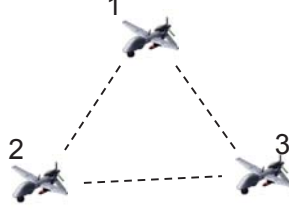
Figure 4.3: A Fully Connected Communication Network for 3 Collection Assets

$$\sum_{i \in J_a} \sum_{\substack{j \in J_a \\ j \neq i}} c_{ijt} \geq \frac{|J_a|(|J_a| - 1)}{2} \quad \forall t \in T \tag{4.24}$$

where $J_a \subseteq I$ represents the set of collection assets in a connected component a. It is important to note that $J_a \cap J_{a', a' \neq a} = \emptyset$ and $\underset{a}{\cup} J_a = I$. Constraints (4.16) - (4.24) are then added to the mathematical program of Sections 4.4.1 - 4.4.3 when the fully connected network topology is assumed for a connected component.

Note: M is a large-enough constant so it enables the behavior described for Constraints (4.13), (4.14) and (4.23). Thus, from Constraint (4.13), $M \geq f_{jrkt}$, from Constraint (4.14), $M \geq \zeta_{jrkt}$, and from Constraint (4.23), $M \geq \overline{\mathrm{CR}_i}$. Given that $f_{jrkt} \leq 1.0$ and $\zeta_{jrkt} \leq 1.0$,

$$M \geq \max\{\max_{i \in I} \overline{\mathrm{CR}_i}, 1.0\} \tag{4.25}$$

4.5   Pictorial Representation of the Output of the Mathematical Model

Based on the concepts described in Sections 4.1 - 4.4, a simulation was implemented to show the applicability and potential of our mathematical programming model to study the influence of decentralization level on solution quality. The assignment of 3 information collection assets was considered, particularly a set of UAVs, in an area of operation represented by a grid of 5×5 cells as shown in Figure 4.4. It is assumed all UAVs are autonomous, with a single on-board sensor. Assets were tasked to collect information for a search mission (i.e., $R = 1$) in which the information value on each cell represents the likelihood of finding a high value target at that cell. In Figure 4.4, areas

of low information gain (e.g., the middle of a lake while searching for a car) are denoted by yellow oval A, while those of high information gain are denoted by yellow oval B. The planning horizon was assumed to be 5 time-steps.

Three identical UAVs were modeled:

1) On-board sensors are assumed to be radars, having a discretized effectiveness of collecting information as shown in Figure 4.5.

2) UAVs can only move in horizontal and vertical directions; no diagonal movement is allowed.

3) All unmanned aerial systems will have the same initial potential information gain map.
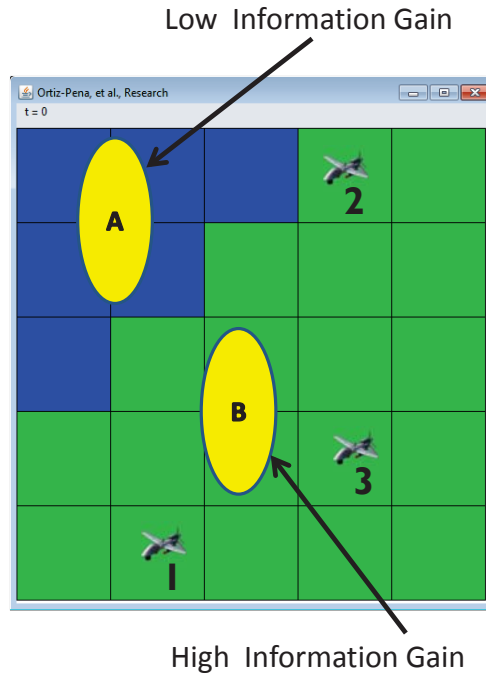
Figure 4.4: Area of operation: (A) represents a low potential information gain area; (B) represents a high potential information gain area

Values of other relevant parameters during the simulation are captured in Table 4.1.

First, a centralized framework was evaluated in which all information collected by each UAV is assumed to be available at a "central" controller. This allows optimal coordination of all collection assets in the area of operation to maximize the information gain for the mission.
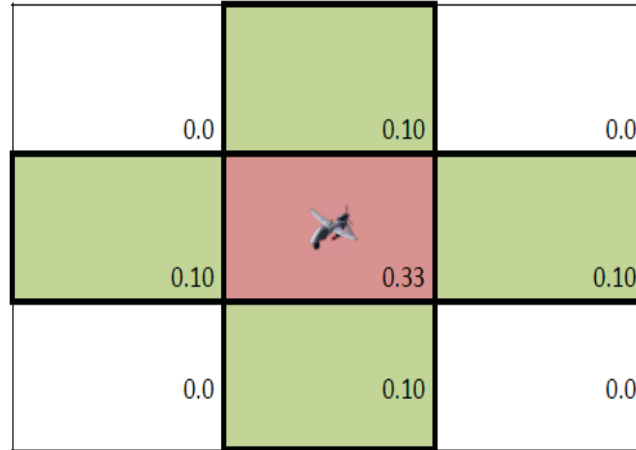
Figure 4.5: Sensor Model (values represent sensor's discretized effectiveness acquiring the potential information of cell)

Table 4.1: Mathematical Program and Experiment Parameters for Model Evaluation

Parameter	Value
Mathematical Program	
I	$\{1, 2, 3\}$
T	$\{1, 2, \ldots, 5\}$
K	$\{1,2,\ldots,25\}$ (a 5-by-5 grid area)
R	$\{1\}$
$\overline{\text{CR}}_i$	10 (centralized framework) 0 (decentralized framework)
w_{rt}	1.0 $(\forall r \in R, t \in T)$
M	10

For this case, in the mathematical programming model, the set I includes all collection assets and the communication range for each of them, $\overline{\text{CR}}_i = 10$. The routes for each collection asset for this centralized framework are shown in Figures 4.6, 4.8, 4.10, 4.12, 4.14 for time-steps $t = 1, \ldots, 5$, respectively. A decentralized framework in which each collection asset is operating independently,

with no coordination or communication among the team members was also evaluated. For this case, each unmanned vehicle system is solving the mathematical programing model considering only its own collection asset. The MILP is solved independently for each asset i in the set I. The routes for each collection asset for this decentralized framework are shown in Figures 4.7, 4.9, 4.11, 4.13, 4.15 for time-steps $t = 1, \ldots, 5$, respectively.
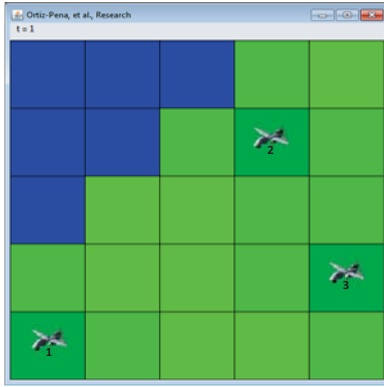
Figure 4.6: Centralized Solution ($t = 1$)
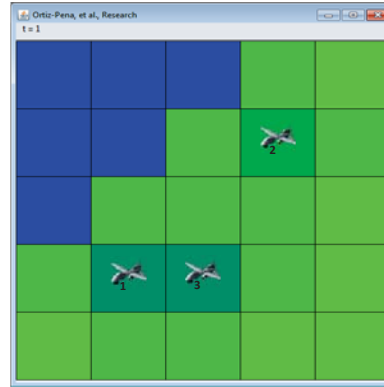
Figure 4.7: Decentralized Solution ($t = 1$)
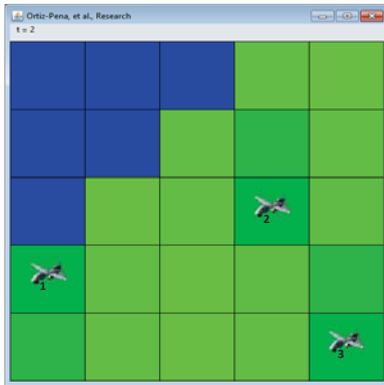
Figure 4.8: Centralized Solution ($t = 2$)
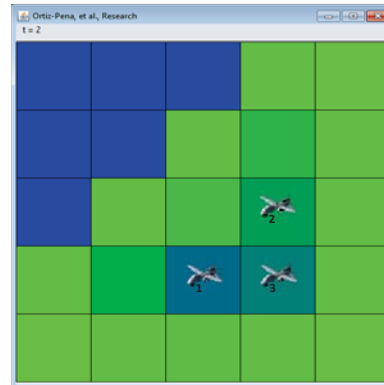
Figure 4.9: Decentralized Solution ($t = 2$)

From Figures 4.6, 4.8, 4.10, 4.12, 4.14, note how the centralized, coordinated solution, in general, distributes the UAVs over the area of interest. From t=1 to t =4, UAVs are assigned to areas in which their sensors' coverage do not overlap. At time-step = 5, when the sensor coverage of UAV 1 and 3 overlaps, the potential information gain in the area of operation is relatively constant
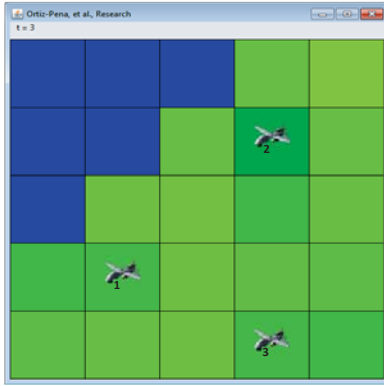
Figure 4.10: Centralized Solution ($t = 3$)
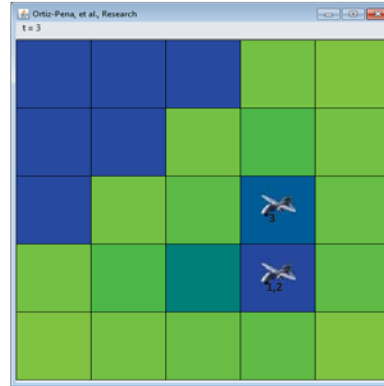
Figure 4.11: Decentralized Solution ($t = 3$)
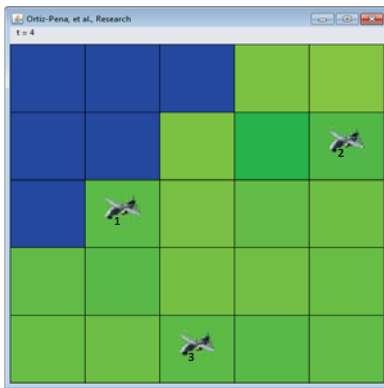
Figure 4.12: Centralized Solution ($t = 4$)
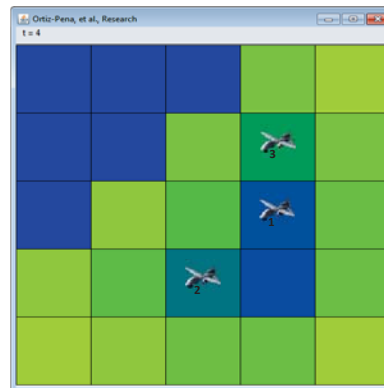
Figure 4.13: Decentralized Solution ($t = 4$)

and low (compared to the solution for the decentralized framework at the same time-step, Figure 4.15). For the decentralized solution on Figures 4.7, 4.9, 4.11, 4.13, 4.15, each UAV is trying to maximize its own potential information gain, with no consideration for the effectiveness of the other UAVs in the area of operations. In this framework, UAVs tend to travel to the same area of high potential information gain, including visiting the same cell simultaneously (see Figure 4.11). Note that the solutions shown are the optimal allocation of UAVs, solving the mathematical programming model described in Sections 4.2 - 4.4 using `CPLEX` Interactive Optimizer 12.2 [50].

As shown in this section, the mathematical programming model described in Sections 4.2 - 4.4 define a framework to determine the routes of cooperative assets collecting information, based
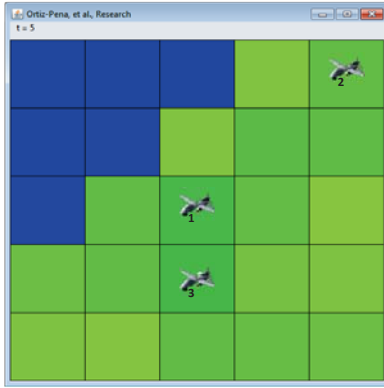
Figure 4.14: Centralized Solution ($t = 5$)   **Figure 4.15:** Decentralized Solution ($t = 5$)
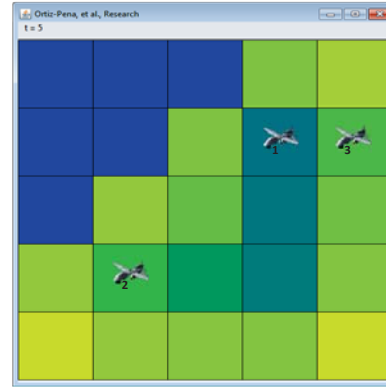
on the representation of potential information gain in discretized maps derived in Chapter 3. As is well-known, there is no polynomial time approximation algorithm for the vehicle routing problem or traveling salesman problem [51], both directly related to the derived mathematical model. Consequently, the same holds for the derived mathematical formulation. Heuristic and solution approaches need to be developed to find acceptably good solutions that are computational efficient. This is the topic discussed in Chapter 5. Extensions to the mathematical program to represent additional operational constraints are discussed in Chapter 6. In Chapter 7, the mathematical program is used as the framework to evaluate the degradation of solution quality as a centralized system moves to a decentralized framework considering different communication network topologies.

Chapter 5

Solution Approach to Mathematical Programming Framework

5.1 Introduction

Although the mathematical program presented in Chapter 4 provides a framework to define the optimal trajectory of autonomous information gathering assets maximizing potential information gain, it becomes intractable for relative small Area of Operations (AOs) (i.e., number of cells) and mission timelines (i.e., number of time-steps in the planning horizon). This becomes a research challenge since routing of assets over relatively large AOs and extensive planning timelines is envisioned. The solution strategy defined to address this issue consists of solving a set of subproblems using the same framework described in Chapter 4. Subproblems will be defined using a combination of time cascades and space aggregation algorithms, described in Section 5.2 and Section 5.3, respectively. In Section 5.4, an analysis of the impact of the combined time and space aggregation approaches to the solution quality (i.e., overall information gain) on various scenarios and the time to obtain such solutions is presented.

5.2   Time Cascade Approach

Consider the definition of routes for a set of cooperative, autonomous information gathering assets using Equations (4.1) - (4.24) from Chapter 4 over a Planning Horizon (PH). Instead of defining the complete route for each asset at once, the evaluation of a subset of time-steps at a time is proposed. This subset of time-steps is referred to as a *Rolling Horizon (RH)* and it constitutes a subproblem to be solved using Equations (4.1) - (4.24). While solving this subproblem, the number of time-steps considered as the planning horizon, T in Section 4.2, is replaced by the rolling horizon. No other changes are required to define the optimal route of the set of information gathering assets to maximize the potential information gain within the rolling horizon.

Once the route of each asset is obtained within a RH, only a number of time-steps from the solution of this subproblem will be considered in the final solution (i.e., the route of each asset). This subset of time-steps is referred to as a *Fixed Window (FW)*. Note that $PH \geq RH \geq FW \geq 1$. The routes for the entire PH are then defined by solving multiple RHs, each solving the routing problem for a certain number of time-steps. Each stage is referred to as a *cascade* in this work . Once a cascade is completed (i.e., a subproblem defined, solved and appropriate steps from the solution fixed), a new rolling horizon is defined starting from the last fixed time-step in the solution. A new cascade is then solved. In this approach, subsequent RHs may overlap. This gives the opportunity to revisit decisions made only with limited information (i.e., the value of potential information gain from cells outside the rolling horizon in a cascade is not considered). When the RH includes the last time-step in the PH, the solution from that subproblem completes the final solution of the routing problem; routes for each information gathering assets are defined.

Figure 5.1 shows an overview of the time cascade approach for a sample routing problem consisting of a PH of 10 time-steps, a RH of 3 time-steps and a FW of 1 time-step. The first cascade, Cascade 1, consists of solving a subproblem considering time-steps t_1, t_2, and t_3. As will be described below, information from the remaining time-steps in the planning horizon is aggregated while solving each subproblem. The solution of the mathematical program described in Chapter 4 consists of an assignment, x_{jkt}, of a cell k in the discretized AO for each time-step t of the planning horizon, for each collection asset j. For Cascade 1 in Figure 5.1, the solution will be an assignment $\{x_{jkt_1}, x_{jkt_2}, x_{jkt_3}\}$ for each asset j under consideration. Given that FW = 1, the values of x_{jkt_1}, $\forall j, \forall k$, will be part of the final solution. A new cascade, Cascade 2, is then defined. Cascade 2
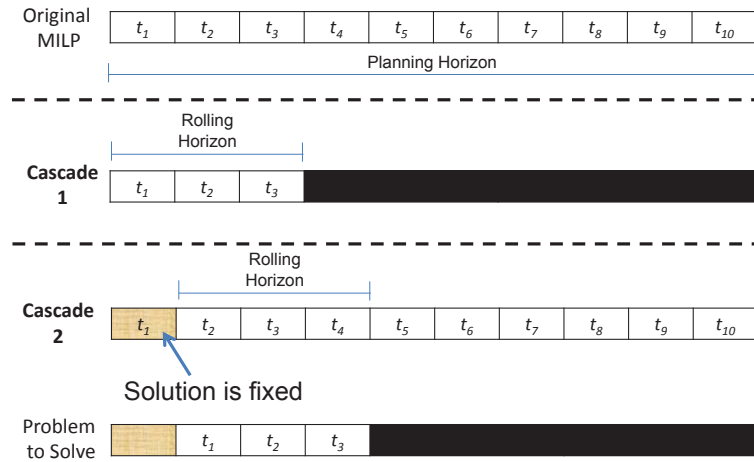
Figure 5.1: Overview of Time Cascades Approach

will consist of solving a subproblem for time-steps t_2, t_3, and t_4. The same process defined above is repeated until Cascade 8, where the subproblem for time-steps t_8, t_9 and t_{10} is defined. The solution obtained for this last subproblem completes the definition of the routes $\{x_{jkt_1}, x_{jkt_2}, \cdots, x_{jkt_{10}}\}$ for each asset j over the 10 time-steps of the planning horizon.

Note that while solving each cascade, certain areas of the discretized geographical space will not be considered, even when those areas might be visited if the complete planning horizon was considered at once. It is desirable to the solution strategy using the time cascade approach to define a mechanism to consolidate some of the information about those cells so that decisions (moves) made at an earlier stage consider potential future gain. The aggregation of information from feasible future moves that are not part of a cascade's rolling horizon is presented in Section 5.3.

5.3   Space Aggregation Approach

The time cascade approach is based on the idea of reducing the number of time-steps considered while solving the mathematical program defined in Chapter 4. Using this approach provides the opportunity to also reduce the number of grid cells considered while solving the subproblem in each cascade. Given the number of time-steps in each rolling horizon and the (known) kinematic constraints of each autonomous vehicle, the cells that could be reached in each cascade are identified. The set K in Section 4.2, is replaced by considering only those cells (rather than the complete,
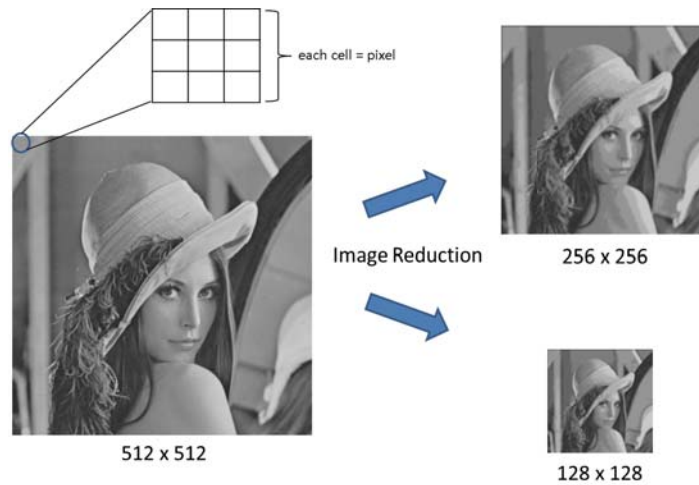
Figure 5.2: Sample of Digital Image Compression

discretized AO).

Although the time cascade approach can reduce the number of decision variables considered in the mathematical program, it introduces the risk of defining a suboptimal set of routes because decisions are made on each cascade based on only a subset of the feasible space. If information about cells outside of the RH were considered when solving each cascade problem, better solutions would result.

In image processing, a digital image is simply an array of numbers [52]. Each element in this array is referred to as a picture element, or pixel as shown in Figure 5.2. This figure shows an example of digital image compression. Note that the compressed images preserve "relevant" features that allow the original image to be recognized. Figure 5.3 shows the general steps used while compressing an image. A numerical example of this process is shown in Figure 5.4. Motivated by this observation, and considering Information Gain Maps (IGMs) as digital images, the following approach is defined to preserve relevant information from the IGMs while solving each subproblem in the time cascade approach: information from cells that might be visited in the planning horizon are aggregated to the cells that could be assigned on each subproblem in each cascade. Let us refer to a cell that might be assigned in the last time-step of a rolling horizon and whose value will be updated after aggregation as a *cell of interest*. The following procedure is defined:

1. An aggregation window is defined capturing adjacent cells to the cell of interest. The aggre-
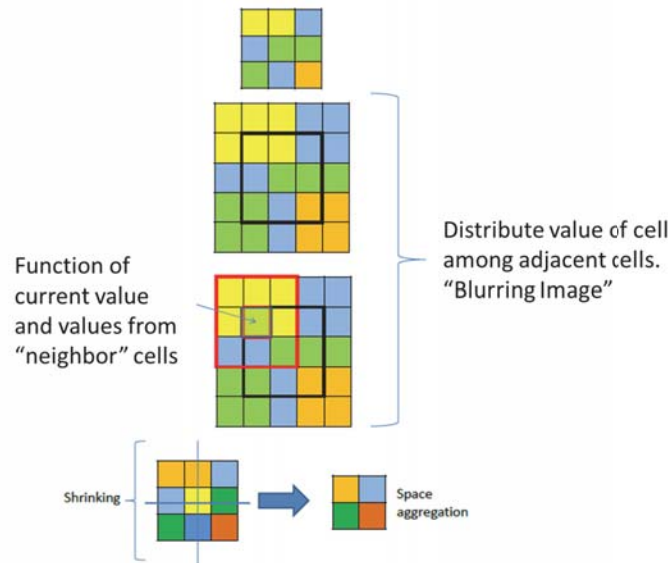
Figure 5.3: General Digital Image Compression Process
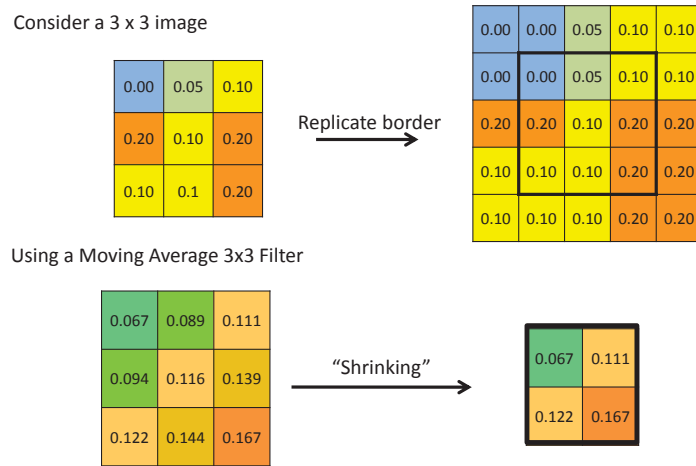
Figure 5.4: General Digital Image Compression Process - Numerical Example

gation window will only consider cells that will not be evaluated as part of the rolling horizon.

2. An aggregation function is applied to the cell in the aggregation window. The aggregation function performs, for example, the blurring and shrinking steps in Figure 5.3.

3. The resulting value from the aggregation function replaces the value of the cell of interest.

Figure 5.4 depicts the steps considered in this approach for an aggregation window of 9 cells and

the arithmetic mean of these cells as the aggregation function.

The decision to assign a cell to a collection asset should be based not only on the current reward of this cell but on the potential to move to other feasible cells to collect additional information. Based on this observation, an aggregation function that identifies the path that maximizes the potential information gain from the cell of interest over the remaining time-steps in the planning horizon is defined. The Bellman-Ford algorithm [53] is used to define such a path for each cell of interest in a subproblem.

Bellman-Ford is an efficient procedure used to find all shortest paths in a graph, $G(V, E)$, from one source to all other nodes in the graph, where V is the set of vertices and E is the set of edges. This problem is also referred to as the single-source shortest path problem for weighted directed graphs. The weights on the edges of E were updated to identify the path that maximizes the potential information gain from the cell of interest. The algorithm initializes the distance to the source vertex to 0 and all other vertices to ∞. It then does $|V| - 1$ passes ($|V|$ is the number of vertices) over all edges relaxing, or updating, the distance to the destination of each edge. Finally it checks each edge again to detect negative weight cycles, in which case it returns false. Weights may be negative. The time complexity of the Bellman-Ford algorithm is $O(|V||E|)$, where $|E|$ is the number of edges.

Let $\overline{T}$ be the remaining time-steps in the planning horizon when a subproblem is defined. $\overline{T} = \{1, 2, \ldots, PH - RH + t\}$ where t is the initial time-step of the cascade. T is the set of time-steps in the planning horizon (as defined in Section 4.2). Moreover, let $\overline{k}$ be a cell of interest on a subproblem.

Let F_k be the set of cells that any of the vehicles under consideration could visit from cell k. Parameter $\psi_{ik''k'k}$ (as defined in Section 4.2) is used to define F_k. The set V is created from the set F_k. Let $V_{\bar{t}}$ be the set of cells that could be visited at time-step $\bar{t}, \bar{t} \in \overline{T}$.

$$V_1 = \overline{k} \tag{5.1}$$

Now, $\forall \bar{t} \in \overline{T}, \bar{t} > 1$

$$V_{\bar{t}} = \cup F_k, \quad \forall k \in V_{\bar{t}-1} \tag{5.2}$$

Finally,

$$V = \cup V_{\bar{t}} \quad \forall \bar{t} \in \overline{T} \tag{5.3}$$

Let $e_{k,k'}$ be an edge in E for each $k \in V_{\bar{t}}$ and $k' \in F_k$. The weight of each edge

$$e_{k,k'} = 1 - \max\{f_{1k0} + \bar{t} * D_{1k}, 1.0\}, \forall k \in V_{\bar{t}} \tag{5.4}$$

where f_{1k0} is the initial potential information gain from cell k, and D_{1k} is the maximum increase of potential information gain at time t due to obsolescence of collected information on cell k. Both are parameters of the mathematical program of Chapter 4. Note that $G(V, E)$ is defined once for each subproblem. Without loss of generality, since a single mission was assumed to describe the solution approach, a single collection requirement $(R = 1)$ is assumed while defining these parameters. The same approach would be applied when multiple collection requirements (and corresponding IGMs) are considered in a mission.

Given the best path over the remaining time-steps to complete the planning horizon, the aggregation function is defined as a weighted average of the potential information gain values of the cells in the path and their respective distance to the cell of interest. This aggregation function for a cell of interest $\bar{k}$ is represented mathematically as

$$\overline{f}_{\overline{k}} = \frac{\sum_{\bar{t} \in \overline{T}} w_{\bar{t}} \max\{f_{1k_{\bar{t}0}} + \bar{t} * D_{1k_{\bar{t}}}, 1.0\}}{|\overline{T}|} \tag{5.5}$$

where $k_{\bar{t}}$ is the potential information gain for cell k, when k is the $\bar{t}$th move on the identified best path by the Bellman-Ford algorithm and $w_{\bar{t}}$ is a weighting parameter on the assigned cell at time $\bar{t}$. The weighting parameter $w_{\bar{t}}$ can be used to discount the contributions of cells that are far in the future to the value of $\overline{f}_{\overline{k}}$.

Section 5.4 presents an analysis of the impact of the combined time and space aggregation approaches to the solution quality (i.e., overall information gain) on various scenarios and the time to obtain such solutions.

5.4   Experimental Results

A study was conducted to analyze the impact of the combined time and space aggregation approaches to the solution quality (i.e., overall information gain) and the time to obtain such solutions. All subproblems were solved using `CPLEX` Interactive Optimizer 12.2 [50]. The time cascades and space aggregation approach were implemented in `MATLAB R2011b` [49]. Table 5.1 captures the parameters under consideration in the study. Two types of IGMs were considered: (1) 1 Hot-Spot, and (2) Random. Figure 5.5 shows an example of an IGM with a single hot spot. The location of the hot spot was randomly selected for each case considered. Figure 5.6 shows an example of a random IGM. For this type of IGM, the value of each cell was randomly selected from a uniform distribution $U(0,1)$. A 10 time-step route for a single vehicle over a 15×15 grid area was defined. Rolling Horizon and Fixed Window were varied. Moreover, the impact of the vehicle's sensor effectiveness collecting information was studied.

Table 5.1: Mathematical Program and Experiment Parameters for Solution Approach Evaluation

Parameter	Value
Mathematical Program	
I	$\{1\}$
T	$\{1,2,\ldots, \text{RH}\}$
K	$\{1,2,\ldots,225\}$ (a 15-by-15 grid area)
R	$\{1\}$
$\overline{\text{CR}}_i$	3.0 ($\forall i \in I$)
w_{rt}	1.0 ($\forall r \in R, t \in T$)
Solution Approach	
$w_{\bar{t}}$	$e^{-\lambda\,(\bar{t}-1)}$
λ	$-\ln(0.90)$
Design of Experiment	
n (number of trials)	100
Information Gain Maps	100
Type of Information Gain Maps	1 Hot-Spot and Random
Rolling Horizon (RH)	$\{3, 4\}$
Fixed Window (FW)	$\{1, 2, 3\}$
sensor effectiveness	$\{0.25, 0.50, 0.75\}$
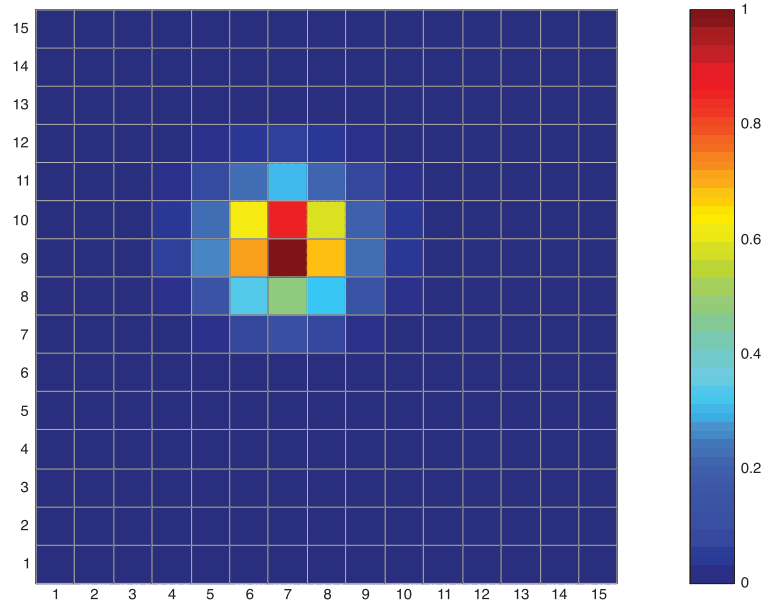
Figure 5.5: Sample IGM with 1 Hot-Spot to Evaluate Solution Approach

For each combination of IGM type and sensor effectiveness, 100 different test cases were defined. Let P represent the set of these cases. The vehicle's initial location and initial IGM were randomly defined for each of these cases. Each of the cases were solved first by applying the time cascade approach but with no space aggregation. Space aggregation as described in Section 5.3 was then enabled. Overall potential information gain from the defined route and the time to obtain that solution was captured. Several metrics were computed. Let $z_{\text{no aggregation},p}$ and $t_{\text{no aggregation},p}$ be the overall potential information gain from the defined route and time to obtain the solution, respectively, when space aggregation was not applied in the solution approach while solving case p. Similarly, let $z_{\text{with aggregation},p}$ and $t_{\text{with aggregation},p}$ be the overall potential information gain from the defined route and time to obtain the solution, respectively, when space aggregation was applied in the solution approach while solving case p. Note that

$$P = P_{\text{solution improved}} \cup P_{\text{solution worsened}} \cup P_{\text{no difference}}$$

where

$$p \in P_{\text{solution improved}} \text{ if } z_{\text{with aggregation},p} - z_{\text{no aggregation},p} > 0;$$
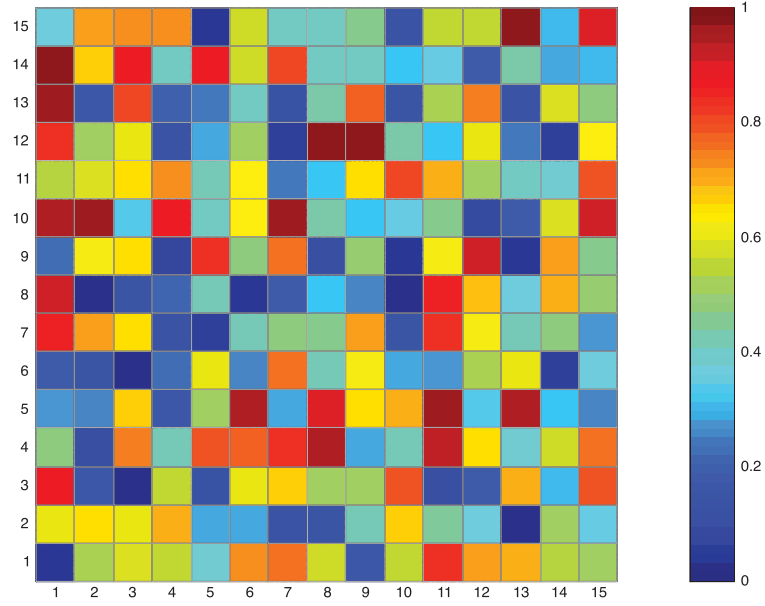
Figure 5.6: Sample Random IGM to Evaluate Solution Approach

$$p \in P_{\text{solution worsened}} \text{ if } z_{\text{no aggregation},p} - z_{\text{with aggregation},p} > 0; \text{ and,}$$

$$p \in P_{\text{no difference}} \text{ if } z_{\text{with aggregation},p} = z_{\text{no aggregation},p}.$$

The following metrics were considered in the study:

- Percentage of cases where Solution Improved When Space Aggregation was Applied =

$$\frac{|P_{\text{solution improved with aggregation}}|}{n} 100\%$$

- Percentage of cases where Solution Worsened When Space Aggregation was Applied =

$$\frac{|P_{\text{solution worsened with aggregation}}|}{n} 100\%$$

- Average Percentage Increase in Solution Value when Solution Improved with Space Aggregation =

$$\frac{1}{|P_{\text{solution improved}}|} \sum_{p \in P_{\text{solution improved}}} \frac{z_{\text{with aggregation},p} - z_{\text{no aggregation},p}}{z_{\text{with aggregation},p}} 100\%$$

- Average Percentage Increase in Solution Value when Solution Worsened with Space Aggregation =

$$\frac{1}{|P_{\text{solution worsened}}|} \sum_{p \in P_{\text{solution worsened}}} \frac{z_{\text{no aggregation},p} - z_{\text{with aggregation},p}}{z_{\text{no aggregation},p}} \, 100\%$$

- Average Time to Solve Problem using Solution Approach without Space Aggregation =

$$\frac{1}{n} \sum_{p=1}^{n} t_{\text{no aggregation},p}$$

- Average Time to Solve Problem using Solution Approach with Space Aggregation =

$$\frac{1}{n} \sum_{p=1}^{n} t_{\text{with aggregation},p}$$

Results are summarized in Table 5.2 - Table 5.4 and used for the analysis that follows.

Figure 5.7 - Figure 5.9 show a comparison of the average percentage increase in solution value when space aggregation was applied as part of the solution approach for a RH = 3 time-steps and FW = 1, 2 or 3 time-steps, respectively. Similarly, in Figure 5.10 - Figure 5.12, a comparison is shown on the average percentage increase in solution value when space aggregation was applied as part of the solution approach for a RH = 4 time-steps and FW = 1, 2 or 3 time-steps, respectively. From these figures, it is evident that applying space aggregation as part of the solution approach has no impact on the solution quality, on average, when the type of IGM is Random. Although for any of the combinations of RH, FW and sensor effectiveness, the percentage number of cases in which the solution improved was over 16%, the best average percentage increase in solution value was 2.73%. Likewise, the average percentage increase in solution value was less than 4% on the cases in which the solution worsened when space aggregation was applied. The value of each cell in an IGM of type Random was defined, independently, from a uniform distribution $\sim U(0,1)$. The expected value for any cell of interest during the space aggregation phase would then be the same, providing no relevant information to exploit as part of the solution strategy.

The improvement observed when space aggregation was applied to the solution approach for IGMs of 1 Hot-Spot was significant. Although not all the cases considered resulted in an improvement, on average, 38% of the solutions obtained when space aggregation was part of the solution

Table 5.2: Summary of Results - Information Gain Improved with Solution

Type of IGM	Sensor Effectiveness	Rolling Horizon	Fixed Window	% Cases Solution Improved	Avg % Increase Solution Value
1 Hot-Spot	0.25	3	1	32.00	35.58
			2	32.00	34.13
			3	20.00	43.91
		4	1	50.00	27.17
			2	42.00	26.22
			3	40.00	26.46
	0.50	3	1	34.00	34.18
			2	38.00	33.54
			3	36.00	28.85
		4	1	52.00	19.75
			2	50.00	22.13
			3	34.00	25.45
	0.75	3	1	28.00	35.92
			2	28.00	35.92
			3	36.00	32.98
		4	1	38.00	25.23
			2	46.00	22.67
			3	42.00	27.78
Random	0.25	3	1	30.00	1.28
			2	20.00	1.90
			3	34.00	2.60
		4	1	34.00	1.07
			2	20.00	1.31
			3	36.00	1.12
	0.50	3	1	30.00	2.66
			2	22.00	2.32
			3	44.00	2.19
		4	1	16.00	1.38
			2	18.00	1.82
			3	26.00	1.60
	0.75	3	1	36.00	2.17
			2	20.00	2.73
			3	40.00	2.06
		4	1	20.00	1.45
			2	22.00	1.61
			3	28.00	1.64

strategy improved the potential information gain from the route computed without applying space aggregation. The average percentage increase in solution value for these cases was always over 19.75% for the different combinations of RH, FW and sensor effectiveness studied. For the cases where the solution did not improve with the space aggregation approach, the decrease in potential information gain was, on average, 0.67% from the solution obtained when space aggregation was not applied.

The computational cost of using space aggregation as part of the solution strategy is rel-

Table 5.3: Summary of Results - Information Gain Worsened with Aggregation

Type of IGM	Sensor Effectiveness	Rolling Horizon	Fixed Window	% Cases Solution Worsened	Avg % Increase Solution Value
1 Hot-Spot	0.25	3	1	16.00	0.15
			2	32.00	0.80
			3	32.00	0.58
		4	1	12.00	0.21
			2	22.00	0.39
			3	24.00	0.40
	0.50	3	1	14.00	0.64
			2	14.00	1.06
			3	18.00	0.70
		4	1	18.00	0.40
			2	14.00	0.38
			3	22.00	0.49
	0.75	3	1	24.00	0.89
			2	24.00	1.37
			3	18.00	0.96
		4	1	20.00	0.46
			2	16.00	0.59
			3	20.00	1.68
Random	0.25	3	1	58.00	2.69
			2	76.00	2.52
			3	60.00	2.78
		4	1	30.00	1.63
			2	32.00	1.88
			3	26.00	1.87
	0.50	3	1	58.00	2.94
			2	66.00	3.16
			3	52.00	3.57
		4	1	44.00	2.04
			2	38.00	2.52
			3	38.00	2.14
	0.75	3	1	52.00	2.56
			2	64.00	3.15
			3	52.00	3.83
		4	1	40.00	1.89
			2	40.00	2.25
			3	32.00	1.92

atively minimal. Figure 5.13 and Figure 5.14 captures the average time (in seconds) required to obtain a 10 time-steps route for a single vehicle using the described solution strategy for different RHs and FWs. The average time increase to obtain a solution with space aggregation was 7.66% of the time required by the solution approach to define a route without space aggregation. The worst case observed was an average increase of 0.49s. Both, Figure 5.13 and Figure 5.14, capture a similar trend: solving subproblems with a rolling horizon of 4 time-steps increased the time to obtain a solution by 64.36%, relative to the time required, on average, to solve the routing problem for a RH

Table 5.4: Summary of Results - Average Time to Solve (s)

Rolling Horizon	Fixed Window	Avg. Time to Solve (s)	
		No Aggregation	With Aggregation
3	1	2.3220	2.5241
	2	1.3637	1.4778
	3	1.1005	1.1874
4	1	6.6987	7.1933
	2	3.9068	4.1515
	3	2.9979	3.2176

of 3 time-steps, fixing the same number of time-steps. As described in Section 5.2 and Section 5.3, the complexity of the subproblems increase as the planning horizon (i.e., rolling horizon in a cascade) and the number of cells from the IGM increase. From the perspective of a particular RH, increasing the number of time-steps in the FW represents a potential reduction on the subproblems to solve (i.e., less cascades), resulting in a decrease in the time to obtain a solution. For a RH = 3 time-steps, the time to solved the 10 time-steps routing problem was reduced by 41.4% for a FW = 2 time-steps and 52.8% for a FW = 3 time-steps, from the time required to solved the problem with a FW = 1 time-steps. For the case of RH = 4 time-steps, the time to solved the 10 time-steps routing problem was reduced by 42% for a FW = 2 time-steps and 55.3% for a FW = 3 time-steps, from the time required to solved the problem with a FW = 1 time-steps.

Finally, a comparison on the quality of the solution obtained from each of these cases was made. Figure 5.15 - Figure 5.17 shows the average percentage difference between the potential information gain obtained from the route defined using the solution strategy and the best known solution for the cases of RH = 3 time-steps, FW = 1, 2, and 3 time-steps. Similarly, Figure 5.18 - Figure 5.20 shows the average percentage difference between the solution strategy and the best known solution for the cases of RH = 4 time-steps, FW = 1, 2, and 3 time-steps. The best known solution value was obtained by evaluating all cases where the IGM, sensor effectiveness and initial location of the vehicle were the same. The maximum solution value for each of these cases was then used to compare the resulting potential information gain from each of them. Note that for the IGMs with 1 Hot Spot, solutions were on average within 1.35% of the best known solution. When space aggregation was not applied, the smallest average percentage difference was 9.81% for a RH of 4 time-steps and a FW of 1 time-step. As indicated before, for the cases of Random IGMs, there is no statistical benefit or disadvantage of applying space aggregation.
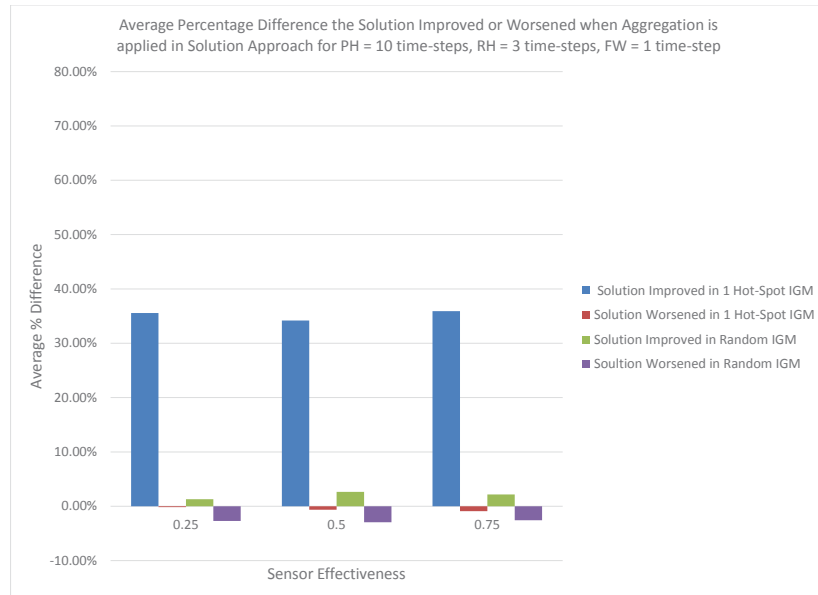
Figure 5.7: Average Percentage Increase in Solution Value when Space Aggregation is applied to Solution Approach for PH = 10 time-steps, RH = 3 time-steps, FW = 1 time-step
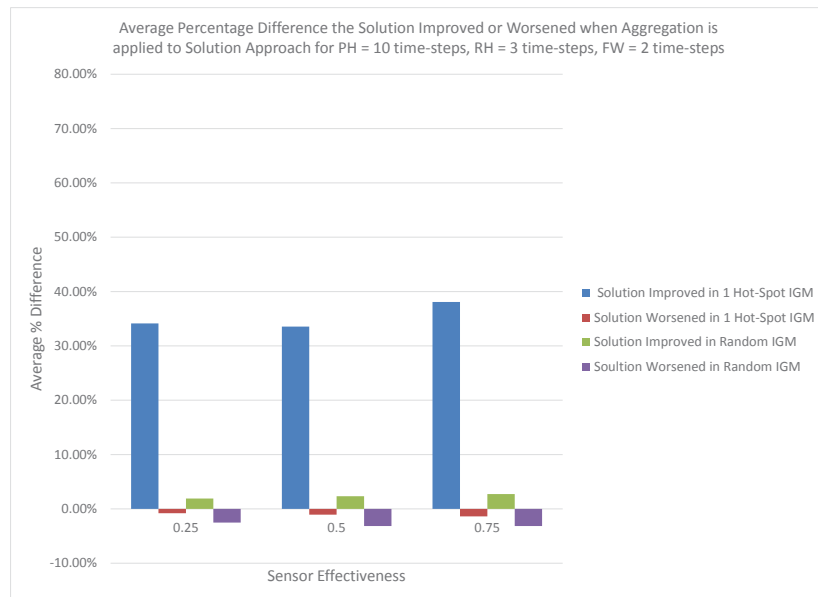
Figure 5.8: Average Percentage Increase in Solution Value when Space Aggregation is applied to Solution Approach for PH = 10 time-steps, RH = 3 time-steps, FW = 2 time-steps
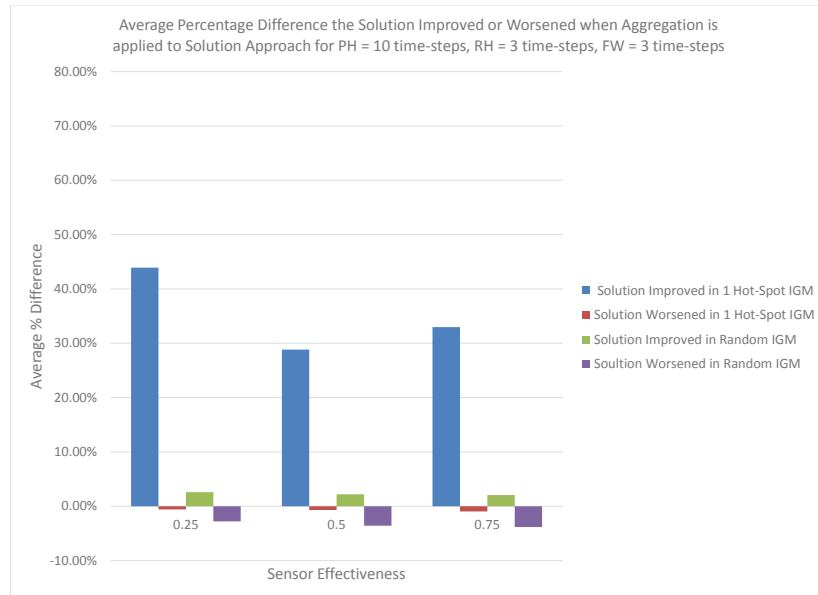
Figure 5.9: Average Percentage Increase in Solution Value when Space Aggregation is applied to Solution Approach for PH = 10 time-steps, RH = 3 time-steps, FW = 3 time-steps
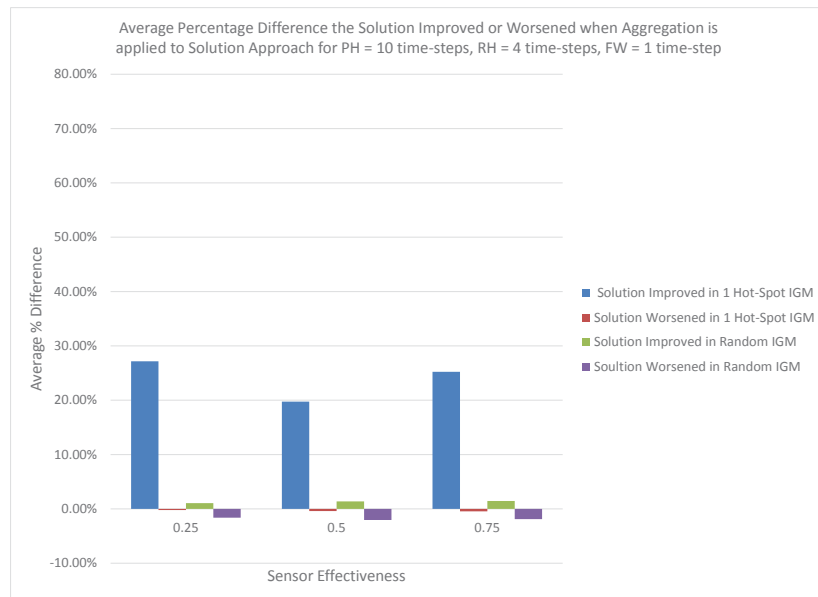
Figure 5.10: Average Percentage Increase in Solution Value when Space Aggregation is applied to Solution Approach for PH = 10 time-steps, RH = 4 time-steps, FW = 1 time-step
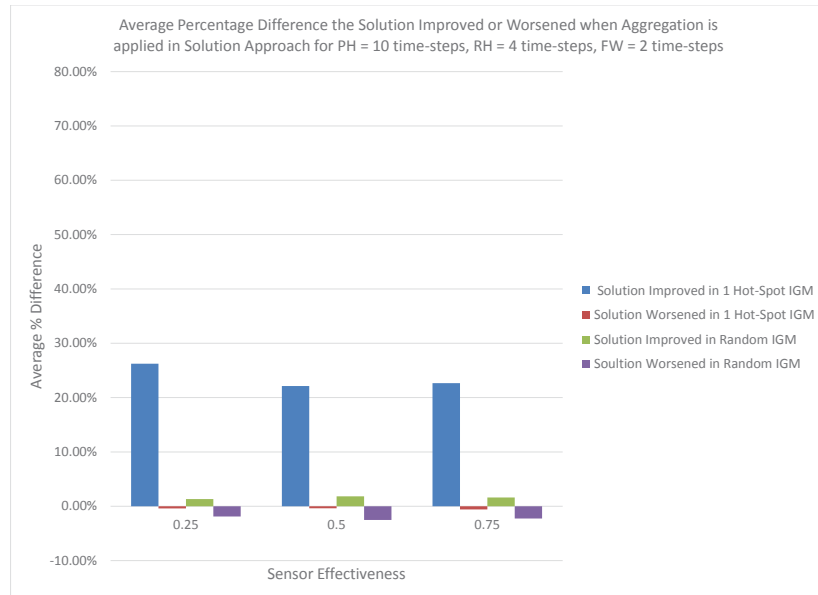
Figure 5.11: Average Percentage Increase in Solution Value when Space Aggregation is applied to Solution Approach for PH = 10 time-steps, RH = 4 time-steps, FW = 2 time-steps
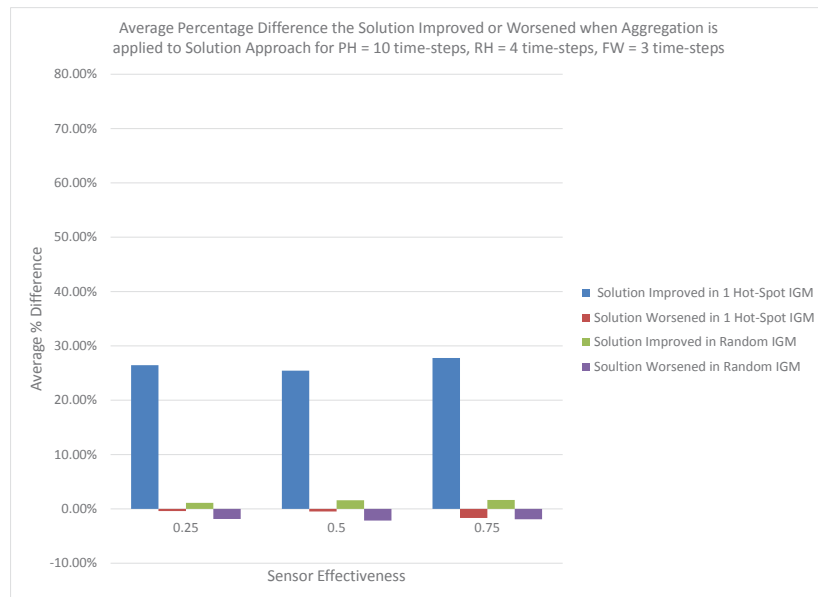
Figure 5.12: Average Percentage Increase in Solution Value when Space Aggregation is applied to Solution Approach for PH = 10 time-steps, RH = 4 time-steps, FW = 3 time-steps
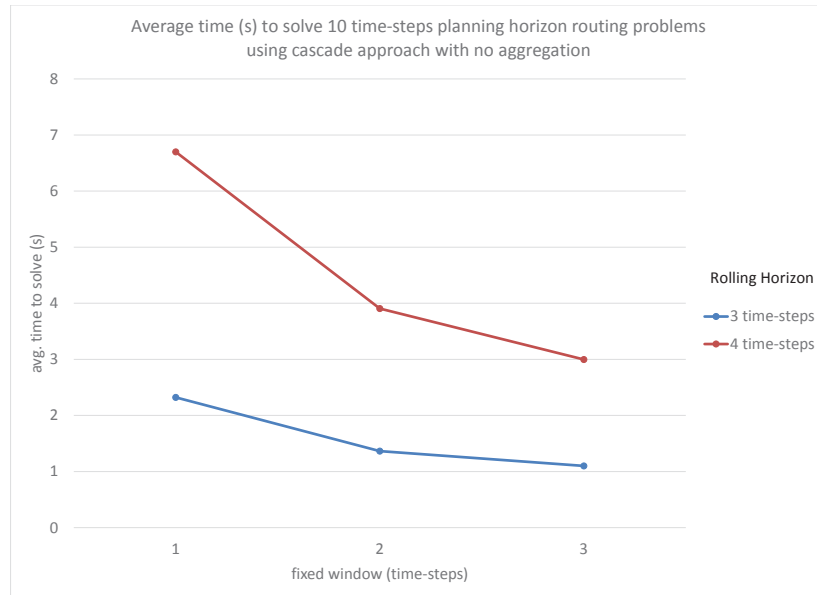
Figure 5.13: Average Time to Solve (s) 10-time step Planning Horizon Routing Problem using Cascade Approach with No Space Aggregation
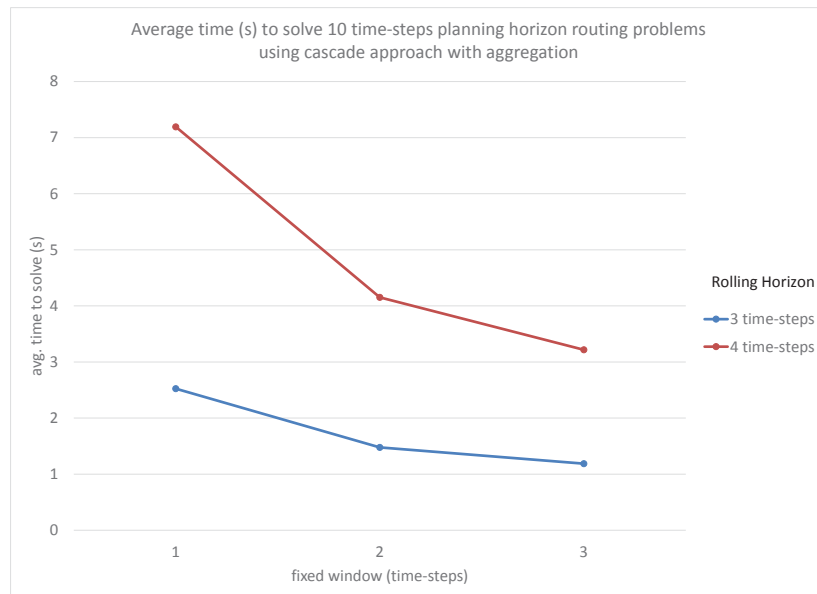
Figure 5.14: Average Time to Solve (s) 10-time step Planning Horizon Routing Problem using Cascade Approach with Space Aggregation
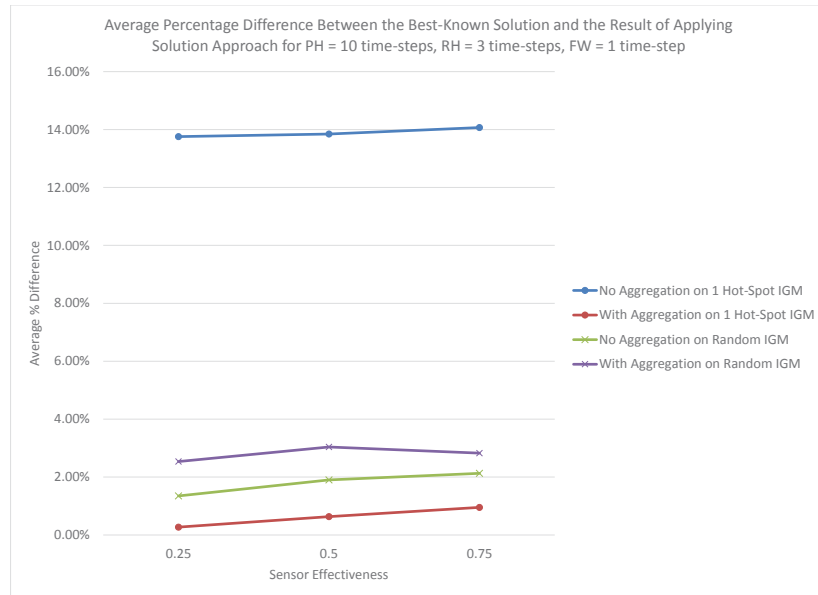
Figure 5.15: Average Percentage Difference Between the Solution Obtained With and Without Aggregation and the Best Known Solution for PH = 10 time-steps, RH = 3 time-steps, FW = 1 time-step
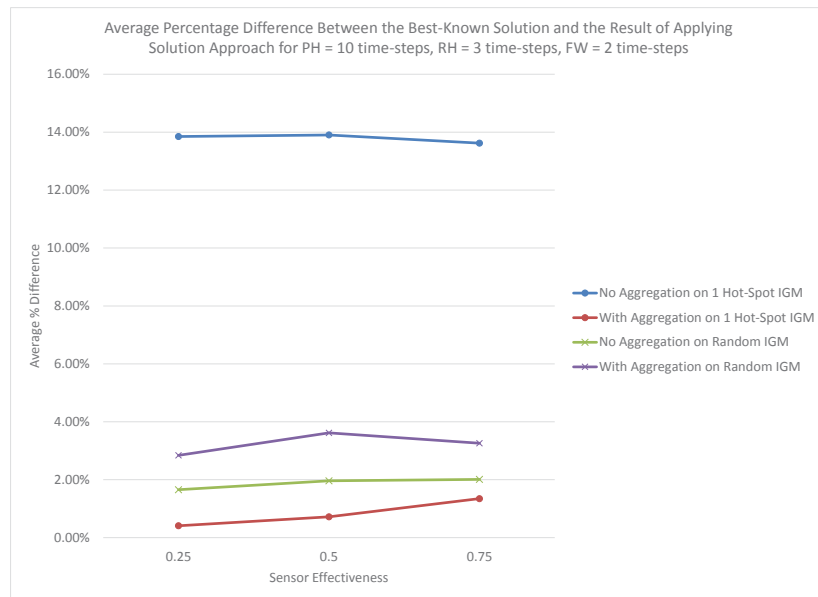
Figure 5.16: Average Percentage Difference Between Solution Quality With and Without Aggregation an the Best Known Solution for PH = 10 time-steps, RH = 3 time-steps, FW = 2 time-step
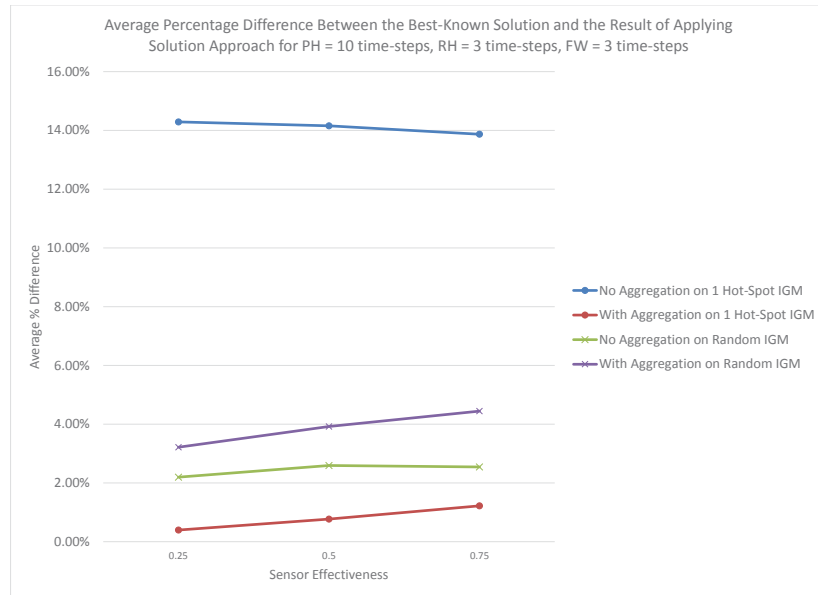
Figure 5.17: Average Percentage Difference Between Solution Quality With and Without Aggregation an the Best Known Solution for PH = 10 time-steps, RH = 3 time-steps, FW = 3 time-step
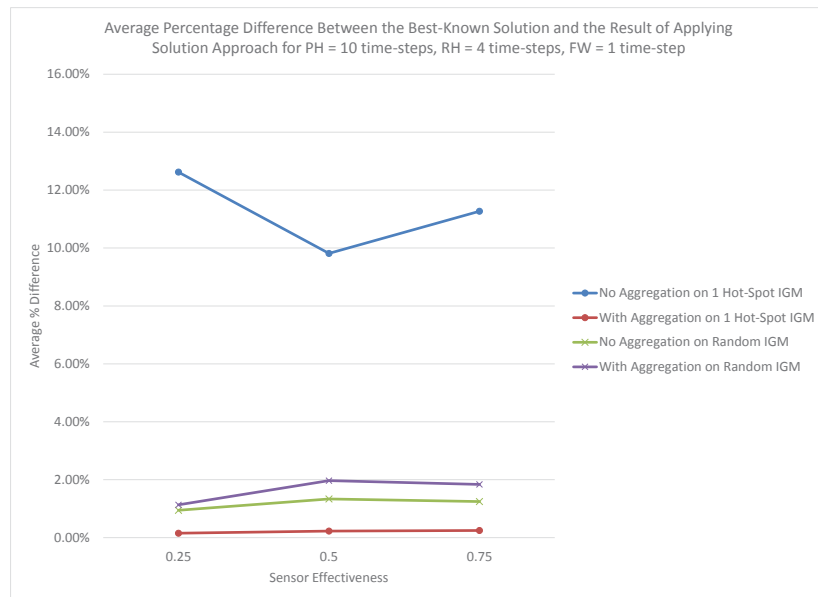
Figure 5.18: Average Percentage Difference Between Solution Quality With and Without Aggregation an the Best Known Solution for PH = 10 time-steps, RH = 4 time-steps, FW = 1 time-step
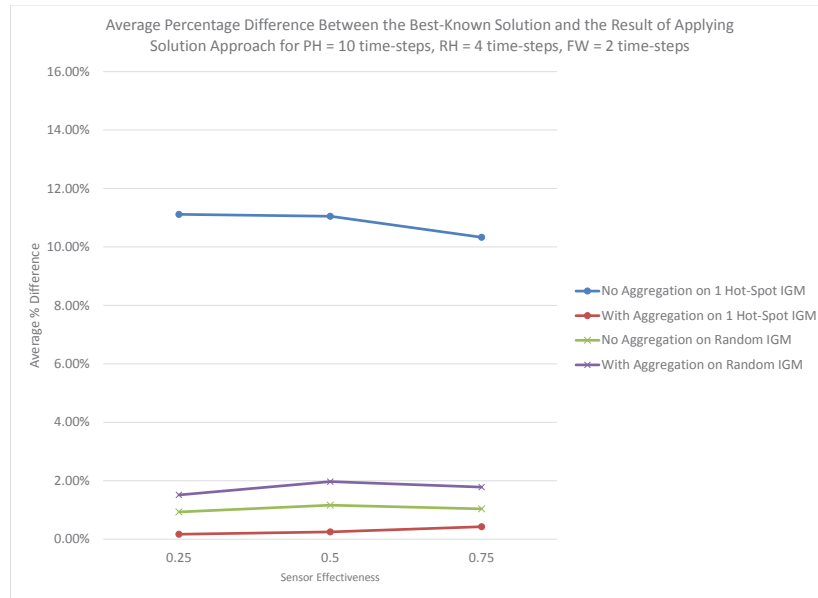
Figure 5.19: Average Percentage Difference Between Solution Quality With and Without Aggregation an the Best Known Solution for PH = 10 time-steps, RH = 4 time-steps, FW = 2 time-step
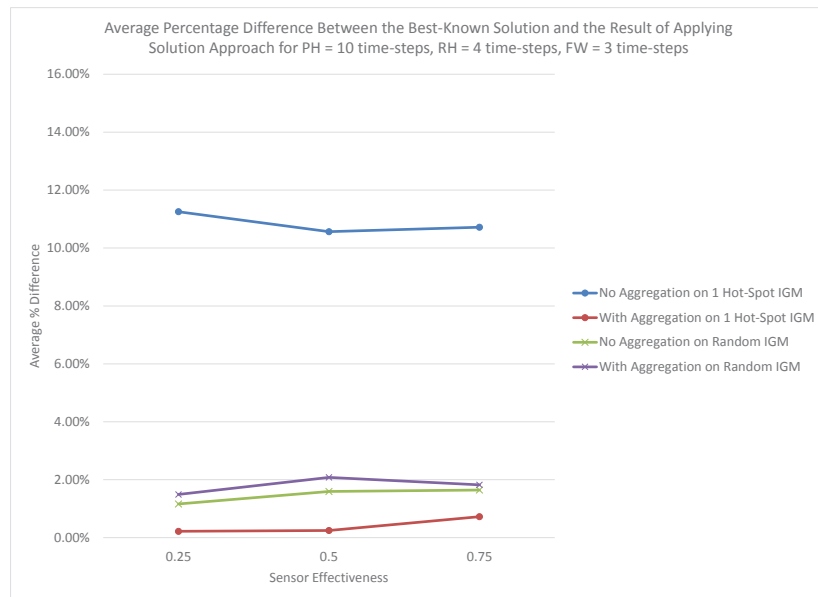
Figure 5.20: Average Percentage Difference Between Solution Quality With and Without Aggregation an the Best Known Solution for PH = 10 time-steps, RH = 4 time-steps, FW = 3 time-step
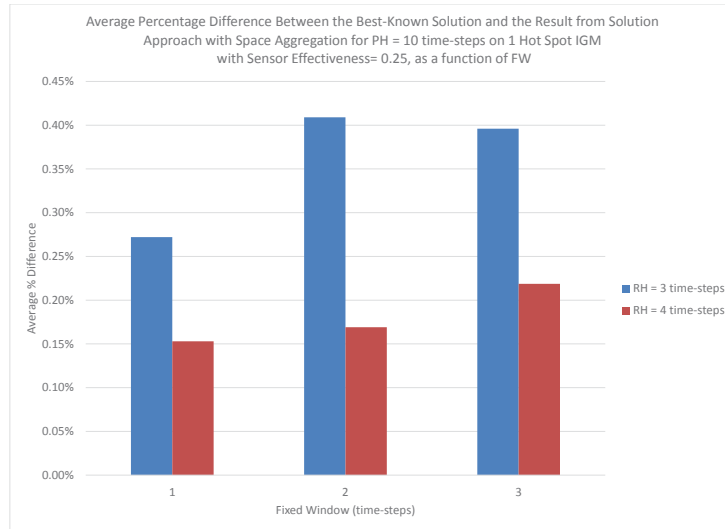
Figure 5.21: Average Percentage Difference Between the Best-Known Solution and the Result from Solution Approach with Space Aggregation for PH = 10 time-steps on 1 Hot Spot IGM with Sensor Effectiveness= 0.25, as a function of FW

In terms of the impact of the FW to the solution quality of the overall solution strategy (i.e., time and space aggregation), Figure 5.21 - Figure 5.23 present a comparison of the average percentage difference between the solution obtained for different FWs and the best known solution for cases on the 1 Hot Spot IGM and sensor effectiveness = 0.25, 0.50 and 0.75, respectively. A similar comparison is made for the cases on the Random IGM and sensor effectiveness = 0.25, 0.50 and 0.75, and shown in Figure 5.24 - Figure 5.26, respectively. Space aggregation was part of the solution strategy for the results shown in these figures. A FW = 1 time-step defined trajectories resulting, on average, in better overall potential information gain. Although the magnitude of the changes are different, this behavior was consistent regardless of the type of IGM and sensor effectiveness. Intuitively, a FW = 1 time-step provides a solution strategy where the routes are cautiously defined by only committing to the initial time-step of the solution of each subproblem in a cascade. This gives the procedure more opportunities to correct any decisions (moves) on the vehicle's path based on the additional information that might be considered on subsequent cascades. As discussed above, the tradeoff is the required computational time to solve the problem.
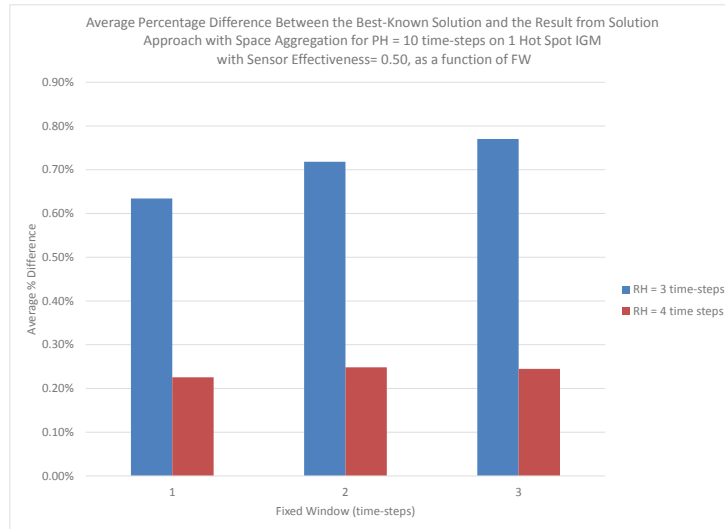
Figure 5.22: Average Percentage Difference Between the Best-Known Solution and the Result from Solution Approach with Space Aggregation for PH = 10 time-steps on 1 Hot Spot IGM with Sensor Effectiveness= 0.50, as a function of FW
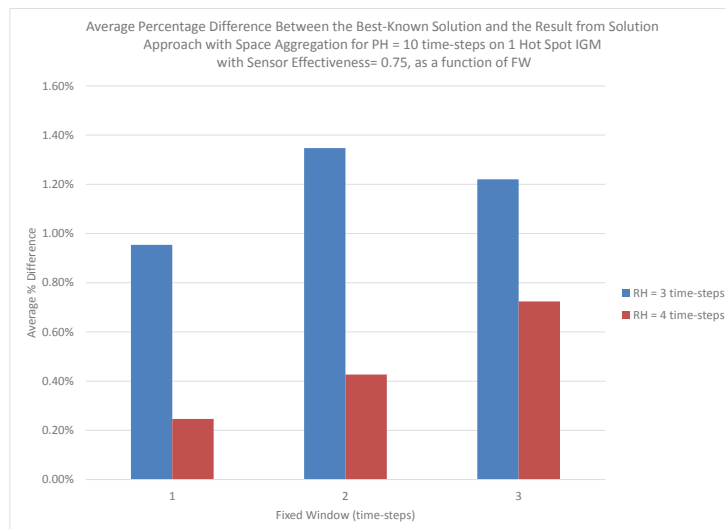
Figure 5.23: Average Percentage Difference Between the Best-Known Solution and the Result from Solution Approach with Space Aggregation for PH = 10 time-steps on 1 Hot Spot IGM with Sensor Effectiveness= 0.75, as a function of FW
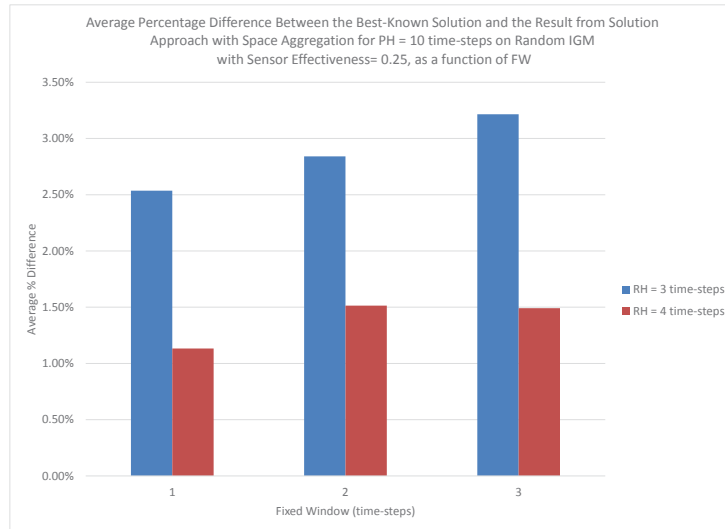
Figure 5.24: Average Percentage Difference Between the Best-Known Solution and the Result from Solution Approach with Space Aggregation for PH = 10 time-steps on Random IGM with Sensor Effectiveness= 0.25, as a function of FW
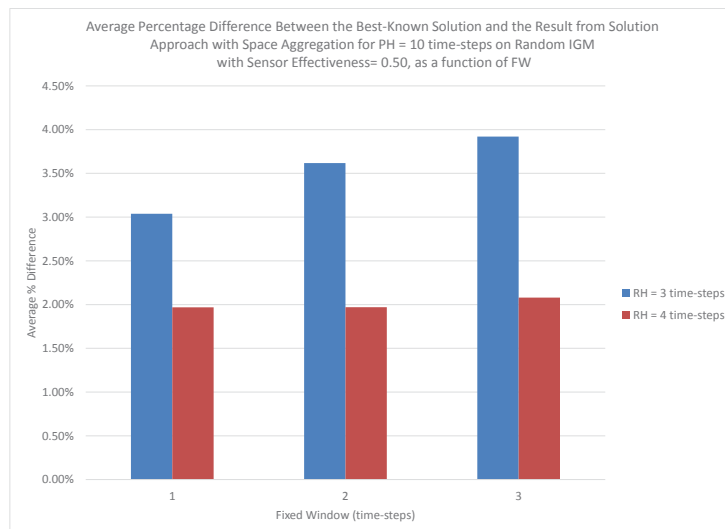
Figure 5.25: Average Percentage Difference Between the Best-Known Solution and the Result from Solution Approach with Space Aggregation for PH = 10 time-steps on Random IGM with Sensor Effectiveness= 0.50, as a function of FW
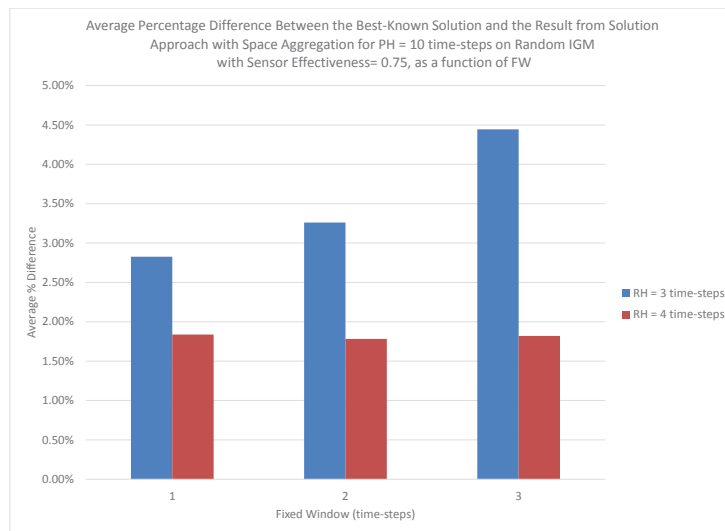
Figure 5.26: Average Percentage Difference Between the Best-Known Solution and the Result from Solution Approach with Space Aggregation for PH = 10 time-steps on Random IGM with Sensor Effectiveness= 0.75, as a function of FW

Chapter 6

Extensions to Mathematical Model

6.1 Introduction

In this chapter, extensions to the mathematical model presented in Chapter 4 are described. Modifications to decision variables and constraints represent the modeling of additional considerations on communication networks and situations among cooperative collection assets . The first update to the Mixed-Integer Linear Program (MILP) includes the addition of control centers or stations to the information gathering system: entities in current operational systems that manage the plans of information collection assets. Control Stations (CSs) can be stationary or move within the Area of Operation (AO). It is assumed that CSs provide no collection capabilities to the mission, although this limitation can be relaxed easily in the formulation. With these assumptions, information exchange occurs between CSs and not directly between collection assets. Collection assets are restricted to remain within communication range of its CS. Section 6.2 captures the updates to the model and results for this extension.

In Chapter 4 it was assumed that, in order to communicate and exchange information, collection assets should be within a bounded communication range to all other assets in the network, effectively creating a fully connected network. This was also the assumption for the communication between CSs with the initial extensions to the model in Section 6.2. A different communication network topology is possible in which assets use other assets as intermediary (or "bridge") nodes to exchange information. In this case, assets are not required to have a direct communication link

(within its communication range) to all other assets in the network: information is exchanged between assets as long as there is a communication path between them. In Section 6.3, updates to the mathematical model are described in order to relax the constraints of a direct communication link topology and allow assets to identify communication paths to exchange information. Theoretical mathematical proofs and numerical examples of the application of these extensions to the mathematical model are also included as part of this section.

Knowledge about an asset (e.g., location, plans, etc.) might be known to other assets even when they are not part of the same network at a given point in time. This information may have an impact in the definition and selection of routes for a collection asset. The concept of *trust* used in this research is introduced in Section 6.4. Trust (with a suitable decay factor as a function of time) on the potential location of assets that are not part of a connected component is considered as part of additional extensions to the optimization model.

6.2   Support to Systems Using Ground Control Stations

Operational collection assets may receive tasking and route plans from remote control centers or stations. These CSs can be stationary or move within the AO. The mathematical program defined in Chapter 4 is updated to support this type of information gathering systems. It is assumed that sensing of the AO is the responsibility of the collection assets; CSs provide no collection capabilities to the mission. This limitation can be relaxed easily in the formulation. Any information sharing occur between CSs and not directly between collection assets. Collection assets, however, are restricted to remain within communication range of its CS over the mission timeline. Section 6.2.1 captures the updates to the mathematical model.

6.2.1   Updates to Mathematical Model

Parameters

The following parameters are defined:

$$\text{CR}_i \quad \equiv \quad \text{communication range of information collection asset } i \text{ to its CS, } \text{CR}_i \geq 0, \ \forall i$$

$$\overline{\text{CR}}_i \quad \equiv \quad \text{communication range of information collection asset } i\text{'s CS to other CSs,} \ \overline{\text{CR}}_i \geq 0, \ \forall i$$

$$\varphi_{ik''k'k} \quad \equiv \quad \begin{cases} 1 & \text{if information collection asset } i\text{'s CS at cell } k'' \text{ at time } t-2 \text{ and} \\ & \text{at cell } k' \text{ at time } t-1 \text{ can be assigned to cell } k \text{ at time } t \\ 0 & \text{otherwise} \end{cases}$$

Main Decision Variables

The following decision variables are considered in the mathematical program:

$$y_{ikt} \quad = \quad \begin{cases} 1 & \text{if information collection asset } i\text{'s CS is assigned to cell } k \text{ at time-step } t \\ 0 & \text{otherwise} \end{cases}$$

$$\Delta_{ijt} \quad \equiv \quad \text{distance from information collection asset } i\text{'s CS to information collection} \ \text{asset } j\text{'s CS at time-step } t$$

$$c_{ijt} \quad = \quad \begin{cases} 1 & \text{if information collection asset } j\text{'s CS and information collection asset } i\text{'s} \\ & \text{CS are within communication range at time-step } t \\ 0 & \text{otherwise} \end{cases}$$

Objective Function

No changes are required to the objective function (4.1) to accommodate the requirements from CSs.

UV Assignment Constraints

$$\sum_{k \in K} \sum_{k' \in K} \eta_{kk'} \, x_{ikt} \, y_{ik't} \leq \text{CR}_i, \quad \forall i \in I, \forall t \in T \tag{6.1}$$

Constraint (6.1) ensures that information collection asset i remains within communication distance of its CS.

Let $b_{ikk't}$ be a binary variable to replace the nonlinear term $x_{ikt}\, y_{ik't}$, where

$$
b_{ikk't} \;=\;
\begin{cases}
1 & \text{if information collection asset } i \text{ is assigned to cell } k \text{ and its CS is assigned} \\
  & \text{to cell } k' \text{ at time-step } t \\
0 & \text{otherwise}
\end{cases}
$$

Constraint (6.1) is then replaced by

$$
\sum_{k \in K} \sum_{k' \in K} \eta_{kk'}\, b_{ikk't} \;\leq\; \mathrm{CR}_i, \qquad \forall i \in I, \forall t \in T \tag{6.2a}
$$

$$
b_{ikk't} \;\leq\; x_{ikt}, \qquad \forall i \in I, \forall k, k' \in K, \forall t \in T \tag{6.2b}
$$

$$
b_{ikk't} \;\leq\; y_{ik't}, \qquad \forall i \in I, \forall k, k' \in K, \forall t \in T \tag{6.2c}
$$

$$
b_{ikk't} \;\geq\; x_{ikt} + y_{ik't} - 1, \qquad \forall i \in I, \forall k, k' \in K, \forall t \in T \tag{6.2d}
$$

CS Assignment Constraints

Similar to Constraints (4.2) - (4.3), the assignment of CSs to a cell k is constrained by

$$
\sum_{k \in K} y_{ikt} = 1, \qquad \forall i \in I, \forall t \in T \tag{6.3}
$$

where Constraint (6.3) ensures that each CS is assigned a (single) cell each time-step t.

$$
\sum_{\substack{k \quad k' \quad k'' \\ k,k',k'' \in K \mid \varphi_{ik''k'k}=1}} o_{ik''k'kt} = 1, \qquad \forall i \in I, \forall t \in T \tag{6.4a}
$$

$$
o_{ik''k'kt} \;\leq\; \frac{y_{ikt} + y_{ik',t-1} + y_{ik'',t-2}}{3}, \qquad \forall i \in I, \forall k, k', k'' \in K \mid \varphi_{ik''k'k} = 1, \forall t \in T \tag{6.4b}
$$

Constraints (6.4) ensure that each CS i is assigned to a cell that can be reached at time-step t, given its assignment $y_{ik'',t-2}$ and $y_{ik',t-1}$ at times $t-2$ and $t-1$, respectively (see Section 6.2.1 for the definition of (parameter) $\varphi_{ik''k'k}$).

Communication Constraints

For communication objectives, consider

$$\Delta_{ijt} = \sum_{k \in K} \sum_{k' \in K} \eta_{kk'} \, y_{ikt} \, y_{jk't}, \quad \forall i, j \in I, \, j \neq i, \forall t \in T \tag{6.5}$$

$$\Delta_{ijt} \quad \leq \quad \overline{\mathrm{CR}}_i + (1 - c_{ijt})M, \quad \forall i, j \in I, \forall t \in T \tag{6.6}$$

Constraint (6.5) can be replaced by the following set of constraints, where the nonlinear term $y_{ikt} \, y_{jk't}$ is replaced by the binary variable $a_{ikjk't}$

$$\Delta_{ijt} \quad = \quad \sum_{k} \sum_{k'} \eta_{kk'} \, a_{ikjk't}, \quad \forall i, j \in I, \, \forall t \in T \tag{6.7}$$

$$a_{ikjk't} \quad \leq \quad y_{ikt}, \quad \forall i, j \in I, \, \forall k, k' \in K, \, \forall t \in T \tag{6.8}$$

$$a_{ikjk't} \quad \leq \quad y_{jk't}, \quad \forall i, j \in I, \, \forall k, k' \in K, \, \forall t \in T \tag{6.9}$$

$$a_{ikjk't} \quad \geq \quad y_{ikt} + y_{jk't} - 1, \quad \forall i, j \in I, \, \forall k, k' \in K, \, \forall t \in T \tag{6.10}$$

6.2.2   Results

Based on the concepts described in Section 6.2.1, a simulation was implemented to show the applicability and potential of the introduced extensions to the mathematical model. The assignment of 2 cooperative autonomous collection assets, in particular Unmanned Aerial Vehicles (UAVs), to surveil the littoral of an area represented by a grid of 10 x 10 cells is considered. Both UAVs are assumed to be controlled by stationary ground CSs. Figure 6.1 shows the selected area of operation and the location of the ground control stations. The CS of UAV 1 is located in cell $k = 83$ (or cell $(3, 9)$), CS of UAV 2 is located at cell $k = 66$ (or cell $(6, 7)$). Values of other relevant parameters during the simulation are captured in Table 6.1.

The littoral surveillance mission consists of two (2) collection requirements: (1) detecting incoming maritime vessels and (2) detecting vehicles approaching the coastline, both suspected to be involved in drug-related activities. A low potential information gain region for collection requirement 2 represents, for example, looking for a car in a body of water. The initial information gain map for each

Table 6.1: Mathematical Program and Experiment Parameters for CS Extension Model

Parameter	Value
Mathematical Program	
I	{1,2}
T	{1,2,...,10}
K	{1,2,...,100} (a 10-by-10 grid area)
R	{2}
$\overline{\text{CR}}_i$	4.0 ($\forall i \in I$)
α	0.5
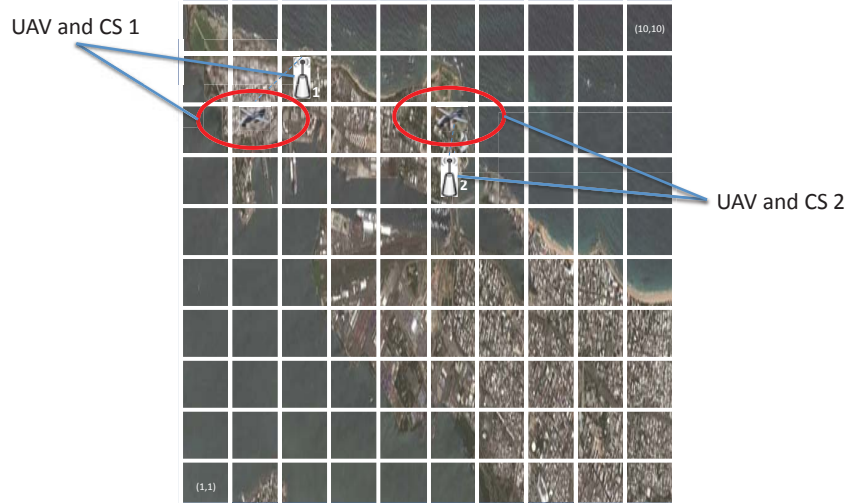
Figure 6.1: Area of Operation and Initial Location of CSs and UAVs

collection requirement is shown in Figure 6.2 and Figure 6.3, for collection requirements 1 and 2 respectively.

On-board sensors, on both UAVs, are assumed to have a discretized effectiveness of collecting information only on the assigned cell. Discretized sensor effectiveness values are captured in Table 6.2. Moreover, UAVs can only move to horizontally or vertically adjacent cells; no diagonal movement is allowed. The communication range between each UAV and its respective CS is 4 distance units.

A decentralized framework in which each UAV is operating independently is considered.

	Collection Requirement 1	Collection Requirement 2
UAV 1	0.75	0.25
UAV 2	0.5	0.5

Table 6.2: Discretized Effectiveness Sensor Suite on each UAV for each Collection Requirement
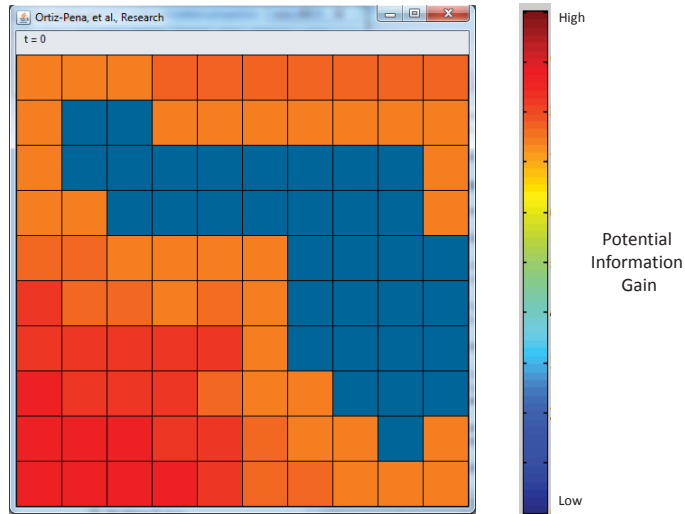
Figure 6.2: Initial Potential Information Gain Map for Collection Requirement 1

Exchange of information and coordination only occurs when the respective CSs are within communication range of each other. For this example, the CSs are stationary and their respective communication radius allow them to share information over the mission timeline. Each unmanned
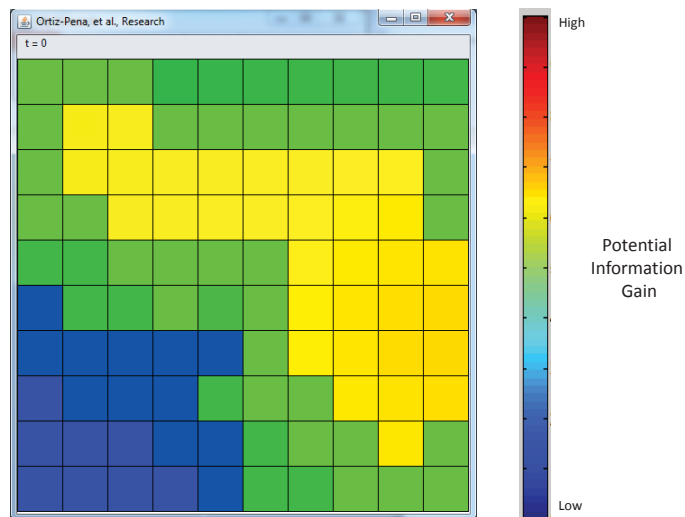
Figure 6.3: Initial Potential Information Gain Map for Collection Requirement 2

vehicle system is solving the mathematical programing model considering only its perceived environment, derived from the information received by the on-board sensors in the UAV, and any information received from neighboring CSs. The UAVs have the same initial potential information gain map and their altitude is assumed to be fixed.

The routes defined for each UAV in 2 situations regarding littoral surveillance are compared. Two cases are considered in which the priorities assigned to each collection requirement differ. In the first case, the priority of surveilling the littoral for incoming vessels is higher than detecting vehicles on land. In the mathematical programming model this is represented by setting $w_{1t} = 0.80$ and $w_{2t} = 0.20$, $\forall t$ in the objective function. The linearized formulation described in Sections 4.2 - 4.4 using CPLEX Interactive Optimizer 12.2 [50] is solved. The routes defined for both UAVs locate them closer to the littoral, keeping both UAVs always within communication range of its CS but maximizing the coverage area (i.e., disjoint sensors coverage area). This is shown in Figure 6.4. In the second case, both objectives were assumed to be equally important ($w_{1t} = 0.50$ and $w_{2t} = 0.50$, $\forall t$). For this case, UAV 1, having the best sensor suite to detect maritime vessels is assigned to cover most of the littoral and UAV 2 is assigned the inland surveillance (see Figure 6.5).
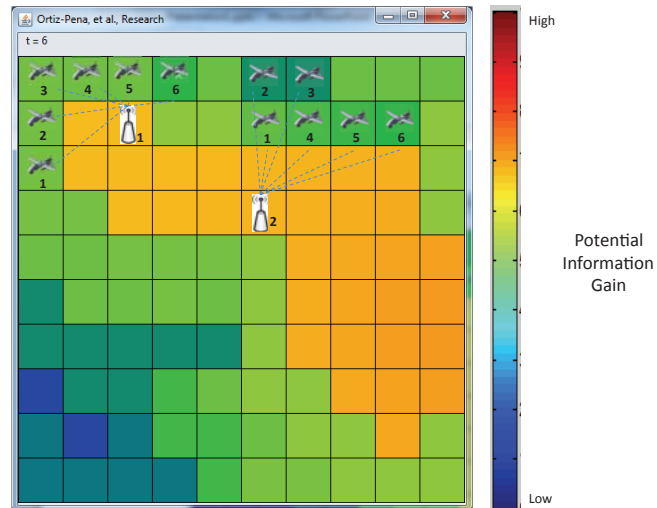
Figure 6.4: Defined Routes for UAVs in Case 1
($w_{1t} = 0.80$ and $w_{2t} = 0.20$, $\forall t$ in the objective function)
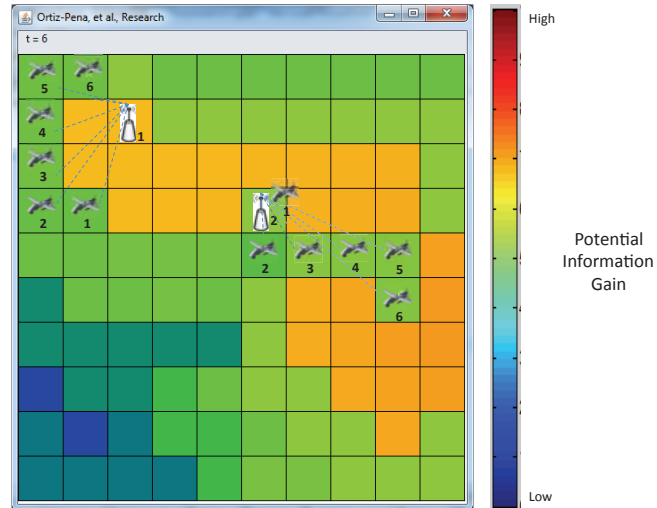
Figure 6.5: Defined Routes for UAVs in Case 2
($w_{1t} = 0.50$ and $w_{2t} = 0.50$, $\forall t$ in the objective function)

6.3   Network Connectivity through Asset Paths

A communication network topology is possible in which assets use other assets as intermediary (or "bridge") nodes to exchange information. In this case, assets are not required to have a direct communication link (within its communication range) to all other assets in the network: information is exchanged between assets as long as there is a communication path between them. In Section 6.3, updates to the mathematical model presented in Sections 4.2 - 4.4 are described in order to relax the constraints of a direct communication link topology and allow assets to identify communication paths to exchange information. Theoretical mathematical proofs and numerical examples of the application of these extensions to the mathematical model are also included as part of this section.

6.3.1   Updates to Mathematical Model

As described above, let

$$c_{ij} \equiv \text{direct communication link between } i \text{ and } j,\ i,j \in J$$

Moreover, let

$$I \equiv \text{set of collection assets in a connected component} = \{1, 2, \ldots, |I|\}$$

The constraints in Section 4.4 that all assets need to be directly connected to all other assets were relaxed. Instead, the relaxation allows each asset to have a communication path to all other assets in its connected component. For each pair of collection assets, $i, j \in I, i \neq j$, there should exists a path, a set of communication links $c_{k,k'} = 1$ so that i can send its information to j. Assume that this set is represented by $C^{(ij)}$

$$C^{(ij)} = \{c_{ik_1}, c_{k_1,k_2}, \cdots, c_{k_n,j}\}$$

where n is the number of required "bridge" assets to connect i and j. When $n = 0$, i and j are connected directly by the communication link c_{ij} so the set $C^{(ij)}$ for this case is

$$C^{(ij)} = \{c_{ij}\}$$

Goal: Define a set of constraints to preserve the connected component I.

6.3.2   Additional Decision Variables

Define

$$y_k^{ij} \equiv i \text{ is connected to } j \text{ via } k = \begin{cases} 1 & \text{if } i \text{ is connected to } j \text{ via } k \\ 0 & \text{otherwise} \end{cases} \quad , i, j, k \in I, i \neq j \neq k$$

6.3.3   Additional Constraints

Consider the following set of constraints to preserve the connected component I:

$$c_{ij} + \sum_{k \in I, k \neq i \neq j} y_k^{ij} = 1 \quad \forall i, j \in I, i \neq j \tag{6.11}$$

$$c_{ik} + c_{kj} + \sum_{k' \in I, k' \neq i \neq j \neq k} y_{k'}^{kj} \geq 2 \cdot y_k^{ij} \quad \forall i, j, k \in I, i \neq j \neq k \tag{6.12}$$

$$\sum_{j \in I, j \neq i} c_{ij} \geq 1 \quad \forall i \in I \tag{6.13}$$

$$\sum_{j \in I, i \neq j} c_{ji} \geq 1 \quad \forall i \in I \tag{6.14}$$

Constraint (6.11) indicates that each pair of assets i and j in I are connected if (1) there exists a direct communication link between i and j, or (2) these assets are connected via another asset k. Constraint (6.12) captures when i is connected to j by a "bridge" asset k that is either (1) directly connected to j, or (2) connected to an asset k' that is connected (not necessarily directly) to j . Constraint (6.13) captures the need to have at least 1 communication link from some asset to i (to receive information from other assets). Similarly, Constraint (6.14) captures the need to have at least 1 communication link out of i (to send information to other assets). Given that this set of constraints enforces that there is a path between each pair of assets $i, j \in I$, (as will be proved in Section 6.3.4), the connected component I is preserved.

Constraints (6.11) to (6.14) replace Constraint (4.24) in the mathematical model when a path between each pair of asset is sufficient to maintain a connected component in the communication network.

6.3.4   Proof that Constraints (6.11) - (6.14) are Sufficient and Necessary Conditions

To show Constraints (6.11) - (6.14) are sufficient and necessary conditions to identify network topologies that preserve a connected component, consider the following:

Theorem 1. *A path connecting i and j is not affected by having additional communication links $c_{k,k'} = 1, k, k' \in I\ k \neq k'$ in the network.*

Proof. Consider the set $C^{(ij)} = \{c_{ik_1}, c_{k_1,k_2}, \cdots, c_{k_n,j}\}$ as the set of communication links defining a path between i and j Adding communication links to $C^{(ij)}$, $c_{k,k'} = 1$, $k, k' \in I$, $k \neq k'$, creates a new set C', where

$$C' = \{c_{ik_1}, c_{k_1,k_2}, \cdots, c_{k_n,j}, c_{k,k'}\}$$

This is simply the union of $C^{(ij)}$ and any additional $c_{k,k'} = 1$ in the network. So,

$$C' = C^{(ij)} \cup \{c_{k,k'}\}$$

Since the set $C^{(ij)}$ is preserved, the path connecting i and j is not affected by additional communication links $c_{k,k'} = 1, k, k' \in I \; k \neq k'$ in the network.   QED

Corollary 1.1. *A path connecting i and j consisting of the direct communication link $c_{ij} = 1$ is not affected by having additional communication links $c_{k,k'} = 1, k, k' \in I \; k \neq k'$ in the network.*

Proof. Consider the set $C^{(ij)} = \{c_{ij}\}$ for the case of a direct communication link between i and j. Adding communication links to $C^{(ij)}$, $c_{k,k'} = 1$, $k, k' \in I$, $k \neq k'$, create a new set C', where

$$C' = \{c_{ij}, c_{k,k'}\}$$

This is simply the union of $C^{(ij)}$ and any additional $c_{k,k'} = 1$ in the network. So,

$$C' = C^{(ij)} \cup \{c_{k,k'}\}$$

Since the set C is preserved, the path connecting i and j is not affected by additional communication links $c_{k,k'} = 1, k, k' \in I \; k \neq k'$ in the network.   QED

Theorem 2. *For any pair of connected assets $i, j \in I$, $i \neq j$, Constraints (6.11) - (6.14) are not affected by additional communication links $c_{k,k'} = 1$, $k \neq i, k' \neq j$ in the network.*

Proof. Lets assume that $C^{(ij)}$ is the set of required communication links $c_{k,k'} = 1, k, k' \in I$ required to establish a path between i and j.

$$C^{(ij)} = \{c_{ik_1}, c_{k_1,k_2}, \cdots, c_{k_n,j}\}$$

where n is the number of required "bridge" assets to connect i and j. Assume adding communication link $c_{k,k'} = 1$, $k \neq i, k' \neq j$ to the network affects the path between i and j by having $c_{ij} = 1$ so the set of Constraints (6.11) - (6.14) will not be enforced.

From Constraint (6.11), $c_{ik} = 1$

$\Rightarrow \sum_{k' \in I, k' \neq i \neq j} y_{k'}^{ik} = 0$

$\Rightarrow y_{k'}^{ik} = 0 \, \forall k'.$

For $c_{k_n,j}$, $c_{k_n,j} = 1 \Rightarrow \sum_{k' \in I, k' \neq i \neq j} y_{k'}^{i,k_n} = 0$

$\Rightarrow y_{k'}^{ik} = 0 \, \forall k'.$

$c_{ik} = 1 \Rightarrow \sum_{k' \in I, k' \neq i \neq j} y_{k'}^{ik} = 0$

$\Rightarrow y_{k'}^{ik} = 0 \, \forall k'.$

Given that c_{ij} and $y_k^{ij} \in \{0,1\}$, Constraint (6.12) will always be satisfied. Moreover, Constraints (6.13) - (6.14) will continue to be met since the summations are over non-negative numbers.

$\Rightarrow$ Contradiction.

$\therefore$ Constraints (6.11) - (6.14) are not affected by additional communication links $c_{k,k'} = 1$, $k \neq i, k' \neq j$ in the network.   QED

Corollary 2.1. *For any pair of assets $i, j \in I$, $i \neq j$, the communication path created by a direct communication link (i.e., $c_{ij} = 1$), Constraints (6.11) - (6.14) are not affected by additional communication links $c_{k,k'} = 1$, $k \neq i, k' \neq j$ in the network.*

Proof. Assume adding communication link $c_{k,k'} = 1$, $k \neq i, k' \neq j$ to the network affects the path between i and j by having $c_{ij} = 1$ so the set of Constraints (6.11) - (6.14) will not be enforced.

From Constraint (6.11), $c_{ij} = 1$

$\Rightarrow \sum_{k \in I, k \neq i \neq j} y_k^{ij} = 0$

$\Rightarrow y_k^{ij} = 0 \, \forall k \in K.$

Given that c_{ij} and $y_k^{ij} \in \{0,1\}$, Constraint (6.12) will always be met. Moreover, Constraints (6.13) - (6.14) will continue to be met since the summations are over non-negative numbers.

$\Rightarrow$ Contradiction.

$\therefore$ Constraints (6.11) - (6.14) are not affected by additional communication links $c_{k,k'} = 1$, $k \neq i, k' \neq j$ in the network.   QED

Theorem 3. *Constraints (6.11) - (6.14) are sufficient to identify a network preserving a connected component*

Proof. Assume Constraints (6.11) - (6.14) do not hold for a set I capturing the set of assets in a connected component. For any pair of assets i and j, let the set C be the set of communication links

$c_{k,k'} = 1, k, k' \in I$ required to establish a path between each i and j.

$$C = \{c_{ik_1}, c_{k_1 k_2}, \cdots, c_{k_n,j}\}$$

where n is the number of required "bridge" assets to connect i and j. Given $c_{ik_1} = 1$, Constraint (6.13) is satisfied. Similarly, given $c_{k_n,j} = 1$, Constraint (6.14) is satisfied.

From (6.11), $\exists! k : y_k^{ij} = 1$. Without loss of generality, let this k be k_1. From Constraint (6.12), $c_{k_1,j} + \sum_{k' \in I, k' \neq i \neq j \neq k_1} y_{k'}^{k_1,j} \geq 1$. However, from Constraint (6.11) applied to the pair of assets k_1 and j, $c_{k_1,j} + \sum_{k' \in I, k' \neq i \neq j \neq k_1} y_{k'}^{k_1,j} = 1$. If $c_{k_1,j} = 1$, Constraint (6.12) is satisfied for i and j using k_1 as the "bridge" asset and we have a path between assets i and j. Otherwise, $c_{k_1,j} = 0$, so $\sum_{k' \in I, k' \neq i \neq j \neq k_1} y_{k'}^{k_1,j} = 1$. $\sum_{k' \in I, k' \neq i \neq j \neq k_1} y_{k'}^{k_1,j} = 1$ in turn implies that $\exists! k' : y_{k'}^{k_1,j} = 1$. Let this k' be k_2. From Constraint (6.12) for k_1, j, and k_2 and using the fact that $c_{k_1,k_2} = 1$, $c_{k_2,j} + \sum_{k' \in I, k' \neq i \neq j \neq k_1 \neq k_2} y_{k'}^{k_2,j} \geq 1$. The same argument is used successively, until (6.12) is applied to assets $k_{n-1,n}$, n and j. For this case, $c_{k_{n-1},k_n} + c_{k_n,j} + \sum_{k' \in I, k' \neq i \neq j \neq k_1 \neq k_2 \neq \cdots \neq k_n} y_{k'}^{k_n,j} \geq 2$. But $c_{k_{n-1},k_n} = 1$ and $c_{k_n,j} = 1$ so the above constraint is satisfied and no additional communication link is required to connect i and j. This is applied to all pairs of assets in the connected component I. As indicated in Theorem 1, if there is a path from any i and j, adding more communication links to the connected component do not affect the path between them.

$\Rightarrow$ Contradiction.

$\therefore$ The set of Constraints (6.11) - (6.14) are sufficient to verify that a set of communication links connect any 2 assets i and j.   QED

Theorem 4. *Constraints (6.11) - (6.14) are necessary to identify a connected component.*

Proof. Consider the set $C^{(ij)}$. Assume communication link $c_{a,b}$ is lost (i.e., $c_{a,b} = 0$), $a, b \in I$, so i and j are no longer connected. Under these conditions, let's assume that Constraints (6.11) - (6.14) hold. Three cases are identified:

1. $a = i$, $b = k$ so $c_{ik} = 0$

2. $a = k_n$, $b = j$ so $c_{k_n,j} = 0$

3. (Without loss of generality) $a = k_1$, $b = k_2$ so $c_{k_1,k_2} = 0$

Case 1: $c_{ik} = 0$.

  If $c_{ik} = 0$, Constraint (6.13) is not satisfied. $\Rightarrow$ Contradiction.

Case 2: $c_{k_n,j} = 0$.

  If $c_{k_n,j} = 0$, Constraint (6.14) is not satisfied. $\Rightarrow$ Contradiction.

Case 3: $c_{k_1,k_2} = 0$.

  Constraint (6.11) for k_1 and k_2 indicates that $c_{k_1,k_2} + \sum_{k \in I, k \neq k_1 \neq k_2} y_k^{k_1,k_2} = 1 \quad \forall k_1, k_2 \in I, k_1 \neq k_2$. Given that $c_{k_1,k_2} = 0$, this implies that $\sum_{k \in I, k \neq k_1 \neq k_2} y_k^{k_1,k_2} = 1 \quad \forall k_1, k_2 \in I, k_1 \neq k_2$. $\Rightarrow \exists! k : y_k^{k_1,k_2} = 1$. Let assume that k is $\bar{k}$.

Constraint (6.12), indicates $c_{k_1,\bar{k}} + c_{\bar{k},k_2 j} + \sum_{k' \in I, k' \neq k_1 \neq k_2 \neq \bar{k}} y_{k'}^{\bar{k},j} \geq 2$. Given that $c_{k_1,k_2} = 0$,

$c_{k_2,j} + \sum_{k' \in I, k' \neq i \neq j \neq k} y_{k'}^{kj} \geq 2$ but from (6.11), $\exists! k : k_2, j$

$c_{k_2,j} + \sum_{k' \in I, k' \neq i \neq j \neq k} y_{k'}^{kj} = 1 \Rightarrow 1 \geq 2 \Rightarrow$ (6.12) is not satisfied $\Rightarrow$ Contradiction.   QED

6.3.5   Numerical Examples

Homogeneous Communication Radii

To show how Constraints (6.11) - (6.14) capture that a given network preserves the connected component, consider a numerical example in which

$$I = \{1, 2, 3, 4, 5\}$$

For the case in which all assets $i \in I$ have homogenous communication radii, $c_{ij} = c_{ji}$. With this,

$$y_k^{ij} = y_k^{ji} \quad \forall i, j, k \in I, i \neq j \neq k \tag{6.15}$$

For the set I and assumptions above, the following constraints, from Constraints (6.11) - (6.14), will be generated:

(from Constraint (6.11))

$$c_{12} + y_3^{12} + y_4^{12} + y_5^{12} = 1 \tag{6.16}$$

$$c_{13} + y_2^{13} + y_4^{13} + y_5^{13} = 1 \tag{6.17}$$

$$c_{14} + y_2^{14} + y_3^{14} + y_5^{14} = 1 \tag{6.18}$$

$$c_{15} + y_2^{15} + y_3^{15} + y_4^{15} = 1 \tag{6.19}$$

$$c_{23} + y_1^{23} + y_4^{23} + y_5^{23} = 1 \tag{6.20}$$

$$c_{24} + y_1^{24} + y_3^{24} + y_5^{24} = 1 \tag{6.21}$$

$$c_{25} + y_1^{25} + y_3^{25} + y_4^{25} = 1 \tag{6.22}$$

$$c_{34} + y_1^{34} + y_2^{34} + y_5^{34} = 1 \tag{6.23}$$

$$c_{35} + y_1^{35} + y_2^{35} + y_4^{35} = 1 \tag{6.24}$$

$$c_{45} + y_1^{45} + y_2^{45} + y_3^{45} = 1 \tag{6.25}$$

(from Constraint (6.12))

$$c_{13} + c_{23} + y_4^{23} + y_5^{23} \geq 2 \cdot y_3^{12} \tag{6.26}$$

$$c_{14} + c_{24} + y_3^{24} + y_5^{24} \geq 2 \cdot y_4^{12} \tag{6.27}$$

$$c_{15} + c_{25} + y_3^{25} + y_4^{25} \geq 2 \cdot y_5^{12} \tag{6.28}$$

$$c_{12} + c_{23} + y_4^{23} + y_5^{23} \geq 2 \cdot y_2^{13} \tag{6.29}$$

$$c_{14} + c_{34} + y_2^{34} + y_5^{34} \geq 2 \cdot y_4^{13} \tag{6.30}$$

$$c_{15} + c_{35} + y_2^{35} + y_4^{35} \geq 2 \cdot y_5^{13} \tag{6.31}$$

$$c_{12} + c_{24} + y_3^{24} + y_5^{24} \geq 2 \cdot y_2^{14} \tag{6.32}$$

$$c_{13} + c_{34} + y_2^{34} + y_5^{34} \geq 2 \cdot y_3^{14} \tag{6.33}$$

$$c_{15} + c_{45} + y_2^{45} + y_3^{45} \geq 2 \cdot y_5^{14} \tag{6.34}$$

$$c_{12} + c_{25} + y_3^{25} + y_4^{25} \geq 2 \cdot y_2^{15} \tag{6.35}$$

$$c_{13} + c_{35} + y_2^{35} + y_4^{35} \geq 2 \cdot y_3^{15} \tag{6.36}$$

$$c_{14} + c_{45} + y_2^{45} + y_3^{45} \geq 2 \cdot y_4^{15} \tag{6.37}$$

$$c_{12} + c_{13} + y_4^{13} + y_5^{13} \geq 2 \cdot y_1^{23} \tag{6.38}$$

$$c_{24} + c_{34} + y_1^{34} + y_5^{34} \geq 2 \cdot y_4^{23} \tag{6.39}$$

$$c_{25} + c_{35} + y_1^{35} + y_4^{35} \geq 2 \cdot y_5^{23} \tag{6.40}$$

$$c_{12} + c_{14} + y_3^{14} + y_5^{14} \geq 2 \cdot y_1^{24} \tag{6.41}$$

$$c_{23} + c_{34} + y_1^{34} + y_5^{34} \geq 2 \cdot y_3^{24} \tag{6.42}$$

$$c_{25} + c_{45} + y_1^{45} + y_3^{45} \geq 2 \cdot y_5^{24} \tag{6.43}$$

$$c_{12} + c_{15} + y_3^{15} + y_4^{15} \geq 2 \cdot y_1^{25} \tag{6.44}$$

$$c_{23} + c_{35} + y_1^{35} + y_4^{35} \geq 2 \cdot y_3^{25} \tag{6.45}$$

$$c_{24} + c_{45} + y_1^{45} + y_3^{45} \geq 2 \cdot y_4^{25} \tag{6.46}$$

$$c_{13} + c_{14} + y_2^{14} + y_5^{14} \geq 2 \cdot y_1^{34} \tag{6.47}$$

$$c_{23} + c_{24} + y_1^{24} + y_5^{24} \geq 2 \cdot y_2^{34} \tag{6.48}$$

$$c_{35} + c_{45} + y_1^{45} + y_2^{45} \geq 2 \cdot y_5^{34} \tag{6.49}$$

$$c_{13} + c_{15} + y_2^{15} + y_4^{15} \geq 2 \cdot y_1^{35} \tag{6.50}$$

$$c_{23} + c_{25} + y_1^{25} + y_4^{25} \geq 2 \cdot y_2^{35} \tag{6.51}$$

$$c_{34} + c_{45} + y_1^{45} + y_2^{45} \geq 2 \cdot y_4^{35} \tag{6.52}$$

$$c_{14} + c_{15} + y_2^{15} + y_3^{15} \geq 2 \cdot y_1^{45} \tag{6.53}$$

$$c_{24} + c_{25} + y_1^{25} + y_3^{25} \geq 2 \cdot y_2^{45} \tag{6.54}$$

$$c_{34} + c_{35} + y_1^{35} + y_2^{35} \geq 2 \cdot y_3^{45} \tag{6.55}$$

Note that Constraint (6.15) and the equality $c_{ij} = c_{ji}$, $\forall i, j \in I$ were included in the constraints above.

Now, consider in particular the case where information collection asset 1 is connected to information

collection asset 2 via a direct communication link, information collection asset 2 is connected to information collection asset 3 via a direct communication link, information collection asset 3 is connected to information collection asset 4 via a direct communication link, and, information collection asset 4 is connected to information collection asset 5 via a direct communication link (as depicted in Figure 6.6). The binary variables capturing this network are:
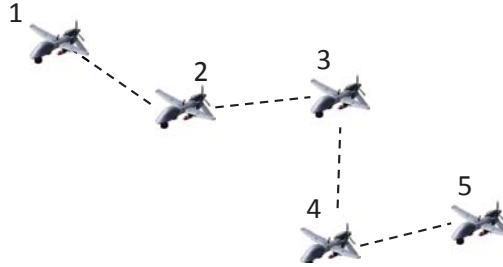
Figure 6.6: Network Connectivity through Asset Paths - Test Case 1

$$c_{12} = 1 \tag{6.56a}$$

$$c_{13} = 0 \tag{6.56b}$$

$$c_{14} = 0 \tag{6.56c}$$

$$c_{15} = 0 \tag{6.56d}$$

$$c_{23} = 1 \tag{6.56e}$$

$$c_{24} = 0 \tag{6.56f}$$

$$c_{25} = 0 \tag{6.56g}$$

$$c_{34} = 1 \tag{6.56h}$$

$$c_{35} = 0 \tag{6.56i}$$

$$c_{45} = 1 \tag{6.56j}$$

To show how the different decision variables capture that the network connectivity (6.56) is a feasible solution (i.e., a connected component) based on the constraints above, observe the following "phases" of the proof:

1. Exploit connectivity information from direct communication links

2. Identify connectivity via network "bridges"

Exploit connectivity information from direct communication links

From Constraint (6.16), and noting that $c_{12} = 1$, we have $y_3^{12} = y_4^{12} = y_5^{12} = 0$. Similarly, from Constraint (6.20), and noting that $c_{23} = 1$, we have $y_1^{23} = y_4^{23} = y_5^{23} = 0$. From Constraint (6.23), and noting that $c_{34} = 1$, $\Rightarrow y_1^{34} = y_2^{34} = y_5^{34} = 0$. Finally, from Constraint (6.25), and noting that $c_{45} = 1, \Rightarrow y_1^{45} = y_2^{45} = y_3^{45} = 0$.

Now, with this information we know that, from Constraint (6.30), $y_4^{13} = 0$. (Note, Constraint (6.30) indicates that $1 \geq 2 \cdot y_4^{13} \Rightarrow y_4^{13} = 0$). Using the same observation, from (6.33), (6.34), (6.37), (6.43) and (6.46), y_3^{14}, y_5^{14}, y_4^{15}, y_5^{24}, and y_4^{25} are equal to 0, respectively.

We can further recognize that from Constraint (6.18), $y_2^{14} = 1$ and, from Constraint (6.32), $y_3^{24} = 1$ (Note, Constraint (6.32) indicates that $1 + y_3^{24} \geq 2 \Rightarrow y_3^{24} = 1$) which further implies that, from Constraint (6.21), $y_1^{24} = 0$. Also, from Constraint (6.50), $y_1^{35} = 0$ (Note, since $y_2^{15} \in \{0, 1\}$ Constraint (6.50) $\Rightarrow y_1^{35} = 0$.)

At this point in the analysis, variables y_2^{13}, y_5^{13}, y_2^{15}, y_3^{15}, y_1^{25}, y_3^{25}, y_2^{35}, and y_4^{35} are still "open", meaning that their value has not been determined.

Identify connectivity via network "bridges"

Observe that from Constraint (6.24), $y_2^{35} + y_4^{35} = 1$ which, from Constraint (6.31) we have $y_5^{13} = 0$, and from Constraint (6.36), $y_3^{15} = 0$. Now, from Constraint (6.17) we have $y_2^{13} = 1$, and from Constraint (6.19), $y_2^{15} = 1$.

These two previous steps allow us to recognize that, from Constraint (6.35), $y_3^{25} = 1$ (i.e., $1 + y_3^{25} \geq 2 \Rightarrow y_3^{25} = 1$), which, since $y_1^{25} = 0$ due to Constraint (6.19), $y_2^{35} = 0$ on Constraint (6.51). Finally, $y_4^{35} = 1$ from Constraint (6.24).

In summary, for this case,

- Information collection asset 1 is connected directly to information collection asset 2 ($c_{12} = 1$), and it is connected to the other information collection assets in the network via this information collection assets ($y_2^{13} = y_2^{14} = y_2^{15} = 1$).

- Information collection asset 2 is connected directly to information collection asset 1 and to information collection asset 3 ($c_{12} = c_{23} = 1$), and it is connected to information collection assets 4 and 5 via information collection asset 3 ($y_3^{24} = y_3^{25} = 1$).

- Information collection asset 3 is connected directly to information collection asset 2 and to information collection asset 4 ($c_{23} = c_{34} = 1$), and it is connected to information collection asset 1 via information collection asset 2 ($y_2^{13} = 1$) and to information collection asset 5 via information collection asset 4 ($y_4^{35} = 1$).

- Information collection asset 4 is connected directly to information collection asset 3 and to information collection asset 5 ($c_{34} = c_{45} = 1$), and it is connected to information collection asset 2 via information collection asset 3 ($y_3^{24} = 1$) and it is connected to information collection asset 1 via this path ($y_2^{14} = 1$).

- Information collection asset 5 is connected directly to information collection asset 4 ($c_{45} = 1$), and it is connected to information collection asset 3 via information collection asset 4 ($y_4^{35} = 1$) and to information collection assets 1 and 2 since either information collection asset 3 or 4 are communicating with them (as indicated above).

Now, let's update the network (6.56) by considering the case when information collection asset 2 and 3 are not within communication distance $\Rightarrow c_{23} = 0$. This network is depicted in Figure 6.7. The binary variables capturing this network are:
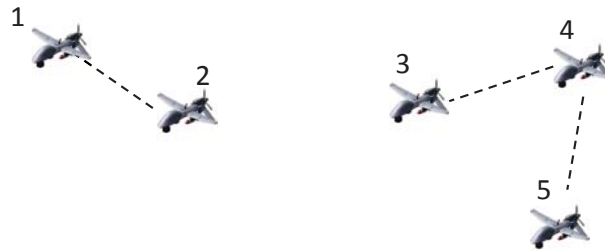
Figure 6.7: Network Connectivity through Asset Paths - Test Case 2

$$c_{12} = 1 \tag{6.57a}$$

$$c_{13} = 0 \tag{6.57b}$$

$$c_{14} = 0 \tag{6.57c}$$

$$c_{15} = 0 \tag{6.57d}$$

$$c_{23} = 0 \tag{6.57e}$$

$$c_{24} = 0 \tag{6.57f}$$

$$c_{25} = 0 \tag{6.57g}$$

$$c_{34} = 1 \tag{6.57h}$$

$$c_{35} = 0 \tag{6.57i}$$

$$c_{45} = 1 \tag{6.57j}$$

Following the same approach above, from the direct communication links, we know that from Constraint (6.16), and noting that $c_{12} = 1$, we have $y_3^{12} = y_4^{12} = y_5^{12} = 0$. From Constraint (6.23), and noting that $c_{34} = 1$, we have $y_1^{34} = y_2^{34} = y_5^{34} = 0$. Finally, from Constraint (6.25), and noting that $c_{45} = 1$, we have $y_1^{45} = y_2^{45} = y_3^{45} = 0$.

Now, with this information we know that, from Constraint (6.30), Constraint (6.33), Constraint (6.34), Constraint (6.37), Constraint (6.39),Constraint (6.42), Constraint (6.43), and Constraint (6.46), decision variables y_4^{13}, y_3^{14}, y_5^{14}, y_4^{15}, y_4^{23}, y_3^{24}, y_5^{24} and y_4^{25} are equal to 0.

We can further recognize that from Constraint (6.18), $y_2^{14} = 1$.

Now, Constraint (6.32) indicates that $1 \geq 2 \cdot y_2^{14} \Rightarrow 1 \geq 2$, identifying that network (6.58) is not a connected component.

As a final case, let's update the network (6.56) by adding a communication link, say between information collection assets 3 and 5 ($\Rightarrow c_{35} = 1$). This network is depicted in Figure 6.8. The binary variables capturing this network are:

$$c_{12} = 1 \tag{6.58a}$$

$$c_{13} = 0 \tag{6.58b}$$

$$c_{14} = 0 \tag{6.58c}$$
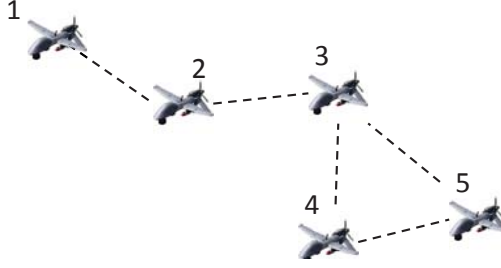
Figure 6.8: Network Connectivity through Asset Paths - Test Case 3

$$c_{15} = 0 \tag{6.58d}$$

$$c_{23} = 1 \tag{6.58e}$$

$$c_{24} = 0 \tag{6.58f}$$

$$c_{25} = 0 \tag{6.58g}$$

$$c_{34} = 1 \tag{6.58h}$$

$$c_{35} = 1 \tag{6.58i}$$

$$c_{45} = 1 \tag{6.58j}$$

Following the same approach above we know :

Exploit connectivity information from direct communication links

From Constraint (6.16), and noting that $c_{12} = 1$, we have $y_3^{12} = y_4^{12} = y_5^{12} = 0$. Similarly, from Constraint (6.20), and noting that $c_{23} = 1$, $y_1^{23} = y_4^{23} = y_5^{23} = 0$. From Constraint (6.23), and noting that $c_{34} = 1$, we have $y_1^{34} = y_2^{34} = y_5^{34} = 0$. From Constraint (6.24), and noting that $c_{35} = 1$, $y_1^{35} = y_2^{35} = y_4^{35} = 0$. Finally, from Constraint (6.25), and noting that $c_{45} = 1$, we have $y_1^{45} = y_2^{45} = y_3^{45} = 0$. Now, with this information we know that, from Constraint (6.30), $y_4^{13} = 0$. (Note, Constraint (6.30) indicates that $1 \geq 2 \cdot y_4^{13} \Rightarrow y_4^{13} = 0$.)

Using the same observation, from Constraint (6.31), $y_5^{13} = 0$. From Constraint (6.33), $y_3^{14} = 0$. From Constraint (6.34), $y_5^{14} = 0$. From Constraint (6.36), $y_3^{15} = 0$. From Constraint (6.37), $y_4^{15} = 0$. From Constraint (6.43), $y_5^{24} = 0$. From Constraint (6.46), $y_4^{25} = 0$.

We can further recognize that from Constraint (6.17), $y_2^{13} = 1$. From Constraint (6.18), $y_2^{14} = 1$ and, from Constraint (6.32), $y_3^{24} = 1$. (Note, Constraint (6.32) indicates that $1 + y_3^{24} \geq 2 \Rightarrow y_3^{24} = 1$.) This further implies that, from Constraint (6.21), $y_1^{24} = 0$. Now, from Constraint (6.19), $y_2^{15} = 1$, which further implies that, from Constraint (6.45), $y_3^{25} = 1$ and, finally, from Constraint (6.22), $y_1^{25} = 0$.

In summary, for this case,

- Information collection asset 1 is connected directly to information collection asset 2 ($c_{12} = 1$), and it is connected to the other information collection assets in the network via this information collection assets ($y_2^{13} = y_2^{14} = y_2^{15} = 1$).

- Information collection asset 2 is connected directly to information collection asset 1 ($c_{12} = 1$) and to information collection asset 3 ($c_{23} = 1$), and it is connected to information collection assets 4 and 5 via information collection asset 3 ($y_3^{24} = y_3^{25} = 1$).

- Information collection asset 3 is connected directly to information collection asset 2 ($c_{23} = 1$) and to information collection asset 4 ($c_{34} = 1$) and information collection asset 5 ($c_{35} = 1$), and it is connected to information collection asset 1 via information collection asset 2 ($y_2^{13} = 1$).

- Information collection asset 4 is connected directly to information collection asset 3 ($c_{34} = 1$) and to information collection asset 5 ($c_{45} = 1$), and it is connected to information collection asset 2 via information collection asset 3 ($y_3^{24} = 1$) and it is connected to information collection asset 1 via this path ($y_2^{14} = 1$).

- Information collection asset 5 is connected directly to information collection asset 3 ($c_{35} = 1$) and to information collection asset 4 ($c_{45} = 1$), and it is connected to information collection assets 1 and 2 since either information collection asset 3 or 4 are communicating with them (as indicated above).

Note on the fully connected (*pairwise connectivity*) network. For this case, $c_{ij} = 1, \forall i, j \in I$. Constraints (6.16) - (6.25) will require that $y_k^{ij} = 0, \forall i, j, k \in I, i \neq j \neq k$. Constraints (6.26) - (6.55) will still be satisfied since $2 \geq 0$ for all of them $\Rightarrow$ a connected component.

Note on a completely disconnected network. For this case, $c_{ij} = 0, \forall i, j \in I$. Constraint (6.11) reduces to $\sum_{k \in I, k \neq i \neq j} y_k^{ij} = 1 \quad \forall i, j \in I, i \neq j$. This indicates that the left-hand side of constraint (6.12) is at most 1; requiring then that all $y_k^{ij} = 0, \forall i, j, k \in I, k \neq i \neq j$. Constraint (6.16) cannot be then satisfied $\Rightarrow$ not a connected component.

Heterogeneous Communication Radii

Consider now the case when $c_{ij} \neq c_{ji}$. Under this assumption, Constraint (6.15) is not valid and can no longer be considered. However, Constraints (6.11) and (6.14) are still sufficient to identify a connected component.

Considering the connected component for the set I above, the following constraints will be generated:

(from Constraint (6.11))

$$c_{12} + y_3^{12} + y_4^{12} + y_5^{12} = 1 \tag{6.59}$$

$$c_{13} + y_2^{13} + y_4^{13} + y_5^{13} = 1 \tag{6.60}$$

$$c_{14} + y_2^{14} + y_3^{14} + y_5^{14} = 1 \tag{6.61}$$

$$c_{15} + y_2^{15} + y_3^{15} + y_4^{15} = 1 \tag{6.62}$$

$$c_{21} + y_3^{21} + y_4^{21} + y_5^{21} = 1 \tag{6.63}$$

$$c_{23} + y_1^{23} + y_4^{23} + y_5^{23} = 1 \tag{6.64}$$

$$c_{24} + y_1^{24} + y_3^{24} + y_5^{24} = 1 \tag{6.65}$$

$$c_{25} + y_1^{25} + y_3^{25} + y_4^{25} = 1 \tag{6.66}$$

$$c_{31} + y_2^{31} + y_4^{31} + y_5^{31} = 1 \tag{6.67}$$

$$c_{32} + y_1^{32} + y_4^{32} + y_5^{32} = 1 \tag{6.68}$$

$$c_{34} + y_1^{34} + y_2^{34} + y_5^{34} = 1 \tag{6.69}$$

$$c_{35} + y_1^{35} + y_2^{35} + y_4^{35} = 1 \tag{6.70}$$

$$c_{41} + y_2^{41} + y_3^{41} + y_5^{41} = 1 \tag{6.71}$$

$$c_{42} + y_1^{42} + y_3^{42} + y_5^{42} = 1 \tag{6.72}$$

$$c_{43} + y_1^{43} + y_2^{43} + y_5^{43} = 1 \tag{6.73}$$

$$c_{45} + y_1^{45} + y_2^{45} + y_3^{45} = 1 \tag{6.74}$$

$$c_{51} + y_2^{51} + y_3^{51} + y_4^{51} = 1 \tag{6.75}$$

$$c_{52} + y_1^{52} + y_3^{52} + y_4^{52} = 1 \tag{6.76}$$

$$c_{53} + y_1^{53} + y_2^{53} + y_4^{53} = 1 \tag{6.77}$$

$$c_{54} + y_1^{54} + y_2^{54} + y_3^{54} = 1 \tag{6.78}$$

(from Constraint (6.12))

$$c_{13} + c_{32} + y_4^{32} + y_5^{32} \geq 2 \cdot y_3^{12} \tag{6.79}$$

$$c_{14} + c_{42} + y_3^{42} + y_5^{42} \geq 2 \cdot y_4^{12} \tag{6.80}$$

$$c_{15} + c_{52} + y_3^{52} + y_4^{52} \geq 2 \cdot y_5^{12} \tag{6.81}$$

$$c_{12} + c_{23} + y_4^{23} + y_5^{23} \geq 2 \cdot y_2^{13} \tag{6.82}$$

$$c_{14} + c_{43} + y_2^{43} + y_5^{43} \geq 2 \cdot y_4^{13} \tag{6.83}$$

$$c_{15} + c_{53} + y_2^{53} + y_4^{53} \geq 2 \cdot y_5^{13} \tag{6.84}$$

$$c_{12} + c_{24} + y_3^{24} + y_5^{24} \geq 2 \cdot y_2^{14} \tag{6.85}$$

$$c_{13} + c_{34} + y_2^{34} + y_5^{34} \geq 2 \cdot y_3^{14} \tag{6.86}$$

$$c_{15} + c_{54} + y_2^{54} + y_3^{54} \geq 2 \cdot y_5^{14} \tag{6.87}$$

$$c_{12} + c_{25} + y_3^{25} + y_4^{25} \geq 2 \cdot y_2^{15} \tag{6.88}$$

$$c_{13} + c_{35} + y_2^{35} + y_4^{35} \geq 2 \cdot y_3^{15} \tag{6.89}$$

$$c_{14} + c_{45} + y_2^{45} + y_3^{45} \geq 2 \cdot y_4^{15} \tag{6.90}$$

$$c_{23} + c_{31} + y_4^{31} + y_5^{31} \geq 2 \cdot y_3^{21} \tag{6.91}$$

$$c_{24} + c_{41} + y_3^{41} + y_5^{41} \geq 2 \cdot y_4^{21} \tag{6.92}$$

$$c_{25} + c_{51} + y_3^{51} + y_4^{51} \geq 2 \cdot y_5^{21} \tag{6.93}$$

$$c_{21} + c_{13} + y_4^{13} + y_5^{13} \geq 2 \cdot y_1^{23} \tag{6.94}$$

$$c_{24} + c_{43} + y_1^{43} + y_5^{43} \geq 2 \cdot y_4^{23} \tag{6.95}$$

$$c_{25} + c_{53} + y_1^{53} + y_4^{53} \geq 2 \cdot y_5^{23} \tag{6.96}$$

$$c_{21} + c_{14} + y_3^{14} + y_5^{14} \geq 2 \cdot y_1^{24} \tag{6.97}$$

$$c_{23} + c_{34} + y_1^{34} + y_5^{34} \geq 2 \cdot y_3^{24} \tag{6.98}$$

$$c_{25} + c_{54} + y_1^{54} + y_3^{54} \geq 2 \cdot y_5^{24} \tag{6.99}$$

$$c_{21} + c_{15} + y_3^{15} + y_4^{15} \geq 2 \cdot y_1^{25} \tag{6.100}$$

$$c_{23} + c_{35} + y_1^{35} + y_4^{35} \geq 2 \cdot y_3^{25} \tag{6.101}$$

$$c_{24} + c_{45} + y_1^{45} + y_3^{45} \geq 2 \cdot y_4^{25} \tag{6.102}$$

$$c_{32} + c_{21} + y_4^{21} + y_5^{21} \geq 2 \cdot y_2^{31} \tag{6.103}$$

$$c_{34} + c_{41} + y_2^{41} + y_5^{41} \geq 2 \cdot y_4^{31} \tag{6.104}$$

$$c_{35} + c_{51} + y_2^{51} + y_4^{51} \geq 2 \cdot y_5^{31} \tag{6.105}$$

$$c_{31} + c_{12} + y_4^{12} + y_5^{12} \geq 2 \cdot y_1^{32} \tag{6.106}$$

$$c_{34} + c_{42} + y_1^{42} + y_5^{42} \geq 2 \cdot y_4^{32} \tag{6.107}$$

$$c_{35} + c_{52} + y_1^{52} + y_4^{52} \geq 2 \cdot y_5^{32} \tag{6.108}$$

$$c_{31} + c_{14} + y_2^{14} + y_5^{14} \geq 2 \cdot y_1^{34} \tag{6.109}$$

$$c_{32} + c_{24} + y_1^{24} + y_5^{24} \geq 2 \cdot y_2^{34} \tag{6.110}$$

$$c_{35} + c_{45} + y_1^{45} + y_2^{45} \geq 2 \cdot y_5^{34} \tag{6.111}$$

$$c_{31} + c_{15} + y_2^{15} + y_4^{15} \geq 2 \cdot y_1^{35} \tag{6.112}$$

$$c_{32} + c_{25} + y_1^{25} + y_4^{25} \geq 2 \cdot y_2^{35} \tag{6.113}$$

$$c_{34} + c_{45} + y_1^{45} + y_2^{45} \geq 2 \cdot y_4^{35} \tag{6.114}$$

$$c_{42} + c_{21} + y_3^{21} + y_5^{21} \geq 2 \cdot y_2^{41} \tag{6.115}$$

$$c_{43} + c_{31} + y_2^{31} + y_5^{31} \geq 2 \cdot y_3^{41} \tag{6.116}$$

$$c_{45} + c_{51} + y_2^{51} + y_3^{51} \geq 2 \cdot y_5^{41} \tag{6.117}$$

$$c_{41} + c_{12} + y_3^{12} + y_5^{12} \geq 2 \cdot y_1^{42} \tag{6.118}$$

$$c_{43} + c_{32} + y_1^{32} + y_5^{32} \geq 2 \cdot y_3^{42} \tag{6.119}$$

$$c_{45} + c_{52} + y_1^{52} + y_3^{52} \geq 2 \cdot y_5^{42} \tag{6.120}$$

$$c_{41} + c_{13} + y_2^{13} + y_5^{13} \geq 2 \cdot y_1^{43} \tag{6.121}$$

$$c_{42} + c_{23} + y_1^{23} + y_5^{23} \geq 2 \cdot y_2^{43} \tag{6.122}$$

$$c_{45} + c_{53} + y_1^{53} + y_2^{53} \geq 2 \cdot y_5^{43} \tag{6.123}$$

$$c_{41} + c_{15} + y_2^{15} + y_3^{15} \geq 2 \cdot y_1^{45} \tag{6.124}$$

$$c_{42} + c_{25} + y_1^{25} + y_3^{25} \geq 2 \cdot y_2^{45} \tag{6.125}$$

$$c_{43} + c_{35} + y_1^{35} + y_2^{35} \geq 2 \cdot y_3^{45} \tag{6.126}$$

$$c_{52} + c_{21} + y_3^{21} + y_4^{21} \geq 2 \cdot y_2^{51} \tag{6.127}$$

$$c_{53} + c_{31} + y_2^{31} + y_4^{31} \geq 2 \cdot y_3^{51} \tag{6.128}$$

$$c_{54} + c_{41} + y_2^{41} + y_3^{41} \geq 2 \cdot y_4^{51} \tag{6.129}$$

$$c_{51} + c_{12} + y_3^{12} + y_4^{12} \geq 2 \cdot y_1^{52} \tag{6.130}$$

$$c_{53} + c_{32} + y_1^{32} + y_4^{32} \geq 2 \cdot y_3^{52} \tag{6.131}$$

$$c_{54} + c_{42} + y_1^{42} + y_3^{42} \geq 2 \cdot y_4^{52} \tag{6.132}$$

$$c_{51} + c_{13} + y_2^{13} + y_4^{13} \geq 2 \cdot y_1^{53} \tag{6.133}$$

$$c_{52} + c_{23} + y_1^{23} + y_4^{23} \geq 2 \cdot y_2^{53} \tag{6.134}$$

$$c_{54} + c_{43} + y_1^{43} + y_2^{43} \geq 2 \cdot y_4^{53} \tag{6.135}$$

$$c_{51} + c_{14} + y_2^{14} + y_3^{14} \geq 2 \cdot y_1^{54} \tag{6.136}$$

$$c_{52} + c_{24} + y_1^{24} + y_3^{24} \geq 2 \cdot y_2^{54} \tag{6.137}$$

$$c_{53} + c_{34} + y_1^{34} + y_2^{34} \geq 2 \cdot y_3^{54} \tag{6.138}$$

Now, consider again the network (6.56). The binary variables capturing this network are now:

$$c_{12} = 1 \tag{6.139a}$$

$$c_{13} = 0 \tag{6.139b}$$

$$c_{14} = 0 \tag{6.139c}$$

$$c_{15} = 0 \tag{6.139d}$$

$$c_{21} = 0 \tag{6.139e}$$

$$c_{23} = 1 \tag{6.139f}$$

$$c_{24} = 0 \tag{6.139g}$$

$$c_{25} = 0 \tag{6.139h}$$

$$c_{31} = 0 \tag{6.139i}$$

$$c_{32} = 0 \tag{6.139j}$$

$$c_{34} = 1 \tag{6.139k}$$

$$c_{35} = 0 \tag{6.139l}$$

$$c_{41} = 0 \tag{6.139m}$$

$$c_{42} = 0 \tag{6.139n}$$

$$c_{43} = 0 \tag{6.139o}$$

$$c_{45} = 1 \tag{6.139p}$$

$$c_{51} = 0 \tag{6.139q}$$

$$c_{52} = 0 \tag{6.139r}$$

$$c_{53} = 0 \tag{6.139s}$$

$$c_{54} = 0 \tag{6.139t}$$

Now, exploiting the connectivity information from direct communication links, from Constraints (6.127), (6.128), and (6.129), and noting that $c_{52} = c_{21} = c_{53} = c_{31} = c_{54} = c_{41} = 0$, we have $y_2^{51} = y_3^{51} = y_4^{51} = 0$. However, from Constraint (6.75), and noting that $c_{51} = 0$, we have $y_2^{51} + y_3^{51} + y_4^{51} = 1$.

$\Rightarrow$ network (6.139) is not a connected component.

Now, considering again the network (6.139) but this time adding a direct communication link between information collection asset 5 and 1 (i.e., $c_{51} = 1$), we have:

$$c_{12} = 1 \tag{6.140a}$$

$$c_{13} = 0 \tag{6.140b}$$

$$c_{14} = 0 \tag{6.140c}$$

$$c_{15} = 0 \tag{6.140d}$$

$$c_{21} = 0 \tag{6.140e}$$

$$c_{23} = 1 \tag{6.140f}$$

$$c_{24} = 0 \tag{6.140g}$$

$$c_{25} = 0 \tag{6.140h}$$

$$c_{31} = 0 \tag{6.140i}$$

$$c_{32} = 0 \tag{6.140j}$$

$$c_{34} = 1 \tag{6.140k}$$

$$c_{35} = 0 \tag{6.140l}$$

$$c_{41} = 0 \tag{6.140m}$$

$$c_{42} = 0 \tag{6.140n}$$

$$c_{43} = 0 \tag{6.140o}$$

$$c_{45} = 1 \tag{6.140p}$$

$$c_{51} = 1 \tag{6.140q}$$

$$c_{52} = 0 \tag{6.140r}$$

$$c_{53} = 0 \tag{6.140s}$$

$$c_{54} = 0 \tag{6.140t}$$

Are Constraints (6.59) - (6.138) sufficient to recognize that network (6.140) is a connected component?

Following the same process above, the following solution was found:

$c_{12} = 1$ (given)	$y_4^{21} = 0$	$y_5^{31} = 0$
$y_3^{12} = 0$	$y_5^{21} = 0$	$y_1^{32} = 0$
$y_4^{12} = 0$	$c_{23} = 1$ (given)	$y_4^{32} = 1$
$y_5^{12} = 0$	$y_1^{23} = 0$	$y_5^{32} = 0$
$y_2^{13} = 1$	$y_4^{23} = 0$	$c_{34} = 1$ (given)
$y_4^{13} = 0$	$y_5^{23} = 0$	$y_1^{34} = 0$
$y_5^{13} = 0$	$y_1^{24} = 0$	$y_2^{34} = 0$
$y_2^{14} = 1$	$y_3^{24} = 1$	$y_5^{34} = 0$
$y_3^{14} = 0$	$y_5^{24} = 0$	$y_1^{35} = 0$
$y_5^{14} = 0$	$y_1^{25} = 0$	$y_2^{35} = 0$
$y_2^{15} = 1$	$y_3^{25} = 1$	$y_4^{35} = 1$
$y_3^{15} = 0$	$y_4^{25} = 0$	$y_2^{41} = 0$
$y_4^{15} = 0$	$y_2^{31} = 0$	$y_3^{41} = 0$
$y_3^{21} = 1$	$y_4^{31} = 1$	$y_5^{41} = 1$

$$y_1^{42} = 0 \qquad\qquad y_2^{45} = 0 \qquad\qquad y_4^{52} = 0$$

$$y_3^{42} = 0 \qquad\qquad y_3^{45} = 0 \qquad\qquad y_1^{53} = 1$$

$$y_5^{42} = 1 \qquad\qquad c_{51} = 1 \text{ (given)} \qquad y_2^{53} = 0$$

$$y_1^{43} = 0 \qquad\qquad y_2^{51} = 0 \qquad\qquad y_4^{53} = 0$$

$$y_2^{43} = 0 \qquad\qquad y_3^{51} = 0 \qquad\qquad y_1^{54} = 1$$

$$y_5^{43} = 1 \qquad\qquad y_4^{51} = 0 \qquad\qquad y_2^{54} = 0$$

$$c_{45} = 1 \text{ (given)} \qquad y_1^{52} = 1 \qquad\qquad y_3^{54} = 0$$

$$y_1^{45} = 0 \qquad\qquad y_3^{52} = 0$$

$\Rightarrow$ network (6.139) is a connected component.

In summary, for this case,

- Information collection asset 1 is connected directly to information collection asset 2 ($c_{12} = 1$), and it is connected to the other information collection assets in the network via this information collection assets ($y_2^{13} = y_2^{14} = y_2^{15} = 1$).

- Information collection asset 2 is connected directly to information collection asset 3 ($c_{23} = 1$), and it is connected to the other information collection assets in the network via this information collection assets ($y_3^{24} = y_3^{25} = y_3^{21} = 1$).

- Information collection asset 3 is connected directly to information collection asset 4 ($c_{34} = 1$), and it is connected to the other information collection assets in the network via this information collection assets ($y_4^{35} = y_4^{31} = y_4^{32} = 1$).

- Information collection asset 4 is connected directly to information collection asset 5 ($c_{45} = 1$), and it is connected to the other information collection assets in the network via this information collection assets ($y_5^{41} = y_5^{42} = y_5^{43} = 1$).

- Information collection asset 5 is connected directly to information collection asset 1 ($c_{51} = 1$), and it is connected to the other information collection assets in the network via this information collection assets ($y_1^{52} = y_1^{53} = y_1^{54} = 1$).

6.4   Trust on Information from Assets Outside the Network Component

Consider the following situation: At time-step t_0, information collection asset 1 and information collection asset 2 shared their respective Information Gain Maps (IGMs) and routes. As assumed before, each route consists of a sequence of cells each collection asset will visit in the next T time-steps. At time-step t, information collection asset 1 and information collection asset 2 are not communicating (e.g,. communication equipment is no longer operational). At time-step $t_0 + T$, information collection asset 1 will define its new route for the next T time-steps. We know that information collection asset 2 is in the area but, since we are not communicating with it, we are not certain on its location nor its route for the next T time-steps.

Research question

From information collection asset 1's perspective, how do we account for the potential collection of information from information collection asset 2 while defining a new route?

6.4.1   Updates to Mathematical Programming Model

Parameters

The following parameters are defined:

$$
\begin{aligned}
\hat{J} &\equiv \text{ set of collection assets not in connected component, indexes } \hat{\jmath} = \left\{1, 2, \ldots, |\hat{J}|\right\}; \hat{J} \subset I \\
p_{\hat{\imath}kt} &\equiv \text{ confidence collection assets } \hat{\imath} \text{ will be on cell } k \text{ at time-step } t
\end{aligned}
$$

Objective Function

No changes are required to the objective function (4.1) to accommodate the potential contribution of collection assets outside the connected component.

Potential Information Gain Constraints

From Section 4, Constraint (4.4) relates the value of cell k at time-step t to its value at time-step $t-1$, the obsolescence rate d_{rkt} and the gain $g_{rk,t-1}$ from the set of collection assets. Constraint (4.4) is repeated below to facilitate description of updates to formulation

$$f_{rkt} \leq f_{rk,t-1} + d_{rkt} - g_{rk,t-1}$$

For the case in which we are considering the potential contribution of collection assets outside the connected component (information collection asset $\hat{j} \in \hat{J}$), f_{rkt} needs to account for the expected information gain from these assets.

g_{rkt} is now represented as constraint

$$g_{rkt} \;\; = \;\; \sum_{j \in J} g_{jrkt} + \sum_{\hat{j} \in \hat{J}} g_{\hat{j}rkt} = \sum_{j \in J \cup \hat{J}} g_{jrkt} \quad \forall r \in R, \forall k \in K, \forall t \in T \tag{6.141}$$

updating Constraint (4.7).

In addition, the following constraint capturing the gain from collection assets outside the connected component is required

$$g_{\hat{j}rkt} \;\; \leq \;\; e_{\hat{j}rkt}\, p_{\hat{j}kt}\, f_{\hat{j}rkt} \quad \forall \hat{j} \in \hat{J}, \forall r \in R, \forall k \in K, \forall t \in T \tag{6.142}$$

Note that the contribution to the overall information gain from collection assets $\hat{j}$ outside the connected component (i.e., $e_{\hat{j}rkt}\, f_{\hat{j}rkt}$) is weighted by the confidence $p_{\hat{j}kt}$ the asset will be at cell k at time t. The smaller the confidence on an asset $\hat{j}$ being at a cell k at time t (e.g., $p_{\hat{j}kt} \approx 0$), the smaller the gain is assumed to be collected from that asset, leaving the collection of information to other assets in the network.

The set of collection assets considered in Constraint (4.11) need to be updated to include all assets (i.e., connected and not-connected). Constraint (4.11) is then updated as follows

$$f_{jrkt} \;\; = \;\; f_{j-1,rkt} - g_{jrkt} \quad \forall j \in \{J \cup \hat{J}\}, \forall r \in R, \forall k \in K, \forall t \in T \tag{6.143}$$

Chapter 7

Measuring the Price of Decentralization

7.1 Introduction

Technology advancements in Intelligence, Surveillance, and Reconnaissance (ISR) automation and the intelligent use of network assets is needed to improve the timely processing and delivery of information products in the emerging Command and Control (C2)/ISR integrated operational environment. Synchronization of activities to maximize the utilization of limited resources (both in terms of quantity and capability) has become critically important to military forces in this environment. Timely and accurate answers to information needs contribute significantly to situational understanding. This requires the increase of information sharing capabilities and planning and control algorithms among current operational and expected future systems to efficiently use all limited resources across domains.

As discussed in Chapter 2, most planning and control algorithms assume a centralized framework [1, 15, 16, 18]. In centralized frameworks, a single node is responsible for determining and disseminating decisions (e.g., tasks assignments) to all nodes in the network. This requires a robust and reliable communication network. In decentralized frameworks, processing of information and decision making occur at different nodes in the network, reducing the communication requirements.

This chapter studies the degradation of solution quality (i.e., potential information gain) as a centralized system synchronizing ISR activities moves to a decentralized framework. The potential information gain value on a discretized area of the Area of Operation (AO) represents a relative prioritization of the likelihood of addressing relevant features of an information deficit for the mission. As described in Chapter 3, this characterization creates an Information Gain Map (IGM). Each collection asset is responsible for sensing the environment. Moreover, each collection asset is responsible for determining its flight plans over the planning horizon, considering mission objectives, its perspective of the environment, and the potential collected information from other assets in its connected component. The primary objective of each asset while defining its plan is then to maximize the overall expected information gain considering available sensing capabilities while preserving the connected component to enable information sharing over the planning horizon in the decentralized framework. The Mixed-Integer Linear Program (MILP) described in Chapter 4 and the solution approach discussed on Chapter 5 provide the framework to define the plans for each collection asset for the study documented in this Chapter. Communication to other assets to exchange information is limited over different communication network topologies. Information is only exchanged when assets are part of the same network. Collection assets are part of the same communication network (i.e., a connected component) if (1) a Fully Connected Network (FCN) exists between the assets in the connected component, or (2) a path between each pair of assets (PPA) in the connected component exists. Equations (4.16) to (4.24) presented in Section 4.4.4 capture the representation of the FCN topology in the mathematical program. A description of Constraints (6.11) to (6.14) and additional updates to the mathematical program to represent the PPA topology are discussed in Section 6.3.1. Multiple connected components may exist among the available collection assets supporting a mission. As described in Section 6.4, in both types of network configuration, the potential location and information collection of assets that are not part of a connected component can be considered as part of the optimization model.

The rest of this chapter is organized as follows: Section 7.2 reviews the concept of the price of decentralization. In Section 7.3, the methodology and results of the experiments to study the impact of the network topology, collection effectiveness and type of IGM to the price of decentralization are presented.

7.2   From Centralized Planning to Anarchy: the Price of Decentralization

The Price of Decentralization (PoD) is defined as a measure on the degradation of solution quality as a centralized system moves to a more decentralized framework. The term "price of anarchy" has been used to refer to the inefficiency of a system when individuals (i.e., agents) maximize decisions without coordination [4]. Researchers have continued using this term to refer to this efficiency-loss ratio [5, 6, 7, 8]. This research extends the concept of Price of Anarchy (PoA) by considering different levels of decentralization. Levels of decentralization are determined by redefining the structure of the network topology used by the collection assets to exchange information. In this research, PoD is defined as

$$\text{PoD} = \left(1 - \frac{\sum_r \sum_t w_{rt} \sum_k g_{rkt}}{\sum_r \sum_t w_{rt} \sum_k g^*_{rkt}}\right) \tag{7.1}$$

where g^*_{rkt} refers to the information obtained by the solution of the centralized framework for collection requirement $r \in R$, from cell $k \in K$, at time-step $t \in T$. Parameters R, K, and T are defined in Section 4.2 and capture the set of collection requirements for the mission, the number of cells representing the AO and the planning horizon, respectively. g_{rkt} in Equation (7.1) is the resulting information gain for collection requirement r from cell k at time-step t by solving the mathematical programming model consisting of Equations (4.1) to (4.15), and the additional constraints for a particular configuration network. As described in Section 4.2, w_{rt} represents a weighting parameter for collection requirement r at time-step t.

Equation (7.1) captures the loss ratio of potential information gain when the solution from a decentralized framework is compared to the solution a centralized framework could attain under the same initial conditions and constraints. In this research, a centralized framework is represented by a network configuration in which all collection assets can share their information. Although there is no "central" node deciding the plans for the assets in this configuration, given that all assets will be aware of all available information for the mission, solving the (deterministic) mathematical program of Chapter 4 will result in the same solution for each asset. Under the assumption of a no latency communication network in this research, this is equivalent to a centralized framework in which the assets broadcast their information to and receive the plans from the "central" node. Note that, under these assumptions, $\sum_r \sum_t w_{rt} \sum_k g^*_{rkt} \geq \sum_r \sum_t w_{rt} \sum_k g_{rkt}$.

7.3   Experimental Results

The purpose of this research is to measure the impact of sensor effectiveness, communication network topology and type of IGM on the PoD metric. Three collection assets, indexed 1, 2, and 3, were considered in a given area of operation. The AO was represented as a grid of 15-by-15 cells. Without loss of generality, it is assumed for these experiments that all information collection assets have a single, on-board sensor. Sensor effectiveness, the ability of a sensor to collect information, was varied in the experiments and is displayed in Table 7.1. As an example, if the sensor effectiveness is given by $\alpha \in [0, 1]$, then a collection asset with this sensor effectiveness will collect $\alpha\%$ of the information available on the collection asset's current cell.

In the developed scenario, the potential information gain value on a discretized area of the AO represents a relative prioritization of the likelihood of addressing relevant features of an information deficit (e.g., finding a high value target at that cell) for the mission. As described in Chapter 3, this characterization creates an IGM. Areas of high information gain are denoted in *red*, while those of low information gain (e.g., the middle of a lake while searching for a car) are denoted in *blue*. Figure 7.1 shows a sample of an information gain map. Ten randomly generated information gain maps were used for these experiments. Analysis is based on the results captured from 10 different trials for each type of network configuration in which the initial location of the assets and information gain maps were randomly determined.
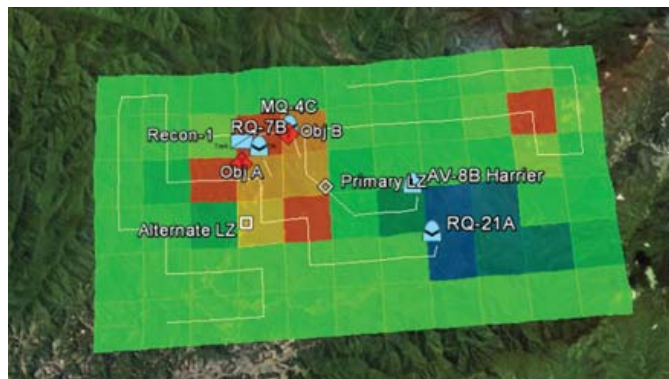
Figure 7.1: Sample Information Gain Map

The planning horizon for the routes to be defined for each asset consisted of 5 time-steps. In the experiments below, however, assets were considered homogeneous: at each time-step, each

asset was allowed to move to any adjacent cells, or remain at the same cell. Moreover, for a given trial in the experiment, all assets started at the same initial location and were assumed to have the same sensor effectiveness. Values of other relevant parameters during the simulation are captured in Table 7.1.

Table 7.1: Mathematical Program and Experiment Parameters for Evaluation of PoD

Parameter	Value
Mathematical Program	
I	{1,2,3}
T	{1,2,..., 5}
K	{1,2,...,225} (a 15-by-15 grid area)
R	{1}
$\overline{\text{CR}}_i$	3.0 ($\forall i \in I$)
w_{rt}	1.0 ($\forall r \in R, t \in T$)
sensor effectiveness	{0.25, 0.50, 0.75}
Design of Experiment	
Number of Trials	10
Type of Information Gain Maps	1 Hot-Spot and Random
Information Gain Maps	10 (for each IGM type)

Using each of the potential network configurations, the solution obtained under distributed planning will be compared with the potential information gain obtained if a "central" node was available and responsible for determining the routes for all information gathering assets supporting the mission.

PoD was computed for multiple runs, under multiple initial conditions, created by varying the starting locations of the collection assets and the initial information gain maps. Moreover, two types of IGMs were considered: (1) 1 Hot-Spot, and (2) Random. Figure 7.2 shows an example of an IGM with a single hot spot. The location of the hot spot was randomly selected for each case considered. Figure 7.3 shows an example of a random IGM. For this type of IGM, the value of each cell was randomly selected from a uniform distribution $\sim U(0,1)$.

Levels of decentralization are defined by fixing the connected components on the communication network structure. Indices within brackets represent the set of collection assets in a connected
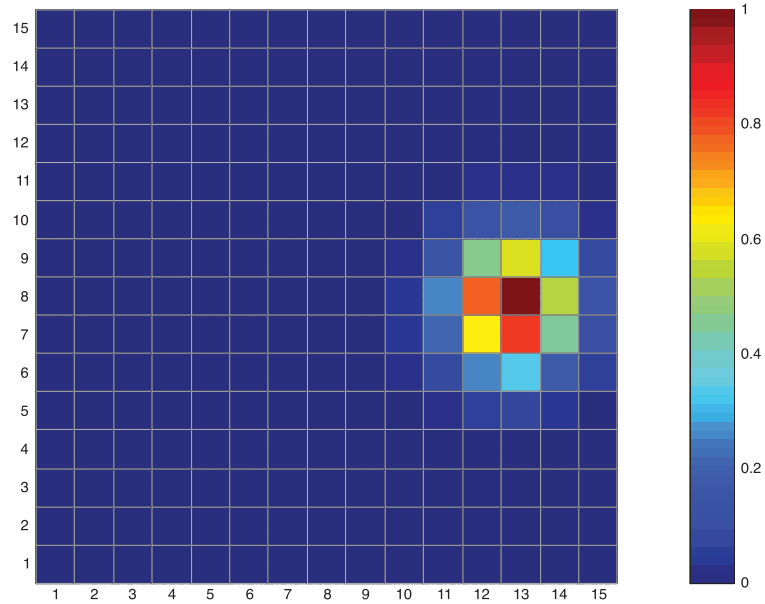
Figure 7.2: Sample IGM with 1 Hot-Spot for Evaluation of Price of Decentralization

component (e.g., [1 2][3] represents that collection asset 1 and collection asset 2 are part of the same connected component and exchange information with each other, while collection asset 3 does not communicate with any other asset in the area of operation). For each connected component, the mathematical program described in Chapter 4 and the corresponding set of constraints for the network topology were solved using CPLEX Interactive Optimizer 12.2 [50]. Solutions were then compared to the potential information gain expected from the best-case known centralized solution for each of the cases. This provides a bound on the PoD since, as discussed in Section 7.2, the centralized solution is guaranteed to not be worse than the decentralized solutions.

Figure 7.4 shows a plot of the average PoD as a function of sensor effectiveness for collection assets on different fully connected network (i.e., pairwise connectivity) topologies on the IGMs with 1 Hot-Spot. The PoD increases as the accuracy of the sensor increases, regardless of the network topology. For the case where one collection asset was operating independently (network topology [1 2][3]) the PoD increased from a 3.36% for assets with a collection effectiveness of 0.25, to a PoD of 14.97% when the effectiveness of the sensors was 0.75. Similarly, for the case where all assets were operating independently (network topology [1]2][3]) the PoD increased from a 26% for assets with a collection effectiveness of 0.25, to a PoD of 45.3% when the effectiveness of the sensors was 0.75.
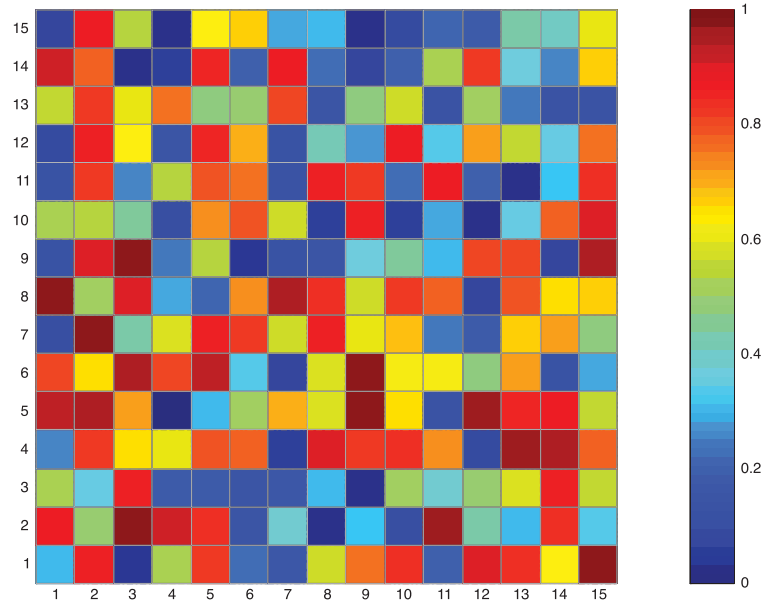
Figure 7.3: Sample Random IGM for Evaluation of Price of Decentralization

PoD for this [1][2][3] network topology is equivalent to PoA. Note also the substantial increase in the PoD for each particular sensor effectiveness but on different network topologies. In Figure 7.5, a plot of the average PoD as a function of sensor effectiveness for collection assets on different PPA (i.e., path connectivity) network topologies on the IGMs with 1 Hot-Spot is shown. Since PPA is a generalization of FCN, under the same initial conditions, the potential information gain obtained by solving the full mathematical program for a PPA network is never worse than the potential information gain obtained from a FCN network. However, it is worth highlighting the trend for each of these network types in the price of decentralization on these experiments: as the accuracy of sensors (better collection effectiveness) increases, the solution quality is more dependent on whether or not the assets are able to communicate, regardless of the type of network topology or type of IGM. The PoD metric in Figures 7.6 and 7.7 show the impact on the lack of coordination for assets with a low sensor effectiveness for different types of IGMs, on the FCN and PPA networks, respectively. In general, less accurate sensors will leave significant information on a sensed cell so additional assets will still benefit by sensing the same cell at the same time. Consider for example a cell with current potential information gain value of 1.0. An asset with on-board sensing capabilities of just 0.25 will leave 0.75 of potential information for other assets to collect. The impact of the lack of coordination

of assets is less evident (i.e., a small PoD) for those cases (as shown in Figures 7.6 and 7.7). From Figure 7.2, there is a single cluster of high potential information gain in a 1 Hot-Spot IGM so any move delaying collection on the area will be have a substantial impact on the overall information gained by the assets. The PoD is relatively the same for an asset with a better sensor effectiveness (≥ 0.5 on this experiment), regardless of the type of IGM. Note that this does not imply that having less accurate (and potentially, cheaper) sensors is not valuable for a mission. However, the price of not coordinating the information gathering activities from these less accurate assets is less when compared to the same situation with highly accurate sensors (20% vs 48% reduction on the potential information gain), regardless of the type of IGM or network type.
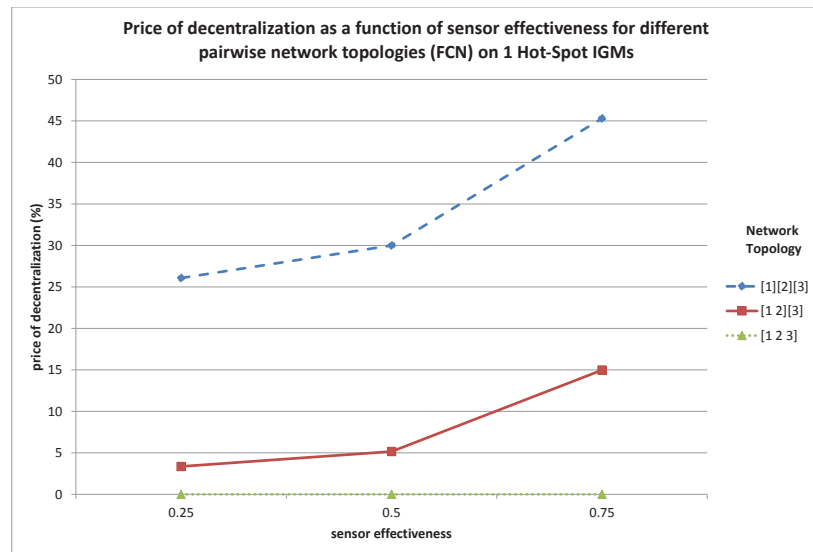
Figure 7.4: Price of Decentralization for Pairwise Sensor Topologies on 1 Hot-Spot IGMs
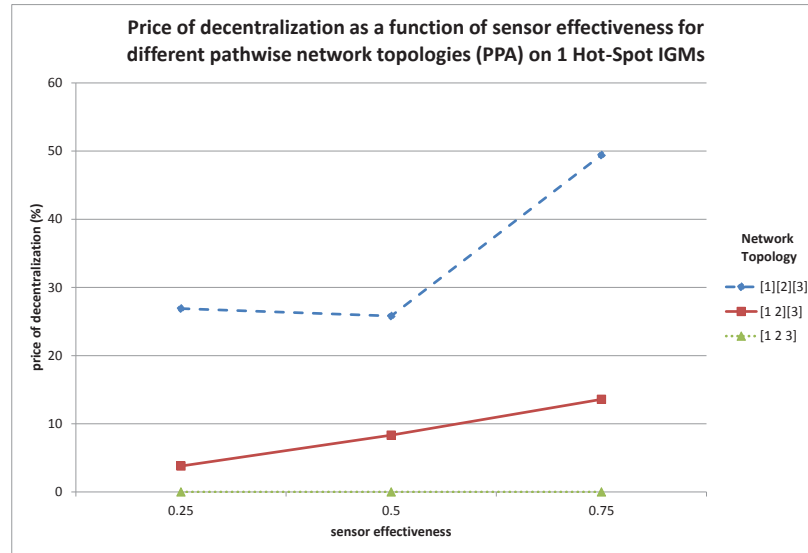
Figure 7.5: Price of Decentralization for Path-based Sensor Topologies on 1 Hot-Spot IGMs
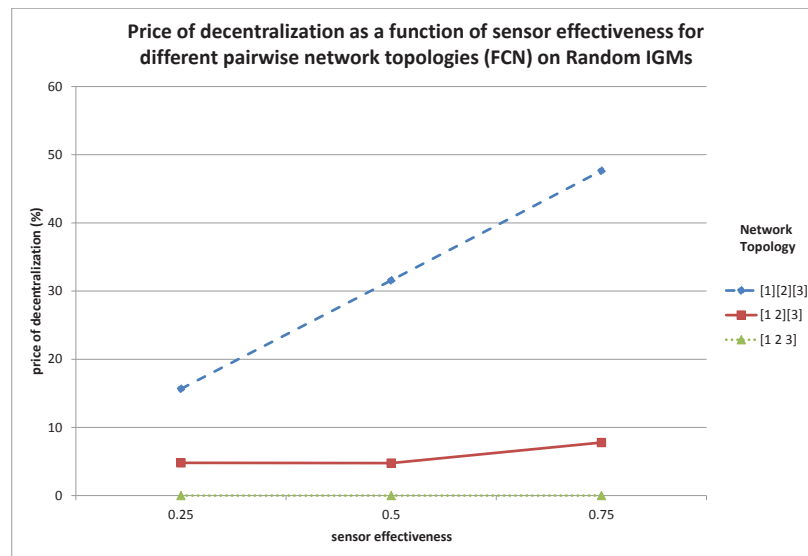
Figure 7.6: Price of Decentralization for Pairwise Sensor Topologies on Random IGMs

Figure 7.7: Price of Decentralization for Path-based Sensor Topologies on Random IGMs

Chapter 8

Conclusions and Future Research Topics

This work addressed the problem of routing cooperative autonomous vehicles (e.g., unmanned vehicles) operating in a dynamic environment to maximize overall information gain. Vehicles (collection assets) are collecting information on multiple objectives, subject to communication network constraints. The Area of Operation (AO) where assets are collecting information is discretized and represented by a set of grid cells.

A rating system based on Keener's method [47] was developed to define Information Gain Maps (IGMs). IGMs assign a numerical value to each cell in the AO based on its potential of having features addressing identified information deficits and objectives in the mission. When considering an IGM, a higher value represents a higher opportunity to obtain relevant information from a cell in the AO to address one or more deficits. The concept of *entropy* as a measure of the amount of information required on the average to describe a random variable was exploited in the developed rating system. Additional scoring functions to better represent the fusion of relevant features from information deficits will the topic of future research.

A rigorous mathematical model was developed as a Mixed-Integer Linear Program (MILP) to determine the optimal routes (i.e., the sequence of moves) of the information collection assets in the AO to maximize the overall potential information to be gained. The model is based on

the representation of potential information gain in discretized maps (i.e., IGMs), the effectiveness of the assets collecting information and an obsolescence rate on the areas visited by the assets. The model assumes assets operate on a decentralized framework. Different communication network topologies were considered. Collection assets are part of the same communication network (i.e., a connected component) if: (1) a fully connected network exists between the assets in the connected component, or (2) a path (consisting of one or more communication links) between every asset in the connected component exists. Multiple connected components may exist among the available collection assets supporting a mission. Extensions to the mathematical model included the evaluation of the potential location of assets that are not part of a connected component. Additional extensions to the mathematical model may consider the endurance of vehicles, time constraints to return to a predefined location (e.g., landing zones), effects of weather on both, mobility and communication capabilities, and other operational limitations.

A solution approach based on multiple aggregation strategies to obtain acceptably good solutions that are computational efficient was developed. Instead of trying to solve the complete route for each asset at once, a strategy in which only a subset of time-steps are evaluated at a time was defined. Using this time cascade approach provided the opportunity to also reduce the number of grid cells considered in each cascade, reducing even more the complexity of the MILP to be solved. A spatial aggregation algorithm was then defined whereby gain information for cells that cannot be reached in a cascade are "aggregated" and used to update the value of selected cells within the rolling horizon. The Bellman-Ford algorithm was used as the basis of this aggregation approach. It defines the path that maximizes the potential information gain for a vehicle on each cell of interest in the subproblem. However, the use of Bellman-Ford algorithm and the definition of the graph G limited the representation of relevant information considered in the modeling of the vehicle routing problem while computing the aggregated cell value. First, the definition of graph G does not include the potential reduction of available information gain from other collection assets in the AO. Moreover, the expected reduction of potential information gain due to the sensor effectiveness of an asset is not captured in the definition of graph G. Approaches to better represent this information will be the subject of future research.

The benefits of applying space aggregation as part of the solution strategy for a random IGM decreased relative to the increase in solution quality observed when aggregation was part of

the solution strategy for the 1 Hot-Spot IGM shown in Chapter 5. Applying aggregation as part of the solution strategy for the 1 Hot-Spot IGM showed an increase of 30% on the solution value (potential information gain); applying aggregation as part of the solution strategy for the Random IGM showed an increase of 4% on the solution value. In the Random IGM, the value of each cell was randomly determined from a uniform distribution so there was no concentration of potential information gain as in the 1 Hot-Spot IGM. Based on these results, the impact of the distance from an information collection asset location to a hot-spot (an area of high potential information gain) in the IGM will be studied as part of future research. Although the computational price to include aggregation as part of the solution strategy was relatively minimal (an average increase of 0.01 seconds), an adaptive solution strategy is envisioned in which, based on a characterization of the IGM, the contribution of aggregation is varied. A study of this characterization is needed and it may include, the variance of the IGM and the distance to clusters of high potential information gain (hot-spots).

The developed mathematical programming model and solution approach were used as a framework to evaluate the degradation of solution quality as a centralized system moves to a decentralized framework. This research defined Price of Decentralization (PoD) as a measure on the degradation of solution quality as a centralized system moves to different levels of decentralization, extending the concept of "price of anarchy" originally defined by the game theory community. A network connectivity matrix captured what assets are in the same communication network and enabled to exchange information. Levels of decentralization were determined by redefining the structure of this connectivity matrix and computing the PoD metric against the information gain from the best-known solution for a centralized framework. Moreover, assets in a connected component were required to maintain (1) pairwise connectivity to all assets in communication network; or, (2) a path between each pair of assets in the communication network. On the latter configuration, assets use other assets as intermediary (or "bridge") nodes to exchange information. Using a set of simulated scenarios where the initial location of assets and the initial information gain maps were defined randomly, the impact of sensor effectiveness, network topology and the type of IGM to the PoD metric was measured. Homogeneous assets (i.e., assets having the same mobility constraints and sensing capabilities) starting at the same location in a discretized area of operation were assumed. Under these conditions, the PoD metric was 45% when the information gathering activities of accurate sensors (0.75 sensor effectiveness) were not coordinated. This contrasts drastically with a PoD value

of 20% when the information gathering activities of less accurate sensors (0.25 sensor effectiveness) were not coordinated. The PoD was relatively the same for an asset with a better sensor effectiveness, regardless of the type of IGM. A study of the impact of heterogeneous collection assets and the effects of the asset's communication range for the different network topologies on the PoD metric is envisioned as future research. Moreover, PoD will be extended to consider available bandwidth, expected latencies and the value of the information flow present in the communication network.

Based on the above results, more complex experiments will be performed, determining how heterogeneous assets impact PoD as a function of the communication topology network. In particular, future work will provide an in-depth analysis of the PoD metric as assets with a mix of sensor effectiveness are available to support a mission. The PoD metric will also be extended to consider available bandwidth, expected latencies and the value of the information flow present in the communication network. The effects of decentralization on other metrics such as the Price of Fairness (PoF) [8] will also be evaluated.

Bibliography

[1] M. J. Hirsch, H. Ortiz-Pena, and C. Eck. Cooperative Tracking of Multiple Targets by a Team of Autonomous UAVs. *International Journal of Operations Research and Information Systems*, 3(1):53–73, 2012.

[2] E. Blasch, P. Valin, and E. Bosse. Measures of Effectiveness for High-Level Fusion. In *Proceedings of the 13th Conference on Information Fusion*, pages 1–8, 2010.

[3] T. Shima, S. J. Rasmussen, and P. Chandler. UAV team decision and control using efficient collaborative estimation. *Journal of Dynamic Systems Measurement and Control*, 129(5), 2005.

[4] C. Papadimitriou. Algorithms, games, and the internet. In *Proceedings of the 33rd Annual ACM Symposium on Theory of Computing*, pages 749–753. ACM, 2001.

[5] J. R. Marden and T. Roughgarden. Generalized efficiency bounds for distributed resource allocation. In *Proceedings of the 48th IEEE Conference on Decision and Control*, 2010.

[6] T. Roughgarden and É. Tardos. How Bad is Selfish Routing? *Journal of the ACM*, 49(2):236–259, 2002.

[7] T. Roughgarden. The price of anarchy is independent of the network topology. *Journal of Computer and System Sciences*, pages 428–437, 2002.

[8] D. Bertsimas, V. Farias, and N. Trichakis. The Price of Fairness. *Operations Research*, 59(1):17–31, 2011.

[9] M. Hirsch, H. Ortiz-Pena, N. Sapankevych, and R. Neese. Efficient flight formation for tracking of a ground target. In *Proceedings of the National Fire Control Symposium*, pages 1–16, 2007.

[10] S. Rasmussen and T. Shima. *UAV Cooperative Decision and Control: Challenges and Practical Approaches*. Society for Industrial and Applied Mathematics, 1st edition, 2008.

[11] L. Bakule. Decentralized Control: An Overview. *Annual Reviews in Control*, 32(1):87–98, 2008.

[12] S. M. Jameson. Architectures for Distributed Information Fusion to Support Situation Awareness on the Digital Battlefield. In *Proceedings of the 4th International Conference on Information Fusion*, pages 7–10, 2001.

[13] The Cooperative Engagement Capability. *Johns Hopkins APL Technical Digest*, 16(4):377–396, 1995.

[14] D. Perugini, D. Lambert, L. Sterling, and A. Pearce. Distributed information fusion agents. In *Proceedings of the 6th International Conference on Information Fusion*, pages 86–93, 2003.

[15] M. M. Polycarpou, Y. Yang, and K. M. Passino. A Cooperative Search Framework for Distributed Agents. In *Proceedings of the 2001 IEEE International Symposium on Intelligent Control*, pages 1–6, 2001.

[16] J.R. Marden and A. Wierman. Distributed welfare games with applications to sensor coverage. In *Proceedings of the 47th IEEE Conference on Decision and Control*, pages 1708–1713, 2008.

[17] Y. Jin, A. A. Minai, and M. M. Polycarpou. Cooperative real-time search and task allocation in UAV teams. In *Proceedings of the 42nd IEEE International Conference on Decision and Control*, pages 7–12, 2003.

[18] V. Shetty, M. Sudit, and R. Nagi. Priority-based assignment and routing of a fleet of unmanned combat aerial vehicles. *Computers and OR*, pages 1813–1828, 2008.

[19] C. C. Murray and M. H. Karwan. An Extensible Modeling Framework for Dynamic Reassignment and Rerouting in Cooperative Airborne Operations. *Naval Research Logistics*, 57(7):634–652, 2010.

[20] J. Kim and J. Crassidis. UAV Path Planning for Maximum Visibility of Moving Ground Targets in an Urban Area. In *Proceedings of the 13th International Conference on Information Fusion*, 2010.

[21] G. A. McIntyre and K. J. Hintz. An Information Theoretic Approach to Sensor Scheduling. In *Proceedings Signal Processing, Sensor Fusion, and Target Recognition V*, volume 2755, pages 304 – 312, 1996.

[22] C. Kreucher, A. O. Hero III, and K. Kastella. A Comparison of Task Driven and Information Driven Sensor Management for Target Tracking. In *Proceedings of the 44th IEEE Conference on Decision and Control, and the European Control Conference*, pages 4004–4009, 2005.

[23] C. M. Kreucher, K. D. Kastella, J. W. Wegrzyn, and B. L. Rickenbach. An Information Based Approach to Decentralized Multi-Platform Sensor Management. In *Proceedings of SPIE*, volume 6249, 2006.

[24] T. Mullen, V. Avasarala, and D. L. Hall. Customer-Driven Sensor Management. *IEEE Intelligent Systems*, 21:41–49, 2006.

[25] Michael J. Hirsch. *GRASP-based Heuristics For Continuous Global Optimization Problems*. PhD thesis, University of Florida, 2006.

[26] M. J. Hirsch, H. Ortiz-Pena, and M. Sudit. Decentralized Cooperative Urban Tracking of Multiple Ground Targets by a Team of Autonomous UAVs. In *Proceedings of the 14th International Conference on Information Fusion*, pages 1–7, 2011.

[27] M. J. Hirsch and H. Ortiz-Pena. Autonomous Network Connectivity and Cooperative Control for Multiple Target Tracking. In *Proceedings of the 27th Army Science Conference*, 2010.

[28] R. L. Raffard, C. J. Tomlin, and S. P. Boyd. Distributed Optimization for Cooperative Agents: Application to Formation Flight. In *Proceedings of the 43rd IEEE Conference on Decision and Control*, pages 2453–2459, 2004.

[29] E. Frazzoli and F. Bullo. Decentralized algorithms for vehicle routing in a stochastic time-varying environment. In *Proceedings of the 43rd IEEE Conference on Decision and Control*, volume 4, pages 3357–3363, 2004.

[30] M. S. Bazaraa, J. J. Jarvis, and H. D. Sherali. *Linear Programming and Network Flows*. Wiley-Interscience, 3rd edition, 2004.

[31] D. Soest, J. List, and T. Jeppesen. Shadow prices, environmental stringency, and international competitiveness. *European Economic Review*, 50(5):1151–1167, 2006.

[32] B. I. Conradie and D. L. Hoag. A review of mathematical programming models of irrigation. *WaterSA*, 30(3):287–292, 2004.

[33] K. Dachraoui and T. Harchaoui. Water Use, Shadow Prices and the Canadian Business Sector Productivity Performance. Economic Analysis Research Paper Series, Statistics Canada, Analytical Studies Branch, 2004.

[34] R. Fare, S. Grosskopf, and W. L. Weber. Shadow Prices and Pollution Costs in U.S. Agriculture. *Ecological Economics*, 56(1):89–103, 2006.

[35] Y. Xue, B. Li, and N. Nahrstedt. Optimal resource allocation in wireless ad hoc networks: A price-based approach. *IEEE Transactions on Mobile Computing*, 5:347–364, 2006.

[36] J. Coles and J. Zhuang. Decisions in Disaster Recovery Operations: A Game Theoretic Perspective on Organization Cooperation. *Journal of Homeland Security and Emergency Management*, 8(1):1772–1787, 2011.

[37] S. Robinson. The Price of Anarchy. *SIAM News*, 37(5), 2004.

[38] E. Koutsoupias and C. Papadimitriou. Worst-case equilibria. In *Proceedings of the 16th Annual Symposium on Theoretical Aspects of Computer Science*, pages 404–413, 1999.

[39] Stuart J. Russell and Peter Norvig. *Artificial Intelligence: A Modern Approach*. Pearson Education, 2nd edition, 2003.

[40] Thomas M. Cover and Joy A. Thomas. *Elements of Information Theory*. Wiley-Interscience, 1991.

[41] http://www.merriam-webster.com/dictionary/information, Accessed December 2013.

[42] A.N. Langville and C.D. Meyer. *Who's #1?: The Science of Rating and Ranking*. Princeton University Press, 2012.

[43] Timothy P. Chartier, Erich Kreutzer, Amy N. Langville, and Kathryn E. Pedings. Sensitivity and Stability of Ranking Vectors. *SIAM J. Sci. Comput*, 33:1077–1102, 2011.

[44] William B. Frakes and Ricardo Baeza-Yates, editors. *Information Retrieval: Data Structures and Algorithms*. Prentice-Hall, Inc., 1992.

[45] Kenneth Massey. Statistical Models Applied to the Rating of Sports Teams. Honors Project in Mathematics, Bluefield College, 1997.

[46] Wesley N. Colley. Colleys bias free college football ranking method: The colley matrix explained. http://www.colleyrankings.com/matrate.pdf, 2002.

[47] J. P. Keener. The Perron-Frobenius Theorem and the Ranking of Football Teams. *SIAM review*, 35(1), 1993.

[48] Gesellschaft für Klassifikation. Jahrestagung, M. Schwaiger, and O. Opitz. *Exploratory Data Analysis in Empirical Research: Proceedings of the 25th Annual Conference of the Gesellschaft Für Klassifikation E.V.* Springer Berlin Heidelberg, 2003.

[49] The MathWorks, Inc. *MATLAB R2011b*. Natick, Massachusetts, United States, 2015.

[50] IBM ILOG CPLEX Optimizer. http://www-01.ibm.com/software/commerce/optimization/cplex-optimizer, Accessed May 2015.

[51] M. R. Garey and D. S. Johnson. *Computers and Intractability: A Guide to the Theory of NP-Completeness*. W.H. Freeman and Company, 1979.

[52] William K. Pratt. *Digital Image Processing: PIKS Inside*. John Wiley & Sons, Inc., 3rd edition, 2001.

[53] Dimitri Bertsekas and Robert Gallager. *Data Networks*. Prentice-Hall, Inc., 2nd edition, 1992.

[54] A. Richards and J. P. How. Decentralized model predictive control of cooperating UAVs. In *Proceedings of IEEE Conference on Decision and Control*, pages 4286–4291, 2004.

[55] R. Smith and R. Davis. Frameworks for cooperation in distributed problem solving. *IEEE Transactions on Systems, Man, and Cybernetics*, 11:61–70, 1981.

[56] P. R. Chandler and M. Pachter. Research issues in autonomous control of tactical UAVs. *Proceedings of the 1998 American Control Conference*, 1, 1998.

[57] J. K. Ho. Computing true shadow prices in linear programming. *Informatica, Lith. Acad. Sci.*, 11(4):421–434, 2000.

[58] M. E. Lübbecke and J. Desrosiers. Selected topics in column generation. *Operations Research*, 53:1007–1023, 2002.

[59] T. Alpcan and L. Pavel. Nash equilibrium design and optimization. In *Proceedings of the 1st ICST international conference on Game Theory for Networks*, pages 164–170, 2009.

[60] P. T. Harker and J. S. Pang. Finite-dimensional variational inequality and nonlinear complementarity problems: a survey of theory, algorithms and applications. *Math. Program.*, 48:161–220, 1990.

[61] Bang Wang. *Coverage Control in Sensor Networks*. Springer Publishing Company, Incorporated, 1st edition, 2010.

[62] Maysum Panju. Iterative Methods for Computing Eigenvalues and Eigenvectors. *The Waterloo Mathematics Review*, 1, 2011.

[63] M.J. Hirsch and D. Schroeder. Dynamic Decentralized Cooperative Control of Multiple Autonomous Vehicles with Multiple Tasks for Urban Operations. In *Proceedings of the AIAA Guidance, Navigation, and Control Conference*, pages 1–19, 2012.

[64] C. Papadimitriou and K. Steiglitz. *Combinatorial Optimization: Algorithms and Complexity*. Dover, 1998.